Studies of the effect of cysteine and heme pocket mutations of the nitric oxide dioxygenase and nitrite reductase activities of human Cytoglobin and Androglobin heme domain

By

John Ukeri

A thesis submitted for the degree of Doctor of Philosophy

School of Life Sciences,

University of Essex,

Wivenhoe Park,

Colchester,

Essex,

UK

April 2020

Abstract

Oxygen delivery to hypoxic tissues along with the interplay between hemoglobins and hypoxic tissues have been an area of interest, the nitrite reductase activity (NiR) and the nitric oxide dioxygenase activity (NOD) working in tandem is a proposed regulatory response which enhances oxygen levels in hypoxic tissues, serving to protect tissues against hypoxia. In hypoxic conditions, NO is generated via the NiR activity, while in normoxic condition NO is consumed via the NOD activity. With NO being a versatile signalling molecule and a potent relaxant of the vasculature, NO homeostasis by the NiR and NOD activity regulates vascular tone in response to oxygen demand. In traditional oxygen carriers like hemoglobin (Hb) and myoglobin (Mb), NO homeostasis via the NOD and NiR activities is seen as an additional function and is well studied and characterised in these globins. Scientific inquiry on hemoglobin superfamily and advances in genomics have led to the discovery of new hemoglobins, including an expanded human hemoglobin family with the discovery of additional members like Neuroglobin (Ngb) Cytoglobin (Cygb) and Androglobin (Adgb). These fresh additions are hexacoordinate, unlike Mb and Hb which have their sixth coordination site vacant in the absence of external ligands, Cygb and Adgb have their sixth coordination site occupied, by a histidine and glutamine respectively. Cygb is a low abundance vertebrate globin of ubiquitous expression, distantly related to Mb and upregulated during cellular hypoxia. Crystallographic data places Cygb as a monomer with free sulfhydryl and dimer with an intermolecular bond between two monomeric subunits. Biochemical studies have observed Cygb also existing as a monomer with an intramolecular disulfide bond, this form of the protein lacks crystallographic data. Adgb is a chimeric globin with a rearranged globin domain, Adgb lacks biochemical characterisation with little information obtained about its biochemical properties. However, Adgb highly is expressed in the testes and gene expression upregulated during spermatogenesis. Despite efforts to probe the biochemical activities of these additional members, their physiological roles are still not clearly defined. In this study, we report that the formation of an intramolecular disulfide bond between cysteines C38 and C83 enhances the

nitrite reductase activity by 50-fold over that of the monomer with free sulfhydryl or 140-fold over that of the dimer with intermolecular disulfide bonds. The NO dioxygenase reactivity of cytoglobin is also very rapid with or without disulfide bond. We have targeted amino acid residues (H81A, L46F, L46W, C38,83S) in Cygb by mapping mutations targeting specific properties of hemoglobin (Hb) and myoglobin (Mb), including O_2 binding and NO binding/scavenging as well as the NiR activity of Ngb, in addition to other rationalised mutations (C38,83S). Mutations of amino acid residues at the distal pocket successfully enhanced or attenuated the NiR and NOD of Cygb, by understanding how particular mutations can affect specific reactivities, these mutations may be used to target the NiR or NOD (e.g. by CRISPR/Cas9) in cell or animal models to help understand the precise role (or roles) of Cygb under physiological and pathophysiological conditions. Ultrafast and laser flash photolysis aided probing of the roles of the cysteines on ligand migration pathway, data suggests the cysteines play a role in ligand entry and exit from Cygb. We have re-evaluated the structural sequence assigned to the globin domain of Adgb (Adgb-GD), and we propose that part of the original structural sequence alignment was in error. Upon correction, we have expressed the Adgb-GD as a stable protein at neutral or alkali pH. Additionally, with a stable form of the protein expressed, we have identified a unique feature of the Adgb-GD. Adgb-GD binds nitric oxide in 5-coordinate heme configuration, unlike any other human globin, but similar to that observed with guanylate cyclase, cytochrome c'. Adgb-GD displays a high nitrite reductase activity, which is influenced by the redox state of the disulfide bond. Spectra characterisation depicts Adgb-GD as a hexacoordinate globin, comparative spectra analysis with Cytochrome C' suggest Adgb-GD may possess similar ligand binding properties.

Acknowledgements

I would like to thank almighty God for inspiration and spiritual guidance. I also give special thanks and appreciation to my dad and mom Mr and Mrs Ukeri, for their sacrifice, support and motivation during the course of my research. I also extend my gratitude to my supervisor Dr Brandon Reeder, and also Prof Mike Wilson, Dr Elizabeth Welbourn and the entire 6.19 research group for their continuous support, patience, and contribution throughout my research. I want to thank Prof Marten Vos for helping with the ultrafast laser experiments, data analysis and hospitality in Paris. I also appreciate to Dr Dimitri A. Svistunenko for help with EPR data and analysis, and Dr Sinan Battah for will cell culture assays. Thanks to Dr Victoria Allen-Baunme and Michelle Simons for their guidance during my first and second year. I also appreciate Dr Ayo Oyelakin, and Mrs Perl Oyelakin for a place to stay and write up during terminal phase of my research and all the members of the DCLM group Colchester for their help and support. Finally, thanks to University of Essex for giving me the opportunity, and the staff, and all the support teams at the school of life sciences

.

Abbreviations

Adgb	Androglobin
ALA	Aminoleuvelinic acid
CO	Carbon Monoxide
Cygb	Cytoglobin
$Dimer_{S-S}$	Dimeric cytoglobin with intramolecular disulfide bond
DMSO	Dimethyl sulfoxide
FAD	Flavin adenine dinucleotide
FHb	Flavohemoglobin
GCs	Globin coupled sensors
Hb	Hemoglobin
IPTG	Isopropyl β-D-1-thiogalactopyranoside
LB	Luria Bertani media
Mb	Myoglobin
$Monomer_{S-S}$	Monomeric cytoglobin with intramolecular disulfide bond
$Monomer_{S-H}$	Monomeric cytoglobin with free sulfhydryl
NaPi	Sodium phosphate buffer
Ngb	Neuroglobin
NiR	Nitrite reductase
NADH	Nicotinamide adenine dinucleotide
NO	Nitric oxide
NOD	Nitric Oxide dioxygenase
Pfu	*Pyrococcus furiosus*
Proli-NONOate	Disodium 1-[(2-carboxylato)pyrrolidin-1-yl]diazen-1-ium-1,2-diolate
SDHb	Single domain hemoglobin
SDS PAGE	Sodium dodecyl sulfate and polyacrylamide gel electrophoresis
TCEP	Tris(2-carboxyethyl)phosphine
TrHb	Truncated hemoglobin

Contents

Chapter 6: General discussion

List of Figures

Chapter 1

Chapter 2:

Chapter 3:

Chapter 4:

Chapter 5:

List of Tables

Chapter 1

GENERAL INTRODUCTION

1.1 Globin structure and evolution

Globins are a diverse family of protein identified in all three kingdoms of life with structural and functional variations (Vinogradov ., 2006). Phylogenetic analysis links the rise of globins to a single ancient gene of bacterial origin. Single-celled eukaryotes possessed globins through lateral gene transfer (Vinogradov ., 2006).

Globins can be structurally classified into a single domain hemoglobins (SDHb) and chimeric globins (Vinogradov ., 2007) see Figure 1.2. The single-domain globins consist of the 3/3 classical hemoglobins like Hemoglobin (Hb), Myoglobin (Mb), Neuroglobin (Ngb) and Cytoglobin (Cygb). The helical configuration of these globins involves the positioning of helices in a 3-over-3 alpha helical sandwich enveloping the heme moiety. Helices A, B and E are on one side of the heme and helices F, G, and H on the other (Vinogradov ., 2007) Helices C and D are shorter and the CD loop region typically contains a highly conserved phenylalanine or tyrosine in the CD1 position that stabilises the heme binding Figure 1.1. The single-domain globins also include truncated 2/2 globins (TrHb) in which the number of helices is fewer (Vinogradov ., 2006), resulting in a short or absent A helix, decreased C-E inter-helical region and helix F mostly occurring as a loop, leaving helices B, E, G, and H to envelope the heme group (Vinogradov ., 2006). Chimeric globins are modular globins with two or more domains, with an N-terminal globin heme domain fused to either a signal-transducing domain, globin coupled sensors (GCs), or a nicotinamide adenine dinucleotide (NAD) and flavin adenine dinucleotide (FAD) domain Flavohemoglobins (FHb) (Vinogradov ., 2007).

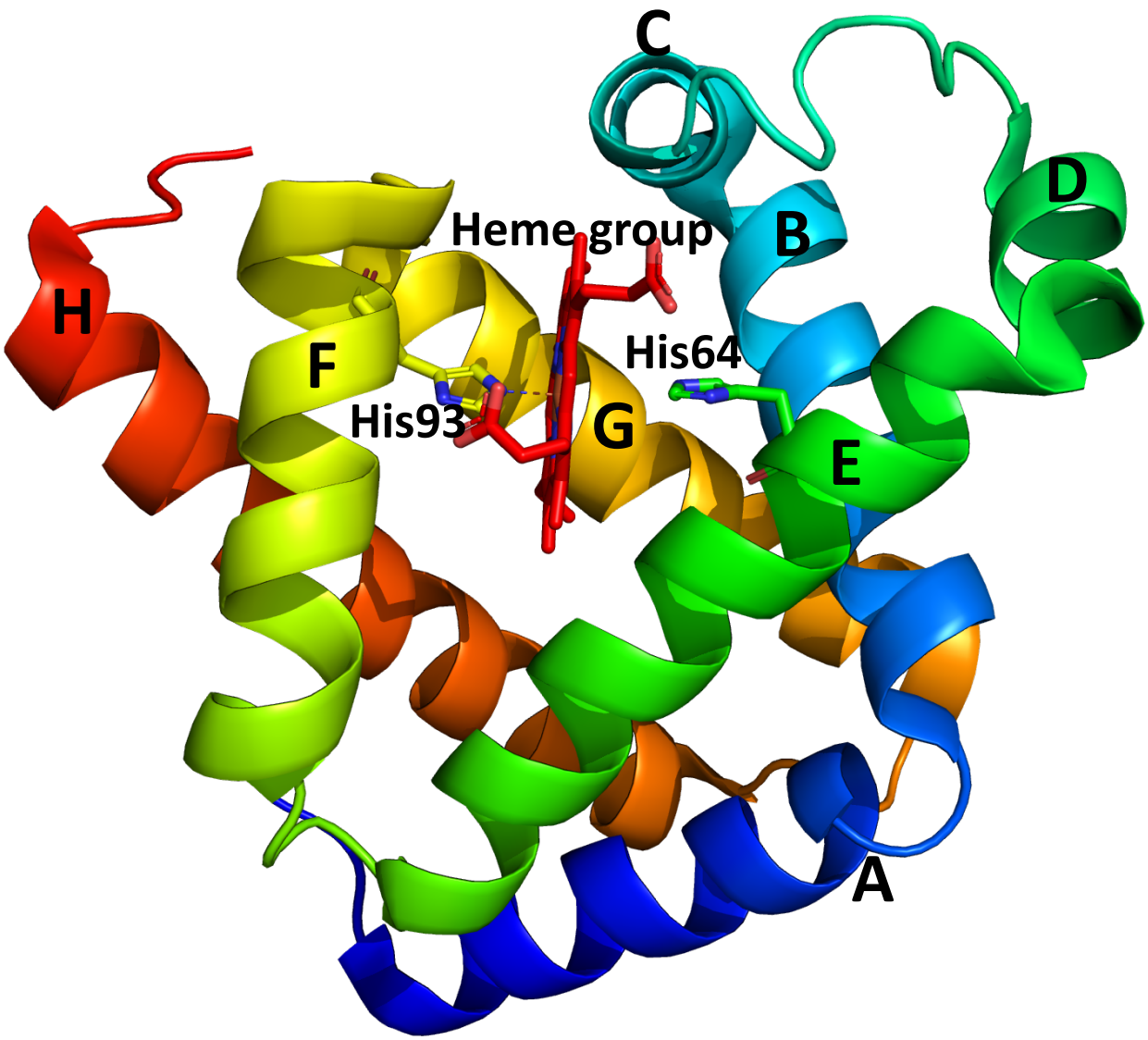

Figure 1.1 structure of horse heart myoglobin PDB ID: 1WLA. Mb structure generated my PyMol molecular graphics software, illustrating the 3/3 helical sandwich with helices H, F, G on one side of the heme plane and helices B, E A on the other side. His64 represents the distal histidine, this histidine aids the coordination of ligands to central heme iron (distal coordination site). His93 represents the proximal, the heme group is attached this histidine, providing stability to the heme plane.

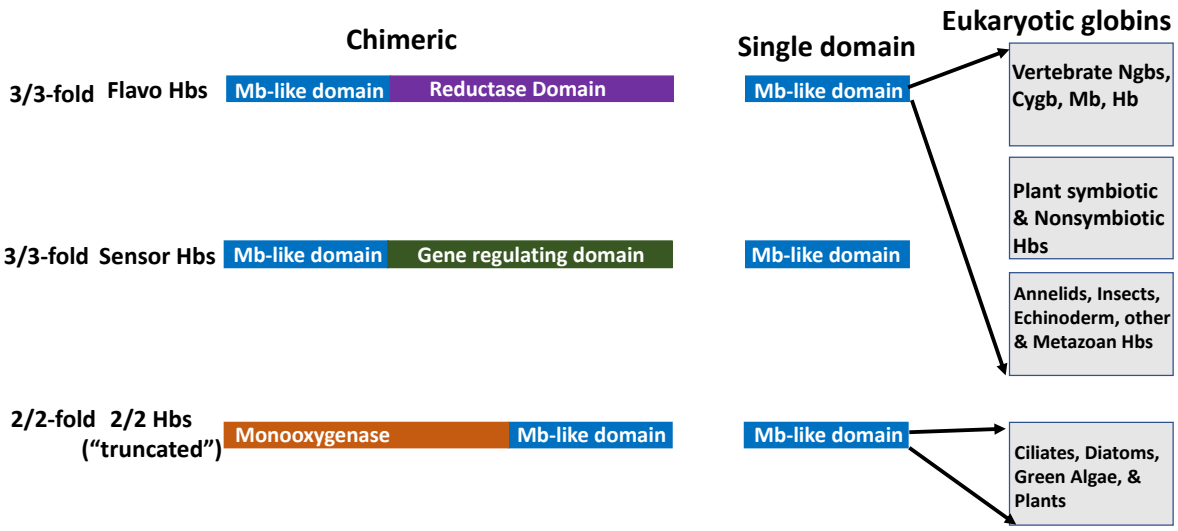

*Figure 1.2 illustration of lineages in the hemoglobin superfamily adapted from ((*Vinogradov *.,* 2008*).* Figure illustrates structural classification of the hemoglobin superfamily. Globins are believed to have evolved from an ancient single domain Mb-like globin (blue). However, divergence events led to the formation of other lineages including incooperation multi-domain globins like: Flavo Hb with reductase domain (purple), Sensor Hb with gene regulating domain (green) and 2/2 Hb with monooxygenase domain (brown).

Phylogenetically, globins can be traced to three lineages (Vinogradov ., 2007) see Figure 1.2. One lineage includes chimeric flavohemoglobins with a NAD and FAD-binding domain homologous to Ferredoxin-$NADP^+$ reductases and related SDHb like Mb, Hb, and Cygb (Vinogradov ., 2007). The second lineage consists of the modular chimeric globin coupled sensors with an N-terminal myoglobin-like sensor domain linked to a C-terminal signalling domain, with related single domain protoglobins (Vinogradov ., 2007). Protoglobins are single-domain globins in bacteria and archaea with sensor domains but devoid of transmitter domain present in globin coupled sensors (Pesce ., 2013). The third lineage consists of abbreviated hemoglobins with a truncated 2/2 alpha-helical structure (Nardini et al., 2007) Figure 1.3.

The globin distribution across the three kingdoms of life shows variations in the distribution of different types of globins across domains (Vinogradov ., 2005, 2006). Bacteria have all three globin lineages, an indication of globins to be of bacterial origin (Frey and Kallio, 2003). Members of the FHb and 2/2 Hb lineages function as enzymes, while members of GCs lineage function as sensors and aerotactic gene regulators (Vinogradov ., 2008; Pesce ., 2013). Presently there are no evolutionary relationships between globin families (Vinogradov .,2008). The emergence of globin complexity may likely have been evolutionary driven due to the advent of multicellularity demanding enzymatic and more tasking operations (Vinogradov and Moens, 2008). At the same time, unicellular organisms thrived using modest sensor-based operations (Martinkova et al., 2013). Globins originally discovered as myoglobin, and heterotetrameric hemoglobin initially assigned role was principally that of oxygen sensing and transport (Wittenberg ., 1975; Dickerson .,1983). With advances in genomics and expanded amounts of experimental data, globins have proved to be diverse structurally functionally and ubiquitous in species (Vinogradov ., 2008). Functions of globins involve the usage of iron cofactors as heme or iron-sulphur cluster, with exception to non-heme globins and Per-Arnt-Sim (PAS) domains, which can bind an array of cofactors (Murray, Delumeau and Lewis, 2005; Freitas ., 2008; Dizicheh ., 2017). Hemoglobins

rely on the coordination of ligands to central iron atom on the heme group, (Hardison, 1996). The iron atom cycle between ferric and ferrous oxidation state, the ferrous state is generally the biologically active form, this allows for binding of external ligands like NO, O_2, CO, and Nitrite, this ability to reversibly bind external ligand is responsible for physiological activities like oxygen transport (Hardison, 1996; Shiva ., 2007; Smagghe .,2008).

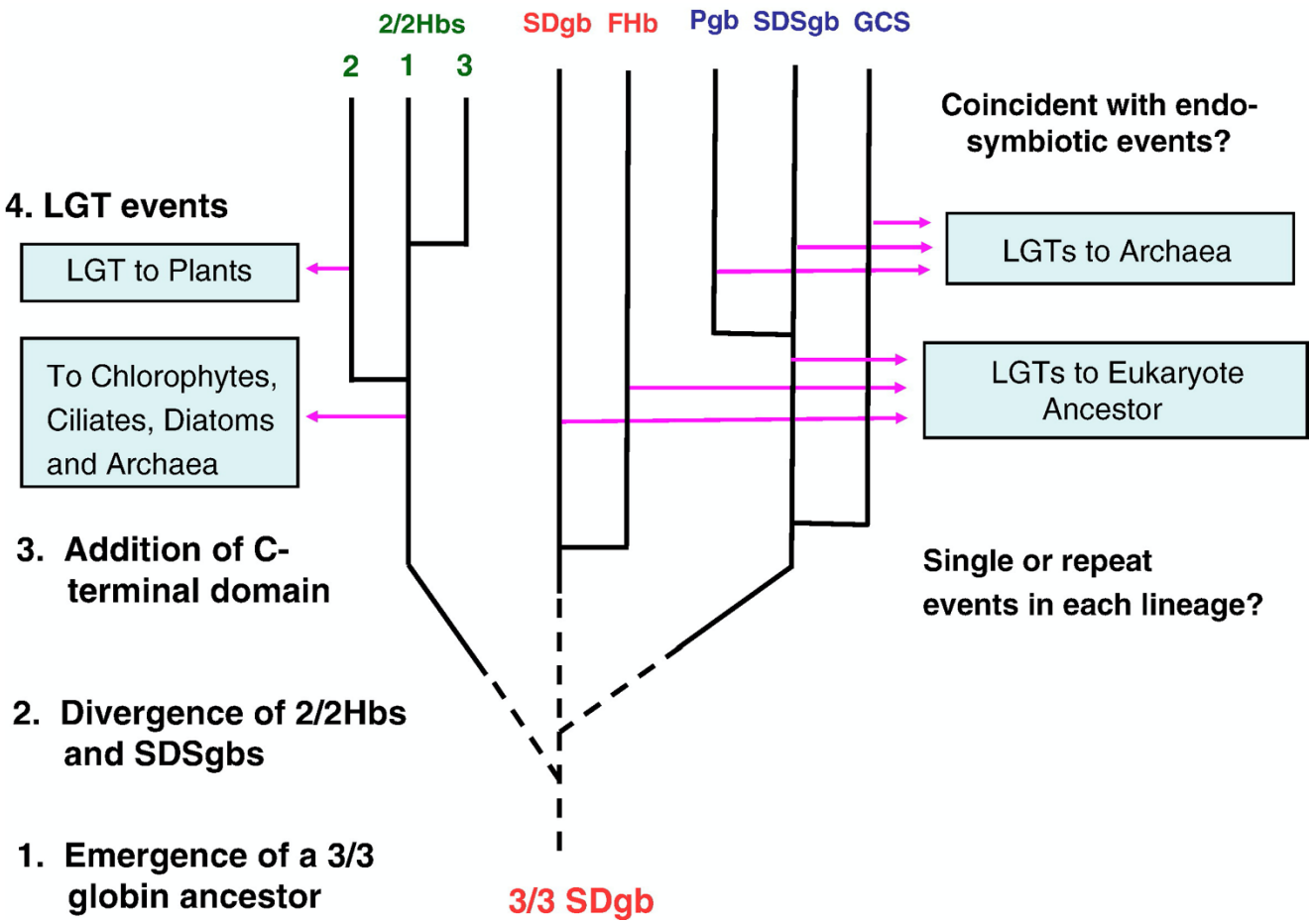

Figure 1.3 Phylogenetic classification of the hemoglobin superfamily. A model depicting globin evolution by (Vinogradov et al., 2007). The ubiquity of globins in all domains of life, is believed to have stimulated by lateral gene transfer events of globins to other domains of life, represented by (Purple arrows) and divergence of an ancestral globin of presumably of bacterial origin, due to presence of all lineages in bacteria. Eukaryotes possibly assimilated globins by lateral gene transfer and/or with symbiotic events.

1.2 Human hemoglobin family

Early members of this family (Mb and Hb) are involved in oxygen transport and storage, these globins are also nitric oxide dioxygenases (NOD) and nitrite reductases (NiR), the NOD and NiR activity have been linked to (NO) homeostasis (Gardner ., 2012; Kamga ., 2012). The functions of the Ngb, Cygb, and Adgb is still not clearly defined (Kakar ., 2010; Hoogewijs ., 2012), however, recent work linked the potential role of Cygb to be that of NO homeostasis as a cytoprotective response against cellular hypoxia (Halligan, Jourd'heuil and Jourd'heuil, 2009; Liu ., 2013; Reeder and Ukeri, 2018).

Members of the human hemoglobin family can utilize metal-bound porphyrin rings for catalytic, electron transfer, and cytoprotective activities such as peroxidase activities. The role of cytochromes was established early in evolution by their use as terminal oxidase in the electron transfer chain, a process key to the generation of energy in life forms (Garcia-Horsman et al., 1994). Due to the planar structure of the heme molecule and central position of the heme iron, this allows for coordination of ligands to the axial ends of the heme iron(Baldwin, 1975) Figure 1.2.1. The heme iron has two available coordination sites, the 5th and 6th coordination sites (Berg Jm, 2002). The heme molecule is attached to the protein via the 5th coordination site, usually via a covalent bond to histidine in the F8 position (De Sanctis et al.). An internal ligand can occupy the 6th coordination site or left vacant for ligation of external ligands. Hemoglobins are characterized, by the coordination complexes of the heme iron, which could be Penta (5-C) with the sixth coordination site accessible to an external ligand or Hexa (6-C) with the sixth coordination site is occupied by an internal ligand (Kakar ., 2010) see Figure 1.2.2.

The biochemical activity of hemoglobins relies on reversible oxidation and binding of external ligands—the central iron atom of the heme group cycles between the Ferric (Fe^{3+}) and Ferrous (Fe^{2+}) oxidation state (Bonaventura et al., 2013). As mentioned previously, the ferrous heme iron

allows binding of exogenous ligands like CO, NO, O_2. This enables a host of biochemical activities, including oxygen storage and transport, nitrite reductase activity (NiR), and nitric oxide dioxygenase (NOD) activity. Biochemical activity results in the formation of ferric iron; to remain in the biologically active ferrous state, heme iron relies on internal reductants such as ascorbate and NADPH (Tong ., 2014). What follows is an examination of each of the five main human globins including a review of the current knowledge about the physiological and pathological roles that they are known to participate in.

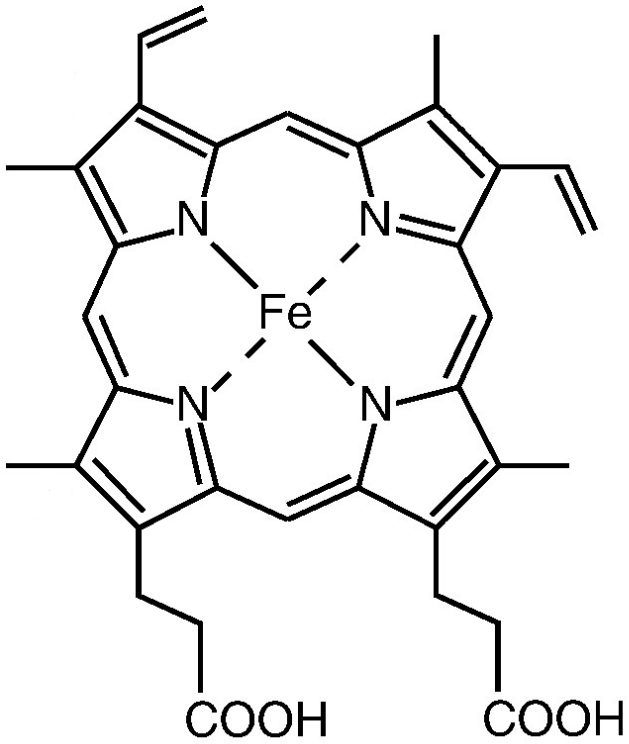

Heme B
(protoheme IX)

Figure 1.2.1. Porphyrin IX macrocyclic ring system (image source: (Hederstedt, 2012)). Skeletal structural of heme b co-factor in the human globin family. Showing the macrocyclic ring system with the central heme iron, the iron cycles between and a ferric (3+) and ferrous (2+) many biochemical activities of hemoglobins occur in the ferrous iron state.

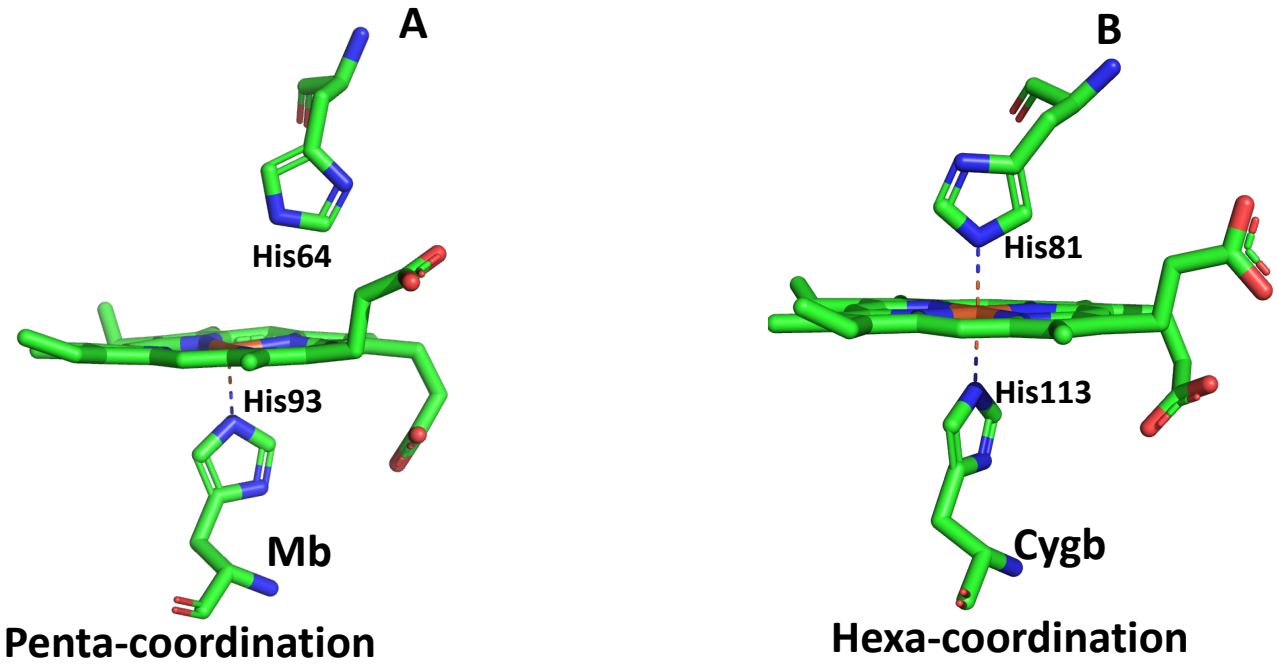

Figure 1.2.2 Distal and proximal coordination sites in Mb and Cygb. Stick structures generated using PyMol molecular graphics software. (A) heme structure of Mb PDB ID: 1WLA illustrating Penta coordination. (B) heme structure of Cygb PDB ID: 2DC3 illustrating Hexa coordination.

1.3 Structure and function of myoglobin

1.3.1 Myoglobin: a globin of skeletal muscle fiber and cardiac tissues

Mb is a vertebrate globin located in the cytoplasm of cardiac myocytes and sarcoplasm skeletal muscle fibre (Koch ., 2016). Mb was the first protein to have to 3-D structure solved (Kendrew ., 1958a), opening the structural-functional paradigm in molecular biology which linked physiological and pathophysiological activities of macromolecules to their structural properties (Kendrew, 1963; Olson and Ghosh, 2008). Mb plays a pivotal role in the physiological capacities of the heart and muscle through oxygen and NO homeostasis in myocytes (Kamga, Krishnamurthy and Shiva, 2012). In contrast with Hb, a heterotetramer that binds oxygen cooperatively, myoglobin is a monomer with just one site for oxygen binding; this results in different binding properties (Ordway and Garry, 2004). Mb binds oxygen noncooperatively displaying a rectangular hyperbolic oxygen saturation curve, while Hb exhibits a sigmoidal shaped binding curve as a result of its cooperative binding (Wittenberg and Wittenberg, 2003). Mb has a higher affinity for oxygen than Hb (~1 mmHg for Mb compared with ~26 mmHg for Hb under physiological conditions). Mb is effective in obtaining oxygen from the bloodstream, it desaturates at the start of muscle activity stabilizing oxygen diffusion to contracting myocyte cells with high energy demands(Wittenberg and Wittenberg, 2003).

1.3.2 Structural properties of myoglobin

Mb has a polypeptide chain of 154 amino acids; it comprises eight alpha helices labelled A-H; activity of this protein relies on the binding of external ligands to the iron atom of the heme group (Kendrew ., 1958b; Perutz ., 1966) see Figure 1.3.2.1. The iron atom has six coordination sites, of which four are occupied by nitrogen atoms of the porphyrin ring system. The fifth site is coordinated to the imidazole side chain proximal His93, which anchors the heme group to the

protein; the sixth coordination site is vacant in the absence of external ligand (Ordway and Garry, 2004). Ligand binding to the sixth coordination site involves formations of a bond with the heme iron and the imidazole side chain of distal His64 (Olson ., 1988). The distal histidine aids the stability of ligands bound to the heme iron (Olson ., 1988). The sixth coordination is the active site of the protein responsible for the assortment of biochemical activities of this globin (Ordway and Garry, 2004).

1.3.3 Physiological activities of myoglobin

Much biological activity like oxygen and NO homeostasis occurs in the ferrous form of the protein (Ordway and Garry, 2004). This protein also performs secondary activities like peroxidation in its ferric state, although the peroxidatic activity of Mb is much slower than classical peroxidases such as cytochrome P450 and catalase. Hence, Mb was used as a pseudo-peroxidase to study peroxidatic mechanisms (George and Irvine, 1955). Later research has shown that Mb does have true peroxidatic activity *in vivo*, although currently only observed in pathological conditions such as acute kidney injury following rhabdomyolysis (muscle injury) (Holt et al., 1999, Boutaud et al., 2010)

The central iron can form a bond with a host of ligands in its Fe^{2+} oxidation state (ferrous), it can be oxygen bound (oxymyoglobin) or not (deoxy myoglobin), ligands like carbon monoxide, nitrite, nitric oxide can also bind to the heme (Ordway and Garry, 2004). Additionally, the heme can be oxidized to the Fe^{3+} state (ferric) (Ordway and Garry, 2004). Apart from oxygen transport and storage, myoglobin possesses some enzymatic functions (Wilson, 2005; Hendgen-Cotta ., 2008; Kamga, Krishnamurthy and Shiva, 2012). Oxymyoglobin decomposes bioactive nitric oxide to nitrate in an enzymatic process called the Nitric Oxide Dioxygenase Activity (NOD activity) (Kamga, Krishnamurthy and Shiva, 2012). The removal of nitric oxide enhances mitochondria respiration because nitric oxide is reversibly inhibitory to terminal oxidases like cytochrome oxidase in the electron transport chain (Shiva ., 2007). Deoxyferrous myoglobin likewise catalyses the generation of nitric oxide from NiR activity, the NOD and NiR enzymatic activities are proposed

to cytoprotective response against cellular hypoxia, regulating NO consumption or production depending on the aerobic/anaerobic condition of the cell (Hendgen-Cotta ., 2008). Other cytoprotective activities of myoglobin also include scavenging of reactive oxygen species to defend against oxidative stress (Totzeck et al., 2014). Ferric myoglobin catalyses the oxidation of organic substrates by hydroperoxides, creating a series of compounds, some of which are potent vasoactive molecules such as the oxidation of arachidonic acid phospholipid side chains to F_2-isoprostanes (Reeder et al., 2007). These activities tend to only be observed under pathological conditions where the Mb has been separated from its anti-oxidant rich, reducing environment of the myocyte (Reeder, 2016).

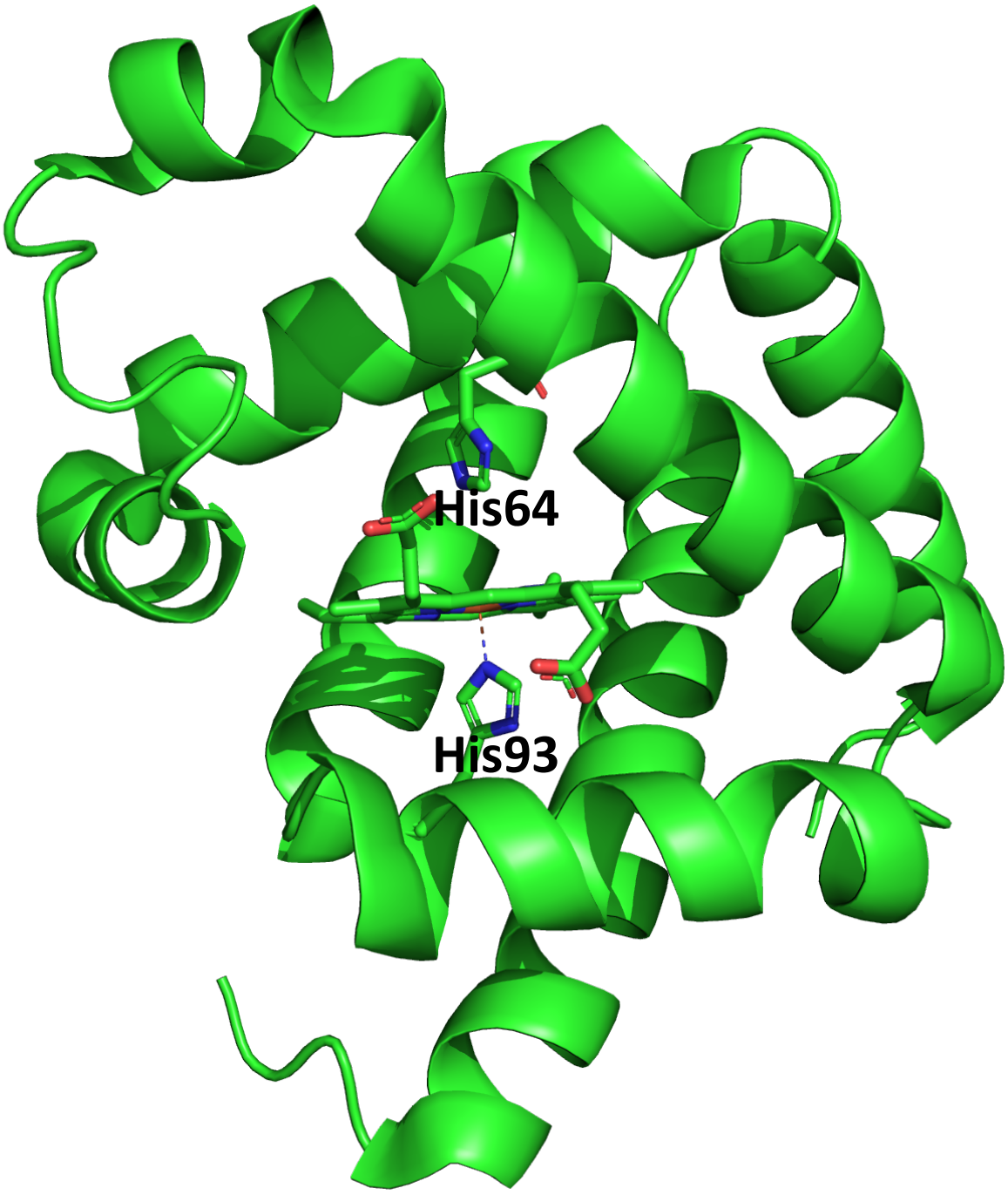

Figure 1.3.2.1 crystal structural of Mb PDB ID: 1WLA. Mb structure generated by PyMol molecular graphics software,of Mb showing distal and proximal histidine.

1.4 Structure and function of hemoglobin

1.4.1 Hemoglobin an erythrocyte globin shuttles molecular oxygen through cooperative binding

Hb is the principal protein of the erythrocyte (red blood cell), delivering oxygen to respiring tissues. Oxygen delivery is crucial for ATP generation by ATP synthase in mitochondria, supplying much of the energy needs of metabolizing cells in the body (Bhagavan and Ha, 2011).

Hb possesses the characteristic globular fold with a hydrophobic centre with houses a heme prosthetic group. Oxygen binding occurs in the ferrous oxidation state (Perutz, 1979). However, Hb readily auto-oxidises in the presence of oxygen to form ferric Hb and superoxide (Bonaventura et al., 2013). Within the erythrocyte there are systems to return the iron to then physiologically active ferrous form by sequestering NADH from glycolysis (the Embden-Meyerhof metabolic pathway (Lo and Agar, 1986, Brown, 1996), in addition, the pentose phosphate pathway utilises NADPH, generated from glucose-6-phosphate dehydrogenase, to neutralise reactive oxygen species such as superoxide (Birben et al., 2012) Hb primarily serves to store and transport molecular oxygen (Perutz ., 1960). Hb is a heterotetramer, binding of oxygen occurs cooperatively, the binding of a single oxygen molecule to one of the subunits triggers a conformational change to allow binding of oxygen to the other subunits (Perutz ., 1960).(Bhagavan ., 2011). Hemoglobin exists in two states, as deoxyhemoglobin in T (tensed) state and oxyhemoglobin in the R (relaxed) state (Bhagavan ., 2011). Cooperative binding of oxygen molecules ensures efficient delivery to respiring tissues (Perutz, 1970).

1.4.2 Structural properties of hemoglobin

Hemoglobins are composed of four subunits, with adult Hb (Hb A_0) consisting of two alpha, and two beta subunits. Each subunit has a protoporphyrin IX prosthetic group associated with a polypeptide chain with amino acid residues 141 (alpha) and 146 (beta) (Dickerson and Geis, 1983).. Human Hb only has two alpha-type subunits, alpha and zeta. The latter is only expressed

in the mesoblastic state of development (Gower 1, $\zeta_2\varepsilon_2$ and Portland, $\zeta_2\gamma_2$) The non-alpha chains include the beta chain of adult Hb, the epsilon chain of embryonic Hb (Gower 1, $\zeta_2\varepsilon_2$ and Gower 2, $\alpha_2\ \varepsilon_2$), delta chain of HBA_2, and also the gamma chains of fetal hemoglobin (Dickerson and Geis, 1983). For adults, ~97% is adult Hb ($\alpha_2\ \beta_2$), ~3% HbA_2 ($\alpha_2\ \delta_2$), and trace fetal Hb ($\alpha_2\ \gamma_2$). Each subunit aligns at the angles of an approximate tetrahedron. The four subunits associate via salts bridges, hydrophobic interactions, van der Waals forces, and hydrogen bonds (PERUTZ ., 1960). The quaternary structure of adult Hb constitutes a pair of identical alpha-beta dimers (alpha1-beta1 and alpha2-beta2) (Berg, ., 2002). The heme iron is coordinated to 4 pyrrole rings of the protoporphyrin IX. The fifth and sixth coordination sites are located on opposite sides of the heme plane (PERUTZ ., 1960). The heme plane rests the histidine side chain of helix F (proximal histidine: His87 (alpha) or His92 (beta), both His F8) (Perutz ., 1960). The distal histidine (His58, alpha and His 63, beta – both His E7) is not bound to the heme iron (PERUTZ ., 1960). However, it aids the stability of ligands bound to the sixth coordination site, for example forming a hydrogen bond to the bound dioxygen (Olson ., 1988; Birukou, Schweers and Olson, 2010). In deoxyhemoglobin, the distal coordination site is vacant for the occupation of external ligands like oxygen; this leaves the iron slightly out of plane (Berg, , 2002). During cooperative oxygen binding, the heme iron rearranges electrons making it smaller, pushing it into the plane of the heme, with the proximal histidine along; this residue situated on an alpha helix also moves this helix along (Berg*t* , 2002), resulting in a 15° rotation of the two alpha-beta dimers, changing the protein from the low O_2 affinity T state to high affinity R state. This conformational change transmits to the subunit paving the way for cooperative binding (Berg, , 2002).

2,3-bisphosphoglycerate (2,3-BPG) within erythrocytes modulates the release of oxygen in target tissues, 2,3-BPG preferentially binds to and stabilizes the T state of Hb, binding between beta chains, enabling the shifting of the oxygen binding curve to the right, lowering the affinity for O_2 and hence releasing O_2 to actively respiring tissue (Bhagavan and Ha, 2011).

1.4.3 Additional potential physiological activities of hemoglobin

The primary role of Hb is the transportation of biomolecular gases like oxygen and carbon dioxide (Dickerson and Geis, 1983). However, like Mb, Hb can also perform enzymatic roles like NiR and NOD activities (Kim-Shapiro, Schechter and Gladwin, 2006) . Nitrite dependent NO generation from nitrite via the NiR activity is allosteric, favouring the T-State (deoxyhemoglobin); this activity utilizes nitrite as a storage pool of bioactive NO as part of a regulatory response against cellular hypoxia which also involves the NOD activity. Hypoxic condition stimulates NO generation through the NiR activity while normoxic conditions favour NO consumption with the NOD activity(Huang ., 2005; Helms and Kim-Shapiro, 2013). While experimental evidence connects NiR activity to vasodilation, the exact mechanism of this process is not clearly understood; it is paradoxical for Hb to generate and consume NO (Cosby ., 2003). However, compartmentalization of the red blood cells, the short life span of NO, and cell-free zones in the endothelium are possible barriers to NO rapid diffusion into the erythrocytes allowing time for NO to regulate vascular tone playing its role as second messenger in the endothelium (Cosby ., 2003; Kim-Shapiro, Schechter and Gladwin, 2006). Like Mb, Hb catalyses the oxidation of organic substrates like lipids and cell membranes by hydroperoxides (Cheng ., 2011). The peroxidase activity of Hb is linked to oxidative stress and cell membrane damage (Cheng ., 2011).

1.5 Structure and function of neuroglobin

1.5.1 Neuroglobin is the globin of neuronal tissues

Ngb was the third addition to the human hemoglobin family, it was discovered in 2000 in human and mouse brain and named neuroglobin(Burmester et al., 2000a). Ngb like Mb and Hb displays the 3/3 globin Fold see Figure 1.1(Vallone ., 2004), however, in contrast with earlier members of the human hemoglobin family, Ngb displays a bis-histidyl six- coordinate heme-Fe atom, ligand binding to the Ngb metal centre is dependent on the dissociation of the distal His(E7)64-Fe bond (De Sanctis et al., 2004b, Trent Iii ., 2001) Figure 1.5.1.1. This made neuroglobin the first vertebrate hemoglobin with hexacoordination similar to plant hemoglobin (Trent Iii and Hargrove, 2002, Garrocho-Villegas *et a*l., 2007) Neuroglobin is predominantly in neuronal tissues (Ostojić et al., 2008, Reuss et al., 2002). From crystallographic data neuroglobin has been observed as a monomer with three cysteine residues, two of these residues forms an intra-molecular disulfide bond (Cys46, Cys55) (Pesce ., 2002; Ascenzi et al., 2013).

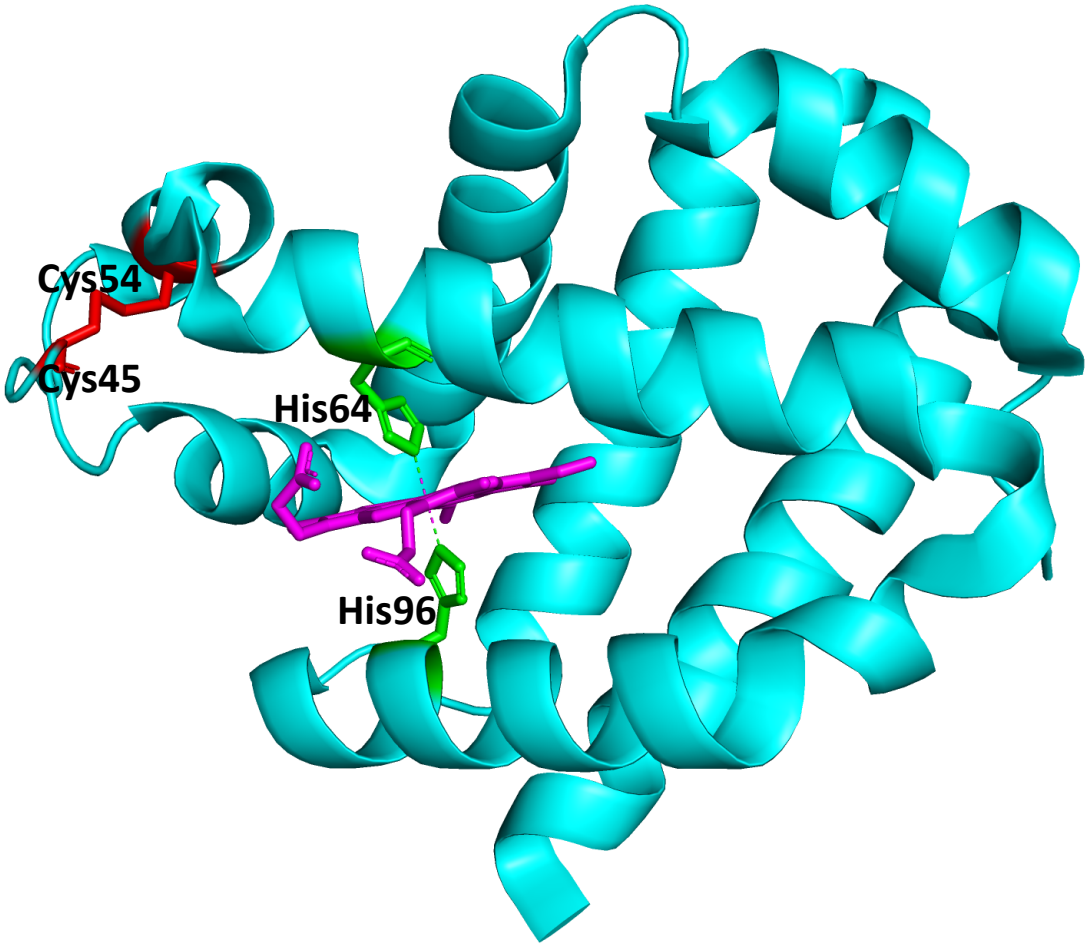

Figure 1.5.1.1. Structure of neuroglobin (PDB ID: 4MPM). Neuroglobin structure generated by PyMol molecular graphics software Showing the proximal and distal coordination sites along with the cysteine residues involved in intramolecular disulfide bond.

1.5.2 Biochemical and functional roles of Ngb

Ngb binds CO in a complex behaviour, which has be characterized as multiphasic binding using flash photolysis suggesting Ngb fluctuates between different conformations, this may due to to modulating effect of the intramolecular disulfide bond between Cys46/55 on the distal His64 (Astudillo et al., 2010, Fago ., 2006). Ngb has a high affinity for NO with low dissociation rate, and ligand binding is competitive depending on the dissociation of distal intrinsic ligand(Van Doorslaer ., 2003). Despite keen interest on study of Ngb, physiological role of this protein is still unclear, proposed roles of Ngb includes that of oxygen delivery to nervous tissues, but high autooxidation rate of Ngb cast doubt on the role of an oxygen carrier (Dewilde *.,* 2001). Like Mb and Hb oxyferrous Ngb performs Nitric Oxide Dioxygenation (NOD), this activity is rapid with a first other rate constant of $360s^{-1}$ (Brunori et al., 2005b, Holmes et al., 2001, Helms et al., 2018). Like Cygb the nitrite reductase activity (NiR), of neuroglobin is modulated by cysteines, this activity is also dependent on displacement of distal histidine by nitrite, as mutation of distal ligand enhances the NiR activity by ~2000 fold (Tiso ., 2011, Tejero ., 2015)

1.5.3 Neuroglobin and Disease

Neuroglobin has been linked to scavenging of reactive oxygen species and hypoxia, the presence of neuroglobin in neuronal tissue have simulated interests in the potential role of neuroglobin as a neuroprotective protein in nervous tissue(Haines et al., 2012, Nayak et al., 2009). Neuroglobin globin has been reported to confer cytoprotection against ischemia in *in vivo* and *in vitro* suggesting a potential cytoprotective role of Ngb (Dietz, 2011, Luyckx *.,* 2018). Ngb is also upregulated in cellular hypoxia hinting Ngb may a have regulatory role against hypoxic insult in neuronal tissues (Terraneo and Samaja, 2017, Zuckerman ., 2017). Studies have also linked

neuroglobin to neurodegeneration and Alzheimer's disease, upregulation of Ngb have been linked with the progression of Alzheimer's disease (Sun et al., 2013, Fiocchetti *.,* 2017)

1.6 Structure and function of Cytoglobin

*1.6.1Cytoglobin a low abundance vertebrate globin with ubiquitous expressio*n

Cytoglobin (Cygb) is a vertebrate co-discovered in 2001 by Kawada . as a stellate cell activation protein (STAP) due to the activation of Cygb in stellate cells, a crucial step in liver fibrosis, and as cytoglobin by Burmester *et a*l., due to expression in all tissue types. It was also re-discovered and mislabelled as histoglobin by Trent et al., in 2002, although only the term Cygb is now used for this protein(Kawada et al., 2001, Burmester ., 2002, Trent Iii and Hargrove, 2002). Cygb is expressed in a wide array of tissues (Burmester ., 2002), in contrast with early members of the human Hb family (Mb and erythrocyte Hb), with well-defined physiological roles, the physiological function of Cygb *in vivo* is not clearly understood. Cygb is a low expression protein, broadly expressed in connective tissues and fibroblasts, but have higher expression levels in the brains, eyes, skeletal, and muscle tissues (Shigematsu et al., 2008b). As opposed to Hb and Mb, where the sixth coordination site is vacant in ferric and ferrous oxidation states (high-spin pentacoordinate), the sixth coordination site of Cygb is occupied by an intrinsic histidine (low-spin hexacoordinate) in the absence of external ligands(Pesce ., 2004). Like vertebrate oxygen carriers, Hb and Mb, Cygb can reversibly bind oxygen. However, the physiological role of oxygen binding is still is in doubt due to its low abundance tissues, particularly tissue with minimal metabolic activities making the possibility this function unlikely. Other proposed roles include collagen synthesis and protection against reactive oxygen species (Mathai ., 2020). Cygb may also have a part in cancer therapy resistance, and fibrotic organ disorder (Chakraborty et al., 2014, Motoyama *et a*l., 2014). There has also been popular support for Cygb in conferring protection against oxidative stress by its NiR and NOD activities; this is due to the upregulation of Cygb during cellular hypoxia and oxidative stress(Emara et al., 2010, Li *.,* 2012a). Cygb additionally undergoes lipid-induced conformational changes from hexacoordinate to pentacoordinate species, a property that appears to be unique to Cygb in hemoglobin superfamily;

this activity may serve as lipid transduction signalling pathway against oxidative stress (Reeder et al., 2011b, Beckerson et al., 2015f).

1.6.2 Structural properties of cytoglobin

Like other members of the hemoglobin family Cygb exhibit the 3/3 globin fold, this protein is composed of eight alpha-helices (De Sanctis *et a*l., 2004). However, there are extended N and C terminal regions consisting of 20 amino acids each, these have no known role in function and little to no structural information from crystallographic data, although some alpha helical properties was observed in one structure in the N terminal region (Mathai ., 2020). The heme group is anchored to the protein by His113 (proximal histidine) at the F8 position, like other human hexacoordinate globins (Ngb and Adgb). The distal histidine, His81, occupies the sixth coordination site of the protein effecting competitive ligand binding kinetics (Trent ., 2001, Pesce *.,* 2004).

Crystallographic information of Cygb reveals a homodimer with two intermolecular disulfide bonds and a monomer with two free cysteines (Cys38/Cys83) (Makino ., 2006a, Sugimoto ., 2004) Figure 1.6.2. In the dimeric protein, two monomeric subunits associate by contact of the cysteine pairs on each monomer, enabling two disulfide bond formation across each subunit. Studies have shown that recombinant Cygb is a mixture of monomer and dimer, with monomeric Cygb exhibiting an intramolecular disulfide bond or free sulfhydryl (Sugimoto ., 2004; Beckerson ., 2015). The state of oligomerization of the protein *in vivo* is unknown but presumed to be monomer due to its low concentration in cells (Lechauve *.,* 2010).

As expressed recombinantly in *E. coli*, Cygb is produced as a monomer with an intramolecular disulfide bond, a monomer with free sulfhydryl, dimer, and minor fractions of higher molecular weight oligomers (Lechauve ., 2010). Monomeric Cygb has a cysteine pair (Cys 38, Cys 83), Cys83 located on the E helix same helix as the distal histidine (His81), with Cys83 on the E9

position and His81 on the E7 position. Due to the proximity of Cys83 to His81 formation of an intramolecular bond between these cysteines moves the equilibrium of His81 from the ON position where it is bound to central heme iron, to the OFF position away from the central heme iron. This can lead to modulation of the distal histidine heme coordination dynamics, depending on whether the cysteines form an intramolecular disulphide or not (Lechauve *.,* 2010). This in turn affects the binding of an exogenous ligand to the distal coordinated site and various enzymatic activities as examined further in Chapter 2 of this thesis(Reeder and Ukeri, 2018). Although no crystal structure exists of the monomer with intramolecular disulfide bond, its formation is predicted to create a more compact structure in which the distal histidine is pulled out of the heme plane, making it more accessible to external ligands (Lechauve et al., 2010). Lack of this disulfide bond creates a more relaxed structure, in which the distal histidine is closer to the heme plane coordination site making it less accessible to exogenous ligands (Lechauve et al., 2010; Tsujino et al., 2014).

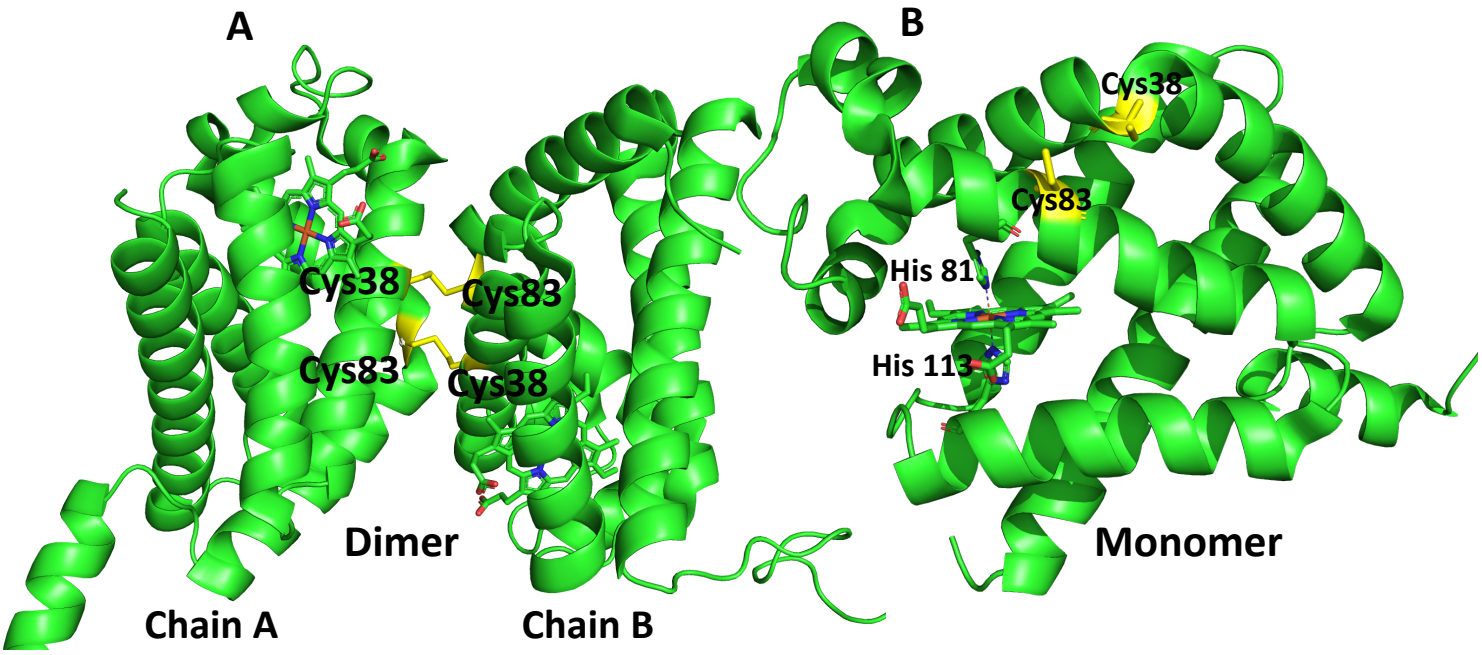

Figure 1.6.2.1. Structure of human cytoglobin (PDB ID: 2DC3) showing the proximal and distal coordination sites along with the cysteine residues in the monomeric unit. (A) Dimeric cytoglobin, (B) Monomeric cytoglobin

1.7 Androglobin a novel chimeric protein in the human globin family

1.7.1 Androglobin is chimeric globin lacking biophysical or biochemical characterizarion

Androglobin (Adgb) is a chimeric protein with a permutated globin domain, the globin domain begins with helices C-H, progresses to an IQ motif then ends with helices A-B. Adgb was first discovered in sea urchin, and later found in 30 metazoan taxa along with 22 vertebrates including humans, this hemoglobin is unusual due to its length of 1667 amino acids (human), with a central globin domain (Hoogewijs et al., 2012). This compares to the 140-160 length of other human globins such as the erythrocyte hemoglobin (Hb) (Perutz, 1960), myoglobin (Mb) and neuroglobin (Ngb) (Trent, Watts and Hargrove, 2001) and the 190-residue length of human cytoglobin (Cygb) with its extended N and C terminal regions (Burmester *.,* 2002). The globin domain of Adgb consists of the typical 8 alpha helical structure (termed A to H) with the 3-on-3 alpha helical fold that encloses the heme moiety. However, highly unusual in the globin family Adgb, is a circularly permuted chimeric globin, an N-terminal calpain-like protease and mainly uncharacterized C-terminal domain sandwich, and a permuted globin domain. A calmodulin-binding IQ motif parts the globin domain placing helices C-H on one side and A-B on the other side (Hoogewijs ., 2012). Previous sequence homology analysis of the flanking regions of the globin domain have yielded no definitive function other than a calpain-like region at the N terminal sequence and an endoplasmic reticulum retention sequence at the C terminus (Hoogewijs *.,* 2012).

crystallographic data has not been obtained for androglobin, clues of about protein assemblage have been obtain sequence analysis, alignment and computation modelling. Androglobin is up made of four domains: (i) The N-terminal calpain-like cysteine protease domain is so-called due to its similarity with human calpain-7. (ii) A circularly permutated globin domain is split in two, sandwiching an internal IQ calmodulin binding motif. (ii) A region with no known domain or motif and (iv) an uncharacterized C terminal domain with an endoplasmic reticulum retention signal. The structure of androglobin is largely unknown, attempts have been to generate possible

structure of the globin domain from sequence analysis as seen in figure 1 and 2 (Hoogewijs ., 2012)

Since its discovery in 2012 very little has been elucidated about the biophysical and biochemical properties of Adgb, or the structural properties of the N and C terminal regions flanking the central heme domain. Hence there have been very little insight into its potential physiological function of the newest member of the hemoglobin superfamily. A knockdown study in cells enhances apoptosis and inhibited proliferation in glioma cell lines, relating to changes in the levels of several protein involved in proliferation (Huang ., 2014). However, there is a complete lack of biochemical and biophysical data with this human hemoglobin. This lack of knowledge is primarily due to the difficulty in generating such a large full-length protein by recombinant techniques and by instabilities of the protein if expressed as only the heme-binding, circularly permuted globin domain.

1.8 New members of the human hemoglobin family

Neuroglobin (Ngb), cytoglobin (Cygb) and androglobin (Adgb) are hexacoordinate human globins, and latter additions to the human hemoglobin family, historically made of pentacoordinate vertebrae respiratory hemoglobin and myoglobin (Burmester et al., 2000, 2002; Hoogewijs et al., 2012). Tissue localization of these hexacoordinate globins are also different from previously discovered hemoglobin and myoglobin. While hemoglobin is localized to circulatory vessels (Dickerson and Geis, 1983) and myoglobin to muscle cells (Wittenberg et al., 1989), cytoglobin is a low abundance protein, expressed in virtually all body tissues (Burmester et al., 2002), neuroglobin is expressed in nervous tissue (Burmester *.,* 2000), and androglobin is predominantly expressed in the testes with a tenfold lower expression in the lungs (Hoogewijs et al., 2012).

1.8.1 New members are hexacoordinate globins

In contrast with pentacoordinate myoglobin and hemoglobin the distal coordination site of hexacoordinate globins are occupied by an endogenous ligand (His 81 for cytoglobin, His 64 for neuroglobin, and Gln 63 for androglobin) in the absence of exogenous ligand (Pesce et al., 2002; De Sanctis et al., 2004). Binding of external ligands therefore proceeds by displacement of the endogenous ligand enabling binding to distal coordination site, leading to competitive ligand binding kinetics (Boron et al., 2015).

Despite the differences in the distal coordination site all globins have overall structural conservation, conservation of the F8 region (proximal histidine) and most have phenylalanine in the CD1 region, to ensure the heme group is stabilized for binding of ligands to distal binding site usually the active site of the heme proteins (Burmester et al.,2014).

1.8.1 Reactivity and additional roles of human hexacoordinate globins

Historically the biological function of human hemoglobins has been oxygen transport and storage (Dickerson et al.,1983). Studies protein expression profile places neuroglobin in nervous tissues, androglobin in the testes and cytoglobin in virtually tissues, positioning hexacoordinate globins outside the traditional location of human globins (Mb: straited muscles and heart, Hb: vasculature), and the expression of the cytoglobin is too low in vasculature to challenge to oxygen delivery capacity of Hb, this has made the oxygen transportation role highly unlikely for hexacoordinate globins (Ascenzi et al., 2013), generating uncertainty about the potential physiological roles of the hexacoordinate members of the human globin family. However, studies on the biochemical properties of these globins have led to proposals on the potential biological functions of these globins.

Potential biological activities of neuroglobin and cytoglobin other than oxygen binding include: cytoprotection for cells against cellular hypoxia or ischemia (Avivi et al., 2010), NO deoxygenase (NOD) (Brunori et al., 2005; Gardner et al., 2010), nitrite reductase activity (NIR) (Tiso et al., 2011; Li et al., 2012), protection against reactive oxygen species also (Burmester and Hankeln, 2009; Singh et al., 2014).

Cytoglobin and neuroglobin are upregulated in cellular hypoxia (Avivi et al., 2010; Emara et al., 2010).

Neuroglobin and cytoglobin may confer cytoprotective functions to cells as reported in earlier studies (Pesce, et al., 2002). In vitro studies of these protein have revealed biochemical NO scavenging is one for the many mechanisms cytoglobin and neuroglobin may carry out their protective function (Liu et al., 2013). NO scavenging activity has been well studied in hemoglobin

and myoglobin, (Azarov et al., 2005; Kamga, Krishnamurthy and Shiva, 2012). Myoglobin is thought to scavenge NO as a cytoprotective mechanism against mitochondria damage due the inhibitory effects of NO against terminal oxidases in the electron transport chain (Kamga et al., 2012). NO activity of cytoglobin has been linked to regulation of vascular tone through the action of soluble guanylyl cyclase, the only known receptor of NO (Liu et al., 2017).

$$Fe^{2+}– O_2 + NO \rightarrow Fe^{3+} — ONOO^- \rightarrow Fe^{3+} + NO_3$$

Equation 1

Like Hb and Mb, oxyferrous cytoglobin and neuroglobin reduces nitric oxide to nitrate with cytoglobin and neuroglobin oxidized to ferric protein (equation 1), the reaction including an intermediate step where peroxynitrite is bound to the ferric iron. (Tiso, J. Tejero, et al., 2011; Li et al., 2012; Ascenzi et al., 2013). The nitric oxide dioxygenase activity of cytoglobin and neuroglobin are modulated by the oxygen levels, at hypoxic or ischemic conditions nitrite is reduced and nitric oxide is produced, this mechanism is thought to be a regulatory response through NO homeostasis in hypoxic/ischemic conditions (Tiso, J. S. Tejero, et al., 2011; Liu et al., 2013).

$$Fe^{2+} + NO^{2-} + H^+ \rightarrow Fe^{3+} + NO + OH^-$$

$$Fe^{3+} + NO \rightarrow Fe^{3+}–NO$$

Equation 1.2

Ferrous cytoglobin and neuroglobin reacts with nitrite (equation 1.2) reducing it to NO and hydroxide. This mechanism is thought to be a mechanism in which NO acts as a signalling

molecule for soluble guanylyl cyclase activation, which helps in vasodilation to enable cells cope in hypoxic or ischemic conditions (Li et al., 2012).

The peroxidase activity is also another potential cytoprotective mechanism of cytoglobin and neuroglobin, these proteins have been reported to be up regulated in the presence of peroxide, this mechanism has been well studied in hemoglobin and myoglobin but the potential role invivo is not well understood (Beckerson et al., 2015a; Beckerson et al., 2015b; ;Tejero et al., 2016)

$$P\text{-}Fe^{2+} + H_2O_2 \rightarrow Protein\text{-}Fe^{4+}{=}O_2\text{-} + H_2O$$

Equation 1.3

$$P\text{-}Fe^{3+} + H_2O_2 \rightarrow P^{\bullet+}\text{-}\ Fe^{4+}{=}O2\text{-} + H_2O$$

Equation 1.4

Where P represents protein and $P^{\bullet+}$ a protein cationic radical

Cytoglobin and neuroglobin reacts with hydrogen peroxide in a two-electron oxidation/reduction reaction in which the protein is oxidized, and hydrogen peroxide is reduced to water (Equation 1.3 and Equation 1.4), (Svistunenko, 2005; Gumiero et al., 2011). The reaction ends with an oxyferryl heme group in both proteins with the formation of water. In redox reaction of ferric protein (Equation 1.4) a protein bound free radicals formed (Beckerson, Svistunenko, & Reeder, 2015b; Gibson, Ingram, & Nicholls, 1958). This reaction has also been widely studied in hemoglobin and myoglobin (Alayash et al., 2004; Gibson et al., 1958; Reeder et al.,, 2005).

Change of heme coordination due to interaction of cytoglobin with lipids like oleate has also been reported (Reeder et al., 2011), though this process is not fully understood structural changes due to interaction of protein with lipids changes the coordination of the protein form low spin hexacoordinate state to high spin pentacoordinate state, and this change in cytoglobin has only been observed in the monomer with intramolecular disulphide bond (Beckerson et al., 2015). The redox state of this intramolecular disulphide bond modulate the binding of exogenous ligand to the distal binding site in monomeric cytoglobin, due the presence of a cysteine residue in the E helix with the distal histidine, it is believed that formation of an intramolecular disulphide bond create a compact structure, which pulls the E helix and consequentially the distal histidine away from the distal binding site allowing access to external ligand (Lechauve et al., 2010; Tsujino et al., 2014). With this bond absent the protein has a relaxed structure, the E helix is relaxed and the distal histidine is closer to the distal coordination site limiting access to external ligand (Lechauve et al., 2010; Tsujino et al., 2014).

Androglobin expression has been associated with post meiotic stages of spermatogenesis with increased expression in fertile males in contrast with infertile male testes, these difference in tissue expression might highlight potential functions of these protein (Hoogewijs, Ebner, et al., 2012). Androglobin, cytoglobin and neuroglobin have all been implicated in cancer pathology ((Chen, Zhao and Meng, 2014; Huang et al., 2014; Zhang et al., 2017). Androglobin and neuroglobin have both been linked with malignant proliferation in nervous tissues with a knockdown of this protein having the opposite effect with the latter being a potential independent prognosis marker due to its over expression in glioma tissues in contrast with normal brain tissues (Huang et al., 2014; Zhang et al., 2017). Cytoglobin plays a dual role in cancer pathology by acting as an inhibitor and promoter of malignancy (Fang et al., 2011). Cytoglobin chromosomal region 17q5 has been reported to be lost in many malignancies (Presneau et al., 2005), with the presence of cytoglobin acting as a tumour suppressant in these malignant tissues (Shivapurkar

et al., 2008). Cytoglobin over expression inhibited cell proliferation and invasion in cultured ovarian cancer cell lines, it also had inhibitory effects in breast, and lung cancer cell line (Shivapurkar et al., 2008; Chen et al., 2014). Cytoglobin acts as a cytoprotectant against oxidative stress and cellular hypoxia/ischemia, this also desensitizes tumour cell against and radiation and oxidative stress used in cancer therapy, making tumour cell cancer therapy resistant (Fang et al., 2011). Cytoglobin is upregulated in malignant tissues, to provide a coping mechanism against oxidative stress, this may serve as a biomarker for cancer diagnosis (Bholah et al., 2015). The role of cytoglobin in cancer therapy resistance may also be a contributory factor to tylosis with oesophageal carcinoma (McRonald et al., 2012).

Chapter 2

Modulating effect of cysteines and disulphide bond formation on the nitrite reductase and nitric oxide dioxygenase activity of cytoglobin

2.1. Introduction

Cytoglobin (Cygb) is a hexacoordinate globin ubiquitously found in the cells of vertebrate (Burmester ., 2002) (Pesce, 2002). There have been numerous suggested physiological functions of Cygb including oxygen sensing (Pesce ., 2002)(Pesce et al., 2002), peroxidase activity (Beckerson et al., 2015a, Ferreira et al., 2015, Lv et al., 2008), lipid peroxidase activity (Ascenzi et al., 2013, Reeder et al., 2011a, Tejero et al., 2016a), scavenging of reactive nitrogen species such as nitric oxide (NO) (Gardner et al., 2010, Halligan et al., 2009a) and scavenging of reactive oxygen species (Fordel et al., 2006, Latina et al., 2016, Ostojic et al., 2008). Nevertheless, the true cellular function (or functions) of Cygb remains unclear. Neuroglobin (Ngb) is a globin similar to Cygb found in high concentrations in neurons (Burmester et al., 2000b) and retinal tissue (Rajendram and Rao, 2007). Both Ngb and Cygb have been proposed to function in NO regulation through NO dioxygenase (NOD) activity (Gardner et al., 2010, Jin et al., 2008, Singh et al., 2013, Van Doorslaer et al., 2003, Zara et al., 2013). In addition to being scavenged by Ngb and Cygb, NO can be generated under conditions of hypoxia, a property particularly noted for Ngb (Jayaraman et al., 2011, Li et al., 2012b, Nicolis et al., 2007, Petersen et al., 2008, Tejero et al., 2015b, Tiso et al., 2011a). Hence it has been proposed that hexacoordinate globins such as Ngb and Cygb under normoxic conditions functions as a NO dioxygenase (NOD) to scavenging NO (Equation 2.1.1) but under hypoxic conditions the globin may switch its function to that of a nitrite reductase (NiR), generating NO (Equation 2.1.2). Therefore, the ferrous protein may serve to protect the functions of NO sensitive redox enzymes such as the terminal oxidase in the electron transport chain by consuming NO (Brittain et al., 2010, Burmester and Hankeln, 2009, Singh et al., 2013) and generate NO to facilitate vasodilation and increased blood flow to the hypoxic tissue (Tejero et al., 2015b, Tiso et al., 2011a).

$$Fe^{2+}\text{-}O_2 + NO \rightleftharpoons Fe^{3+}\text{-}ONOO^- \rightarrow Fe^{3+} + NO_3^- \qquad \text{Equation 2.1.1}$$

$$Fe^{2+} + NO_2^- + H^+ \rightarrow Fe^{3+} + OH^- + NO \qquad \text{Equation 2.1.2}$$

The high autoxidation rate of Ngb casts doubt on the role for Ngb homeostasis *in vivo* (Fago et al., 2004). In contrast, the autoxidation rate of Cygb is low and, in combination with the rapid reduction of Cygb by ascorbate, cytochrome b5 and NADH, promoting the view that the oxidation state of the heme iron *in vivo* is normally ferrous (Amdahl et al., 2017, Gardner et al., 2010, Liu et al., 2012b). The NOD activity of Cygb has previously been shown to be high in rat aorta cells with overexpressed protein and proposed to be a key component in determining the magnitude of the NO response in the vasculature (Halligan et al., 2009a). Additionally, the co-localisation of Cygb with neuronal NO synthase in the brain strongly supports a link between Cygb and NO metabolism (Reuss et al., 2016), as does the protection of Cygb against hepatocyte damage during inflammation (Van Thuy et al., 2017) and the angiotensin-mediated hypertension in aortic smooth muscle cells (Liu et al., 2017a). Knockout of Cygb in mice prolongs NO decay in aortic cells and that NO metabolism in vascular smooth muscle regulates NO flux (Liu et al., 2017a). Taken together, these studies strongly suggest that Cygb is a major pathway of NO metabolism.

The maximal observed rate of human Cygb NOD activity was measured at 430 s^{-1} with no discernible effect of NO concentration between 10 μM and 30 μM (Smagghe et al., 2008). The NiR activity of human Cygb under anaerobic conditions have also been reported. One study has reported no NiR activity for Cygb (Petersen et al., 2008), whilst others have reported some NiR activity of Cygb with rates of reaction that are comparable with other globins such as Ngb and the T (tense) state of human hemoglobin (~0.12-0.14 $M^{-1}s^{-1}$) (Huang et al., 2005, Li et al., 2012b). The reported rate of Cygb NiR activity is an order of magnitude slower than other globins such as myoglobin and the R (relaxed) state of hemoglobin (2-6 $M^{-1}s^{-1}$) (Huang et al., 2005). Consequently, the proposal that Cygb may function as a NiR has not gained support as a potential function of the protein *in vivo*.

The surface exposed cysteines of human Ngb and Cygb can form intramolecular disulfide bonds and are important for the ligand binding and enzymatic properties of both proteins (Astudillo et al., 2013b, Beckerson et al., 2015a, Beckerson et al., 2015e, Tejero et al., 2016a, Tsujino et

al., 2014a). The effect of cysteine oxidation on the NiR activity of Ngb is limited, exerting a twofold decrease in NiR activity with reduced disulfide compared to the protein with an intramolecular disulfide (Tiso et al., 2011a). The intramolecular disulfide bond of Ngb is positioned on the CD loop of the protein structure, but the intramolecular disulfide bond of Cygb spans two adjacent α helices; Cys38 on helix B and Cys83 on helix E. Cys83 is close to the heme iron distal histidine (His81), potentially affecting the distal heme pocket structure depending on the oxidation state of the cysteines. Following generation of the protein by recombinant methods, three forms of Cygb can exist depending on the oxidation state of the cysteines: (i) $dimer_{S\text{-}S}$, where the cysteines form an intermolecular disulfide bond, producing a homodimer (ii) $monomer_{S\text{-}H}$, where the cysteines are reduced, forming a monomer with free sulfhydryls and (iii) $monomer_{S\text{-}S}$, where the cysteines form an intramolecular disulfide on the same protein chain. The $monomer_{S\text{-}S}$ form of the protein behaves significantly different to the $dimer_{S\text{-}S}$ and $monomer_{S\text{-}H}$ forms of the protein. This includes changes in ligand binding properties (Beckerson et al., 2015a), switching of the ligand migration pathway (Astudillo et al., 2013b) and lipid-induced heme iron coordination changes (Ascenzi et al., 2013, Beckerson et al., 2015e, Tejero et al., 2016a). We have reported that this effect on the redox chemistry of the globin is related to an alteration of the distal histidine off-rate (His_{off}) by over 600-fold in the $monomer_{S\text{-}S}$ form of the protein compared to other forms of Cygb (Beckerson et al., 2015a). However, the NO consumption as a function of oxygen concentration is only marginally affected by the oxidation state of the cysteines (Zhou et al., 2017).

Here we have re-examined the capacity of recombinant human Cygb to act as NiR and NOD enzymes as a function of the oxidation state of the surface exposed cysteine residues. The oxidation state of the cysteines showed no discernible effects on the NOD activity of Cygb, the reaction being complete within the dead-time of the stopped-flow instrument. However, the oxidation state of the surface cysteines affected the kinetics of the relaxation of the protein from pentacoordinate to hexacoordinate (bis-his) states, exhibiting moderately higher rates of relaxation with the free sulfhydryl over that of the $monomer_{S\text{-}S}$ and $dimer_{S\text{-}S}$ forms. The effect of

the oxidation state of the cysteines does, however, exert a considerable effect on the NiR activity of Cygb. The second-order rate constant of the NiR activity of Cygb in the $dimer_{S\text{-}S}$ or $monomer_{S\text{-}H}$ states are similar to the low NiR activities previously reported for Cygb and Ngb, but the $monomer_{S\text{-}S}$ form of the protein is over 140 times that of the $dimer_{S\text{-}S}$ form and 50 times that of the $monomer_{S\text{-}H}$ form. These rates are greater than those previously reported for vertebrate globins such as myoglobin and the R state of hemoglobin.

2.2 Materials and Methods.

2.2.1 Materials

Aminoleuvelinic acid and Isopropyl β-D-1-thiogalactopyranoside (IPTG) were purchased from Molekula ltd, UK. Proli-NONOate was purchased from Cayman chemicals, UK. Luria Bertani media was purchased from Melford Laboratories Ltd, UK. Carbon monoxide was purchased from BOC gasses, UK. Tris(2-carboxyethyl)phosphine (TCEP), sodium tetraborate, sodium phosphate (disodium hydrogen orthophosphate and sodium dihydrogen orthophosphate), kanamycin sulfate, sodium imidazole, sodium nitrite and sodium chloride were purchased from Sigma-Aldrich, UK.

2.2.2 Recombinant human cytoglobin expression and purification

Cygb plasmid was constructed from a pET28a inducible vector with the Cygb gene added as a cassette (Origene) with an N terminal cleavable his-tag as previously described (Reeder et al., 2011a). Cygb plasmid was transformation to competent BL21 DE3 *E.coli* cells using heat shock method (42 °C, 90 s), transformed cells were incubated at 37 °C, in solid agar medium in petri dishes overnight. Cygb was expressed by selecting distinct *E.colii* colonies which were cultured in Luria Bertani media containing 50 μg ml^{-1} kanamycin sulfate at 37 °C, in shaking incubator at 120 rpm. Cygb production was induced when optical density of cells was 0.8-1.0 at 600 nm by addition of 500 μM of IPTG. Aminoleuvelinic acid (250 μM) and ferric citrate (50 μM) were added to facilitate heme production. The flasks were bubbled with CO for ~30 s and flasks sealed and incubated overnight at 37 °C, 100 rpm. Cells were harvested by centrifugation (4000 g, 4 °C, 25 min) and cells frozen at -20 °C for storage. Cells were defrosted and lysed by pressure homogenization using an Avestin C3 emulsiflex (15000-20000 psi, two cycles). Cell debris was removed by centrifugation (22000 g, 4 °C, 20 min) and supernatant adjusted to 20 mM sodium phosphate buffer containing 150 mM NaCl and 20 mM imidazole pH 7.4. Hig-tagged protein was

bound to an immobilised metal affinity column (nickel IMAC, 5 ml, GE healthcare), washed with 20 mM sodium phosphate buffer containing 150 mM NaCl and 20 mM imidazole and eluted using 20 mM sodium phosphate buffer containing 500 mM imidazole. Imidazole was removed by dialysis (3 kDa cut-off) against a 5000 ml sodium tetraborate buffer (1 mM, pH 9.5) with at least three buffer exchanges. His tag was cleaved by incubation with the protease thrombin (Sigma-Aldrich, UK) overnight at room temperature with gentle mixing (5 units per mg Cygb). His-tag free Cygb was purified as before using IMAC column using 20 mM imidazole to elute the tag-free protein. Imidazole was removed by dialysis, and protein concentrated using a Whatman centrifuge concentrator (3 kDa cut-off) and stored at -80 °C.

Monomeric and dimeric Cygb were separated by Sephadex G75 column (600 mm x 16 mm) using a GE Healthcare Akta Prime as previously described (Beckerson et al., 2015d, Beckerson et al., 2015a, Beckerson et al., 2015e). The oligomeric sate of the proteins was verified by non-reducing PAGE gel (4 % stacking and 10 % resolving), the protein samples were incubated with the sample buffer (containing 2 % SDS) at room temperature for 1 h, The gels were run at 100 V for 150 min and the tank was kept on ice. Monomeric protein with free sulfhydryl was generated by adding TCEP (5mM) at room temperature for 1 h before removal using a Sephadex G25 column (5x1 cm, GE healthcare). A double cysteine to arginine mutation of Cygb (Cys38Arg/Cys83Arg) was generated by sequential site directed mutagenesis using primers synthesised by Eurofins Scientific, UK, mutagenesis was performed using the Agilent Quikchange II protocol. The polymerase chain reaction (PCR) mix contained: 50ng template DNA, 125ng of each primer (forward and reverse), 3 µL dimethyl sulfoxide (>98% DMSO), 10 mM dNTP mix, 1x *pfu* buffer (Agilent) and 1.5 units *pfu* turbo DNA polymerase (Agilent), using ultrapure H_2O to bring total volume to 50 µL. Sequences were confirmed by Sanger sequencing (GATC Biotech, Germany) following transformation of PCR product into XL1Blue cells and plasmid purification (Qiagen, UK).

2.2.3 Measurement of nitrite reductase and nitric oxide dioxygenase activity

Cygb (5 μM) was reacted with sodium nitrite (0-20 mM) in 0.1 M sodium phosphate buffer pH 7.4 in the presence of ~5 mM sodium dithionite. Dithionite was added immediately prior to nitrite addition to minimise the slow reduction disulfide (Beckerson et al., 2015e). Optical spectra were recorded using an Agilent 8453 diode array spectrophotometer fitted with a multi-cell carriage and temperature control. Rate constants were determined from the time courses Cygb (416 nm- 430 nm) by fitting to exponential functions using the least squares method using Microsoft Excel or Synergy KaleidaGraph.

Cygb (10 μM) in oxygenated 0.1 M sodium phosphate buffer pH 7.4 was reduced to oxyferrous Cygb by addition of 5 mM sodium ascorbate and left for at least 15 minutes to reduce. Complete reduction was checked spectrophotometrically using an Agilent Cary 50 spectrophotometer. Sodium phosphate buffer (pH 7.4, 0.1 M) was degassed using a glass tonometer connected to a supply of argon gas and a vacuum pump via a custom build glass tap system to allow repeated degassing cycles. The degassed buffer was transferred anaerobically to a 10 ml glass syringe. Proli-NONOate was prepared in 25 mM sodium hydroxide to a concentration of 40mM and then purged with argon gas. Proli-NONOate was transferred using a glass Hamilton syringe to the degassed buffer (10-100 μM), under these conditions the Proli-NONOate degrades to generate two molecules of NO. The Oxyferrous Cygb was mixed rapidly with degassed buffer containing in a 1:1 ratio using an Applied Photophysics SX20 stopped-flow spectrophotometer pre-cooled to 11 °C.

2.3 Results

2.3.1 Identification of cytoglobin monomer and dimer by size exclusion chromatography and SDS PAGE

Cytoglobin can exist as a monomer with an intramolecular disulfide bond intramolecular disulfide bonds between Cys38 and Cys83 of a single chain ($monomer_{S\text{-}S}$), a monomer with free sulfhydryl ($monomer_{S\text{-}H}$) or a dimer with an intermolecular disulfide bond between Cys38 of one chain and Cys83 of another ($dimer_{S\text{-}S}$). The fractions of Cygb as dimer and monomer were isolated through size exclusion chromatography (SEC, Sephadex G75). Two major peaks were observed by SEC (Figure 2.3.1.1) eluting at 55 ml and 65 ml for the dimer and monomer respectively. A smaller fraction of higher weight Cygb polymers are observed at <51 ml elution volume. The oligomeric state of the fractions was additionally confirmed by non-reducing SDS-PAGE (Figure 2.3.1.2). The proteins could be seen as a band ~ 40 kDa representing the $dimer_{S\text{-}S}$ and a band ~ 20 kDa representing the monomer. Some monomer was also apparent with the dimer, presumably from cystine reduction prior or during to electrophoresis. This disulphide reduced $monomer_{S\text{-}H}$ does not migrate the same as $monomer_{S\text{-}S}$.

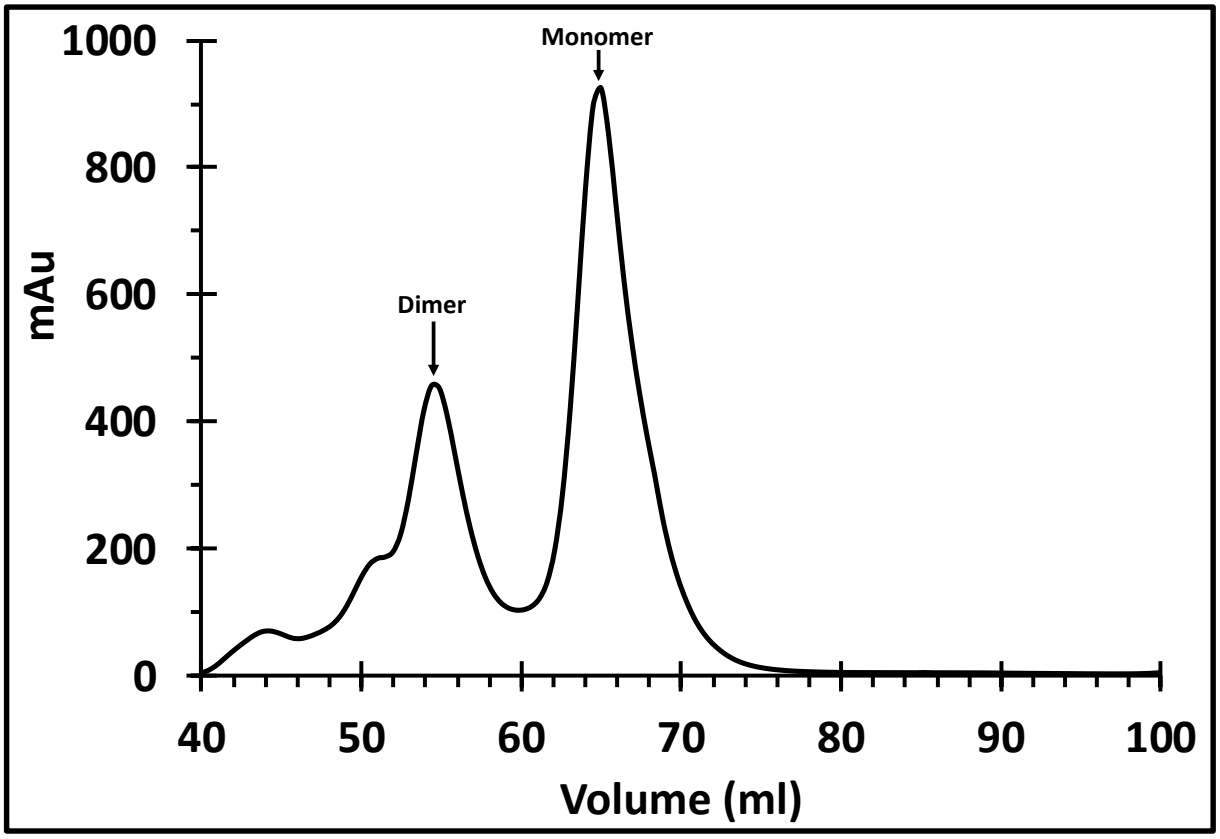

Figure 2.3.1.1 Size exclusion chromatography of recombinant Cytoglobin. The size exclusion column (G-75) elution profile at 280 nm shows 3-4 peaks, with the first smaller peaks at ~45 and 51 ml election volume represents a small fraction of polymerised or aggregated Cygb. The peak at 55ml elution volume represents the Cygb dimer$_{S\text{-}S}$. The final and most prominent peak at ~65 ml elution volume represents the monomer (a mixture of monomer$_{S\text{-}S}$ and monomer$_{S\text{-}H}$).

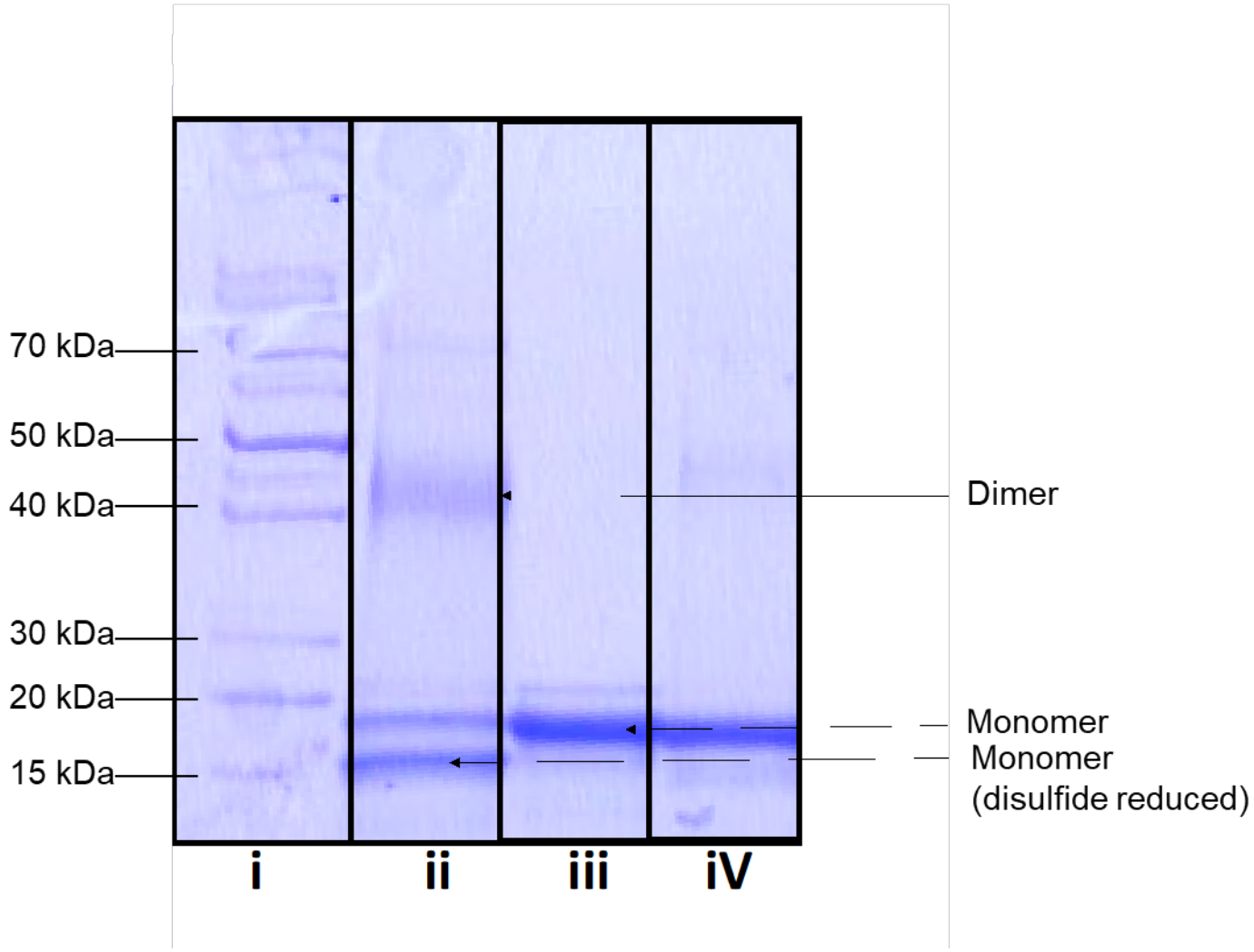

Figure 2.3.1.2. Non-reducing SDS-PAGE of size exclusion column dimer and monomer cytoglobin peaks. Lane (i) ladder side by side with thermofisher 26614 ladder, lane (ii) shows dimeric Cygb (~40 kDa) with also some monomer, lane (iii) monomeric cytoglobin (~20 kDa) and lane (iv) horse heart myoglobin (~17 kDa) for comparison.

2.3.2 Spectral properties of the monomeric and dimeric forms of cytoglobin

Spectra characteristics of monomeric (both $monomer_{S\text{-}S}$ and TCEP reduced $monomer_{S\text{-}H}$) are those of a primarily hexacoordinated globin heme iron in both the deoxyferrous and ferric oxidation states (Figure 2.3.2.1) (Kakar, 2010), due to the presence of two prominent peaks in the alpha and beta region of the visible spectra. This is a feature that indicates an endogenous ligand (the distal histidine, His81) is coordinated to the sixth coordination site of the heme iron. These spectral properties are like other hexacoordinate globins such as Ngb (Dewilde, 2001). The Ferric spectrum of Cygb has a Soret peak of 416nm, with a broad alpha (565nm) and a beta (535nm) region. The addition of a reductant (sodium dithionite) leads to the generation of deoxyferrous species. Reduction leads to a hyperchromic and bathochromic shift in the Soret region from 416nm to 431nm, accompanied by a hyperchromic shift in the alpha/beta bands leading to more defined peaks. The redox state of the cysteines had a minimal impact on the optical properties of the ferric and deoxyferrous spectra. Interestingly the oxyferrous spectra have differences between the $monomer_{S\text{-}S}$ form and other forms of the protein (Figure 2.3.3.1). This is not due to a mixture of ferric and ferrous protein as full reduction by dithionite and rapid re-oxygenation by size exclusion chromatography yields identical oxyferrous spectra.

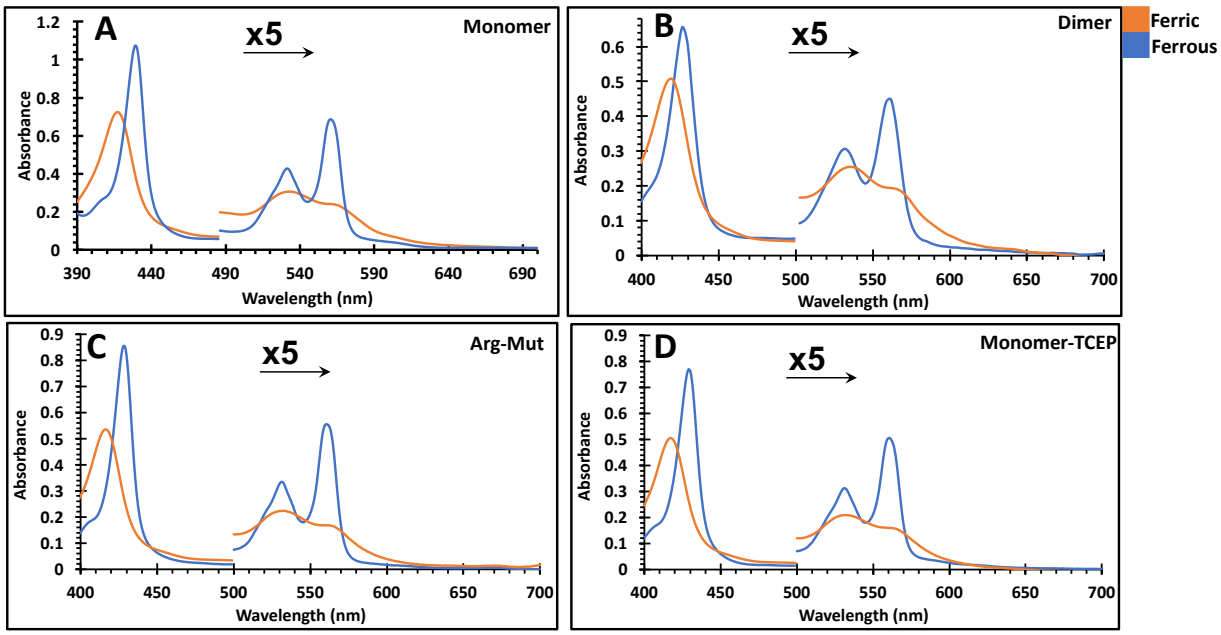

Figure 2.3.2.1. *Optical spectra of monomeric, dimeric, double cysteine arginine mutant and TCEP reduced cysteine cytoglobin*. All proteins were 5μM in 0.1M sodium phosphate buffer (pH 7.4) in the ferric oxidation state (orange) or dithionite-reduced deoxyferrous oxidation state (blue). The spectra of monomeric Cygb (A), dimeric Cygb (B), a double Cys38Arg/Cyg83Arg mutant of Cygb (C) and monomeric Cygb with the intramolecular disulfide bond reduced using TCEP (D). All forms of the protein show classical hexacoordinate heme ligation state in both ferric and deoxyferrous forms.

2.3.3 Effect of disulfide oxidation state on nitrite reductase activity

The reaction of deoxyferrous Cygb with nitrite in the presence of dithionite results in the generation of NO bound ferrous Cygb. The initial and end spectra for the reaction are shown in Figure 2.3.3.1 with all forms of Cygb give essentially identical spectra following nitrite addition, with Cygb final spectra predominantly ferrous-NO due to the presence of dithionite. Following nitrite addition, the optical changes for all forms of Cygb show a hypsochromic shift of the Soret peak from 428 nm to 422 nm, accompanied with decrease in the α and β peaks and an appearance of a shoulder at ~580nm (Figure 2.3.3.2 and 2.3.3.3). However, the kinetics were significantly different with the monomer$_{S\text{-}S}$ exhibiting much faster kinetics compared to the other forms of Cygb (Figure 2.3.3.4). Dimer$_{S\text{-}S}$ Cygb exhibited monophasic reaction kinetics that was fitted to a single exponential function (Figure 2.3.3.5 B) to obtain an observed rate constant (k_{obs}). The monomeric protein showed biphasic reaction kinetics with fast and slow phases (Figure 2.3.3.5 A). Assuming identical optical changes of both forms of the monomeric protein, the protein exhibiting fast reaction kinetics consisted of 86 % of the protein under study, but did show some variation depending on the batch of protein expressed. We interpret this to imply that our monomeric protein was a mixture with an internal disulfide bond (monomer$_{S\text{-}S}$) and free sulfhydryl (monomer$_{S\text{-}H}$). Incubation with dithionite slowly reduces the disulfide as shown in Figure 2.3.3.6 where the amplitude of the fast rate of monomer$_{S\text{-}S}$ decreases as a function of time as the monomer$_{S\text{-}S}$ is converted to slower kinetics of the monomer$_{S\text{-}H}$. Under the conditions of the experiments reported in this chapter, this reduction of disulfide bond resulting from the presence of dithionite was minimal. The Cys38Arg/Cyg83Arg mutant and TCEP reduced kinetics (Figure 2.3.3.5 C and D) where intramolecular disulfides are not possible, the kinetics were monophasic.

The observed rate constant for this reaction with Mb as a function of nitrite concentration showed linear dependence and is presented in Figure 2.3.5.7. The second order rate constant was measured as 2.70 ± 0.19 $M^{-1}s^{-1}$, essentially identical to the previously reported value of 2.9

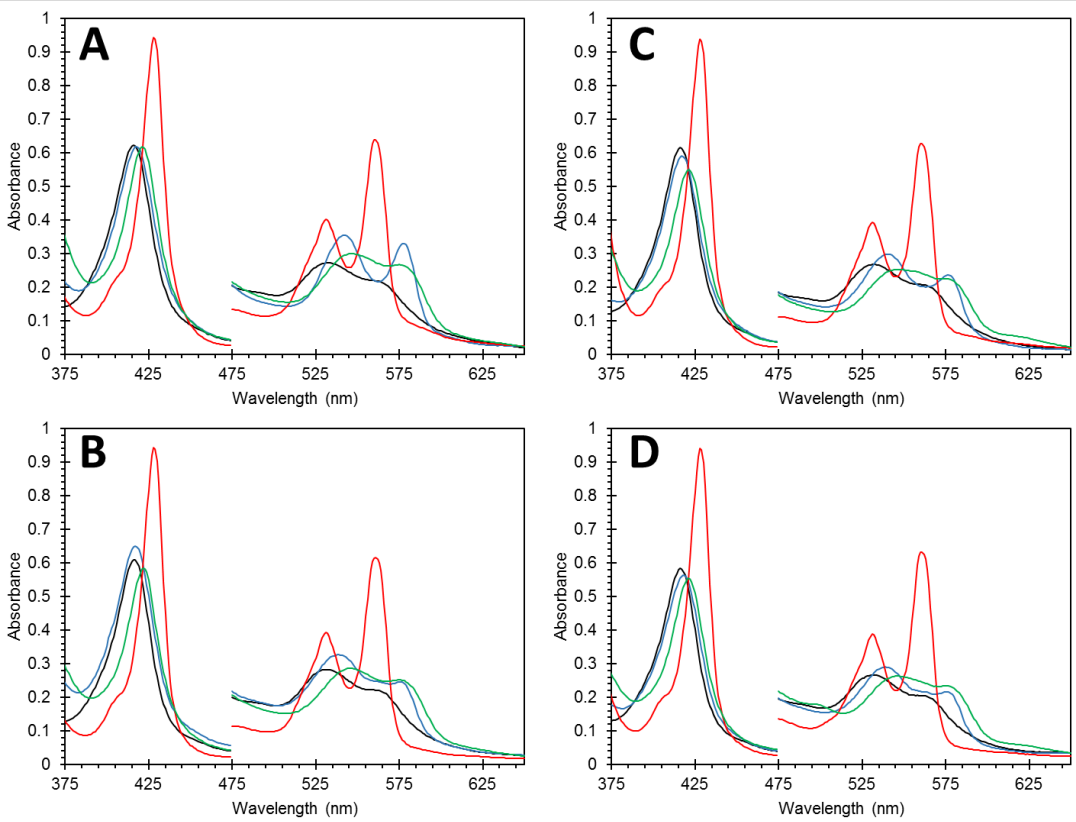

Figure 2.3.3.1. Optical spectra of cytoglobin monomers and dimer. Spectra of cytoglobin monomer with intramolecular disulphide (A), dimer with intermolecular disulphide (B), TCEP reduced monomer with free sulfhydryl (C) and monomer Cys38R/83R mutant (D). Ferric (black line), deoxyferrous (red line), ascorbate-reduced oxyferrous (blue line) and the protein following reaction with nitrite in presnce of dithionite (green line). All proteins were 5μM in 0.1M sodium phosphate buffer (pH 7.4).

$M^{-1}s^{-1}$ under similar experimental conditions (Li et al., 2012b). The rate constant for $dimer_{S\text{-}S}$ Cygb changed linearly as a function of nitrite concentration to yield a second order rate constant of 0.26 $M^{-1}s^{-1}$ ± 0.02 $M^{-1}s^{-1}$ (Figures 2.3.3.7-9). The slow phase from monomer as the slower kinetics, assigned to $monomer_{S\text{-}H}$ form of Cygb were essentially identical to that of the TCEP reduced form of the protein and similar to the C38R/C83R mutant (Figures 2.3.3.7-9). The kinetics of the dominant fast phase of the reaction, assigned to the $monomer_{S\text{-}S}$ Cygb, was nitrite concentration dependent, giving a second order rate constant of 32.3 $M^{-1}s^{-1}$ ± 0.90 $M^{-1}s^{-1}$ (Figures 2.3.3.7 and 2.3.3.9). The monomer from the double cysteine mutant showed second order reaction kinetics of 0.23 $M^{-1}s^{-1}$ ± 0.06 $M^{-1}s^{-1}$, essentially identical to that of the dimeric protein, in line with previously reported NiR rates for Cygb (Li et al., 2012b). The TCEP reduced $monomer_{S\text{-}H}$ Cygb was slightly faster than the dimer and mutant Cygb, giving a second order rate of 0.63 $M^{-1}s^{-1}$ ± 0.05 $M^{-1}s^{-1}$ (Figures 2.3.3.7-9).

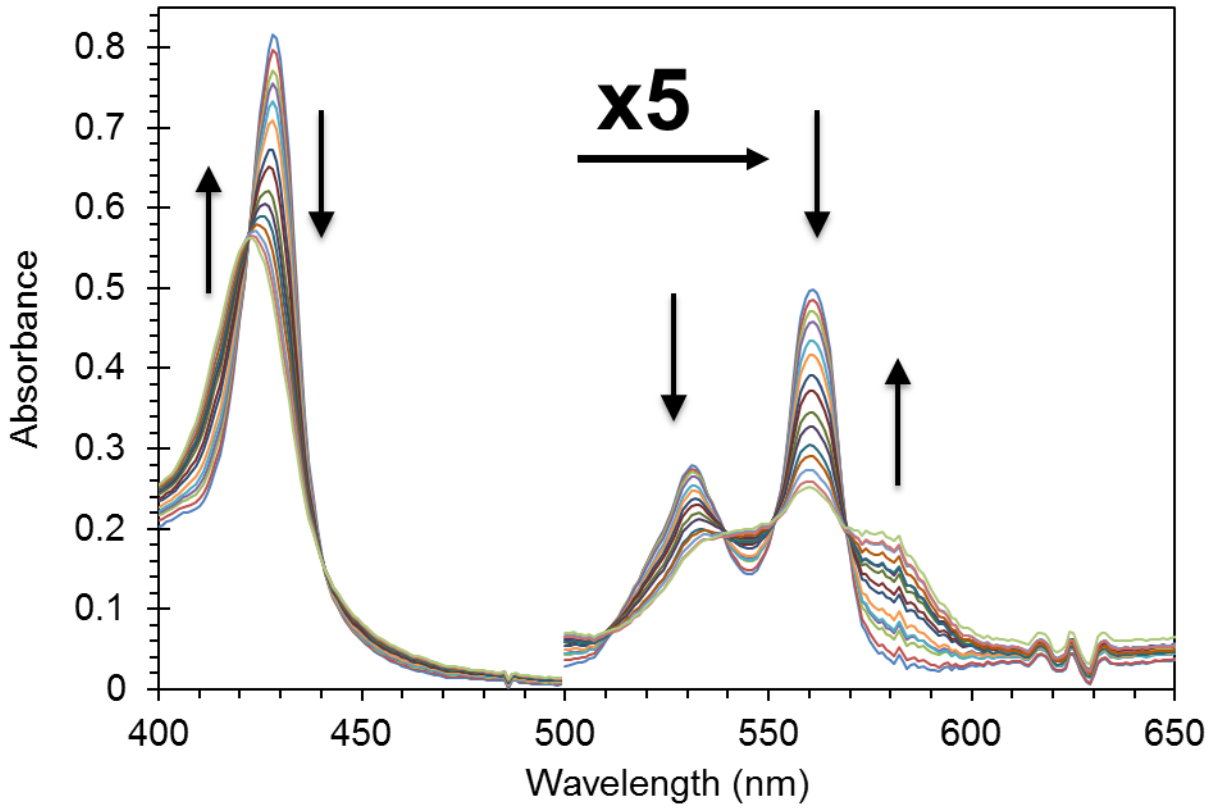

Figure 2.3.3.2 Nitrite reductase activity of cytoglobin showing nitrite-induced optical changes to deoxyferrous-cytoglobin. Experiment was performed in 100 mM sodium phosphate pH 7.4, all proteins were made deoxyferrous by addition of ~5 mM sodium dithionite. Sodium nitrite solution (5 mM) was added to deoxyferrous monomeric Cygb (5 μM) and spectra recorded at 2 s intervals.

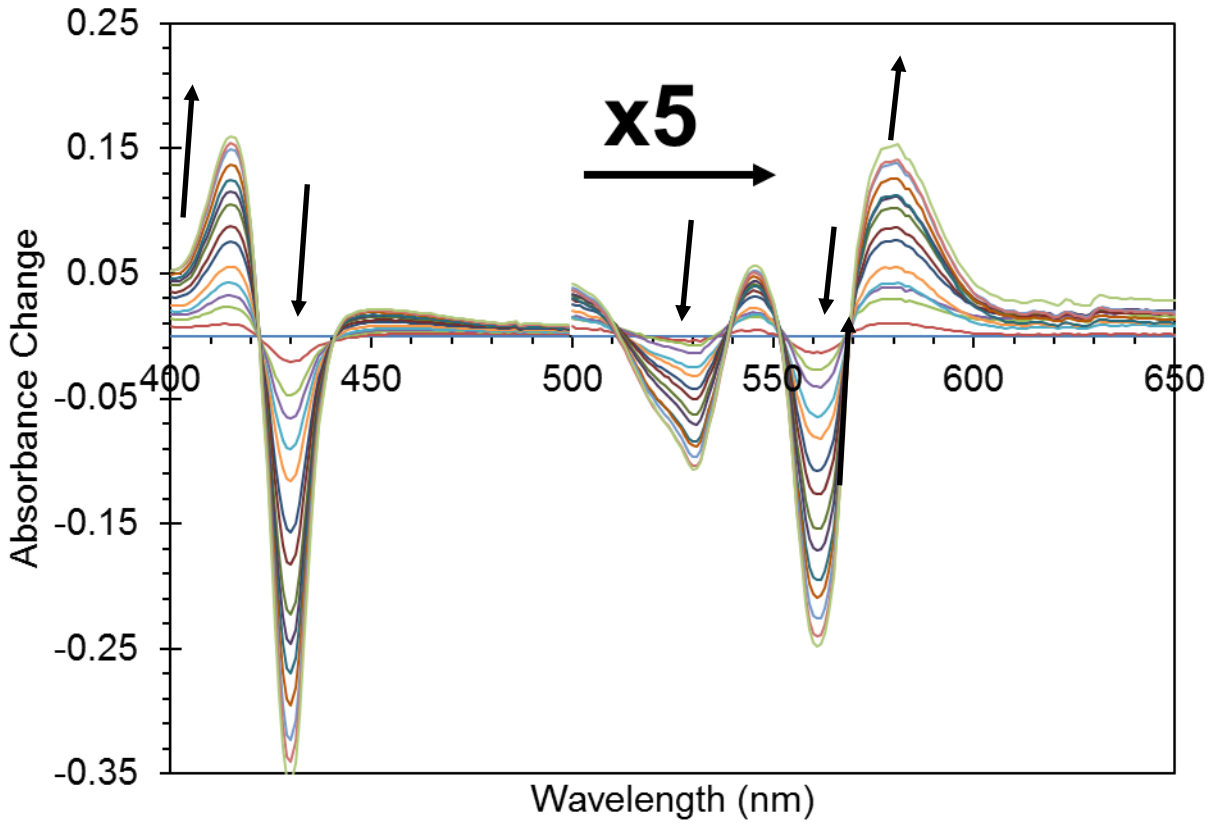

Figure 2.3.3.3 Difference spectra of the nitrite reductase activity of cytoglobin. Spectra from Figure 2.3.3.2 where the spectrum of deoxyferrous protein was removed from all subsequent spectra.

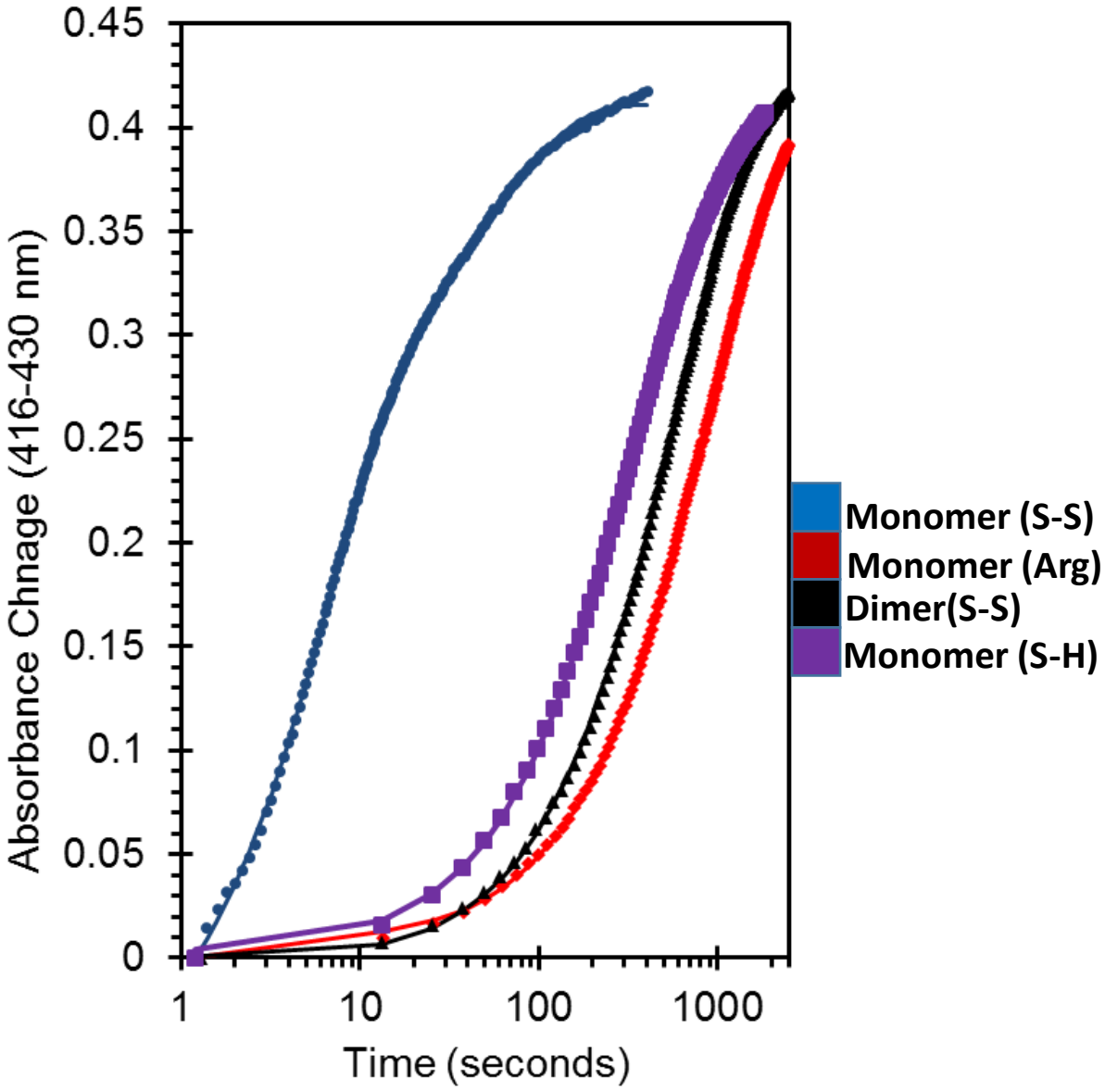

Figure 2.3.3.4. Time course of the nitrite reductase activity of cytoglobin and myoglobin in logarithmic scale. This shows significant differences between the kinetics of the proteins, depending on the redox state of the disulfide bond and oligomeric state. Note that the monomer with intramolecular disulfide ($monomer_{S\text{-}S}$) is two orders of magnitude faster than other forms of the protein.

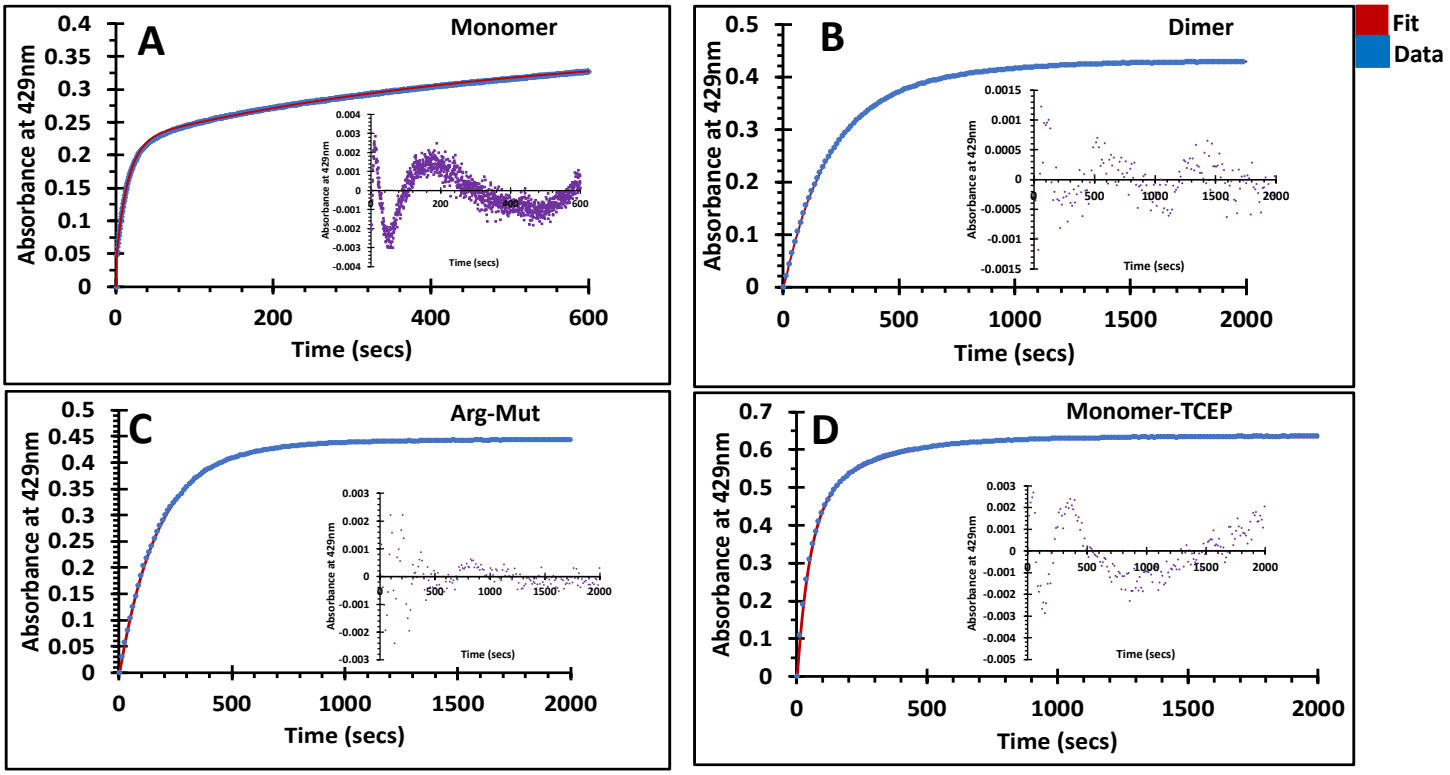

Figure 2.3.3.5 Time course of the nitrite reductase activity at 429nm, of monomeric cytoglobin with intramolecular disulfide. (A), dimeric Cygb (B), cytoglobin double mutant C38R/C83R (Arg-Mut, C) and TCEP reduced cytoglobin (Monomer-TCEP, D). Data points shown in blue. Time courses were fitted using double (A) or single (B, C and D) exponential fits to the data and shown in purple. Inset: Residuals showing accuracy of fit. Reaction was carried with nitrite (3mM) and deoxyferrous Cygb (5 μM) in 100 mM sodium phosphate buffer pH 7.4 at 37 ºC.

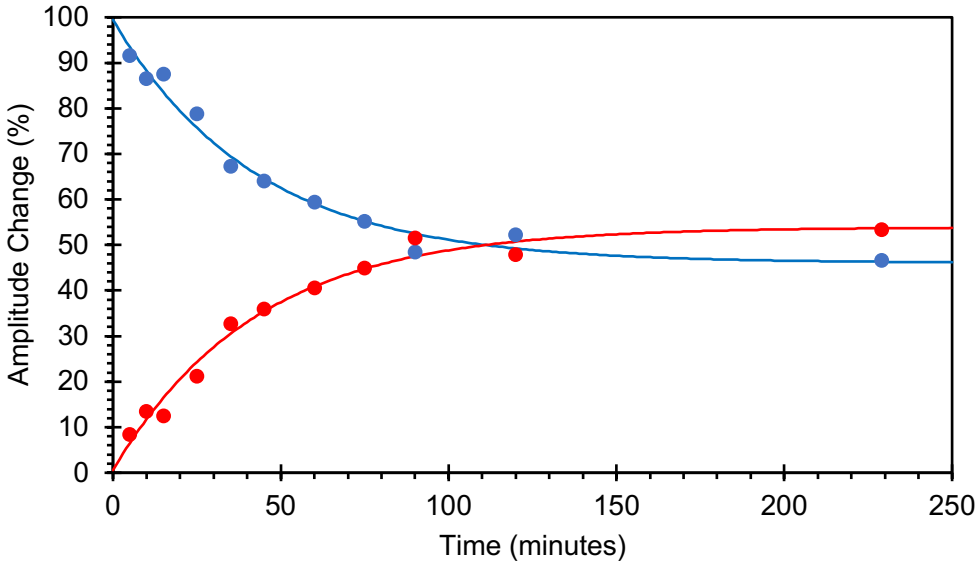

Figure 2.3.3.6. Measurment of dithionite induced reduction of intramolecular disulphide bonds in Monomeric Cygb. Cytoglobin (5 μM) was incubated with dithionite (5 mM) for various times and subsequently mixed with nitrite (10 mM). The changes in amplitude of the fast phase (blue line,) and slow phase (red line,) subpopulations are shown as a function of dithionite incubation time, showing the slow reduction of the disulfide bond. The amplitudes changes were each fitted with a single exponential, $k = 3.92\times10^{-4} \pm 5.8\times10^{-5}$ s^{-1}.

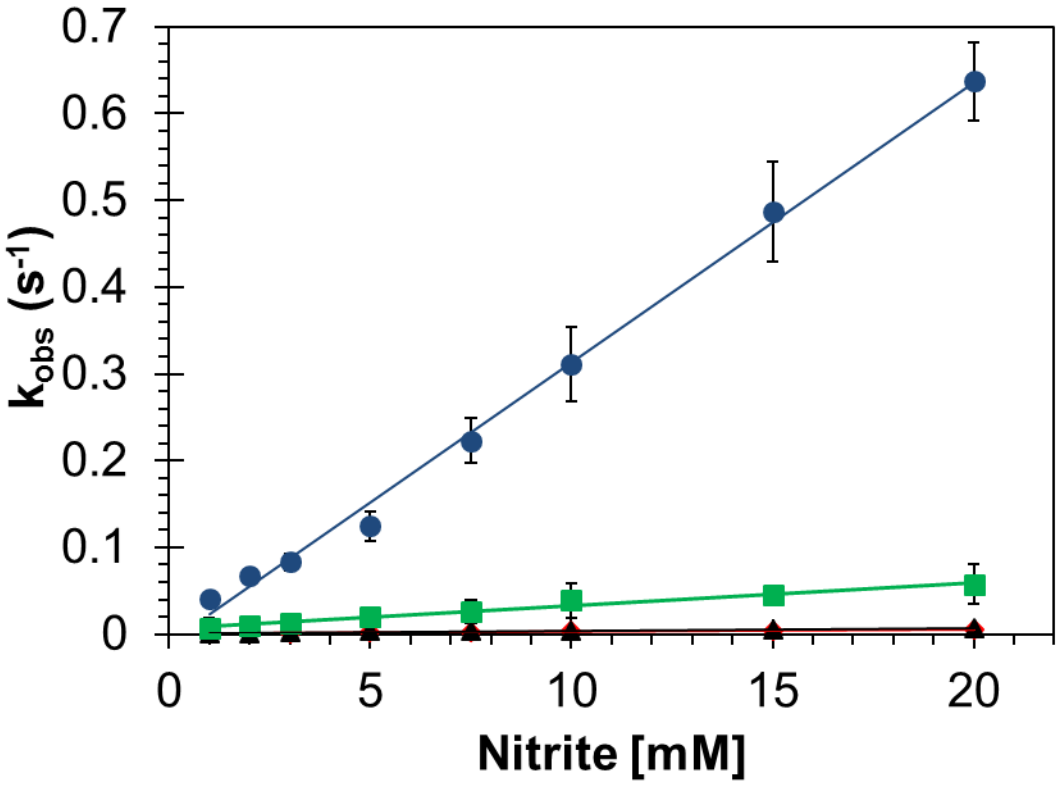

Figure 2.3.3.7. Observed rate constants (ferrous-NO formation) from the reaction of different forms of cytoglobin (deoxy) and nitrite. Monomeric Cygb with intramolecular disulfide (blue), TCEP reduced monomeric Cygb (purple) monomeric Cygb double mutant C38R/C83R (red) and dimeric Cygb with intermolecular disulfide (black). Equine Mb is included for comparison (green)

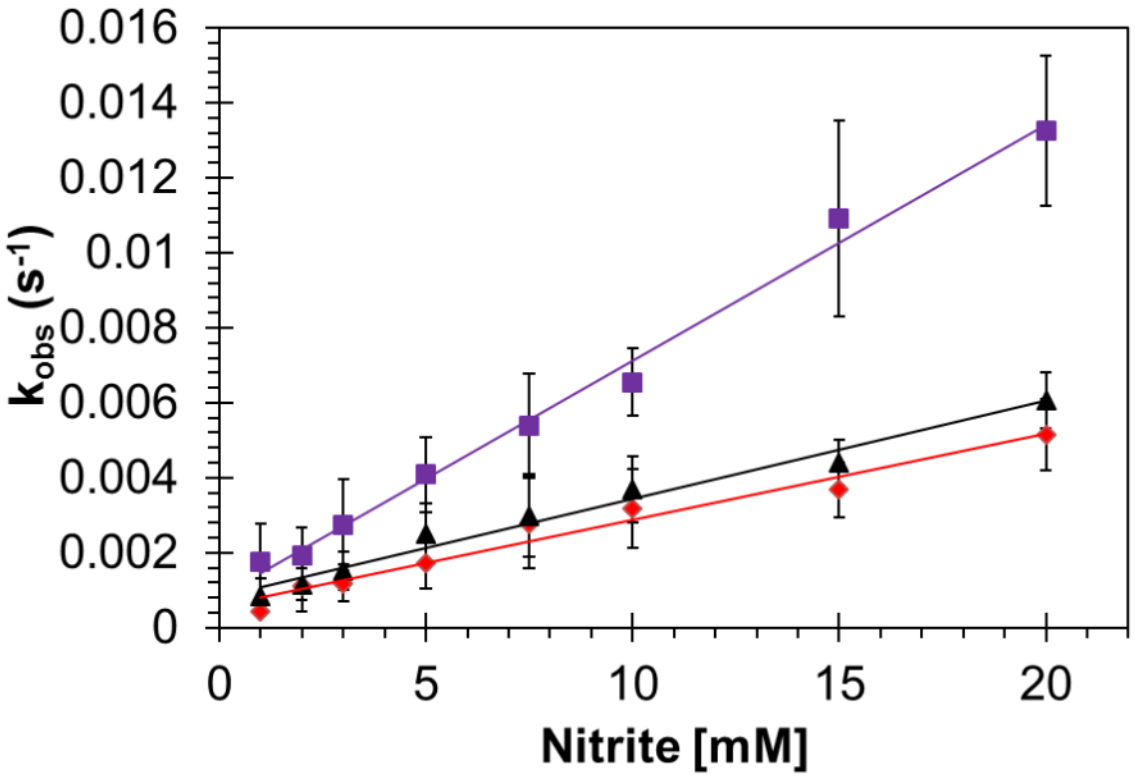

Figure 2.3.3.8. Expansion of observed rate constants (ferrous-NO formation) from the reaction of different forms of cytoglobin showing data for double mutant and dimer.

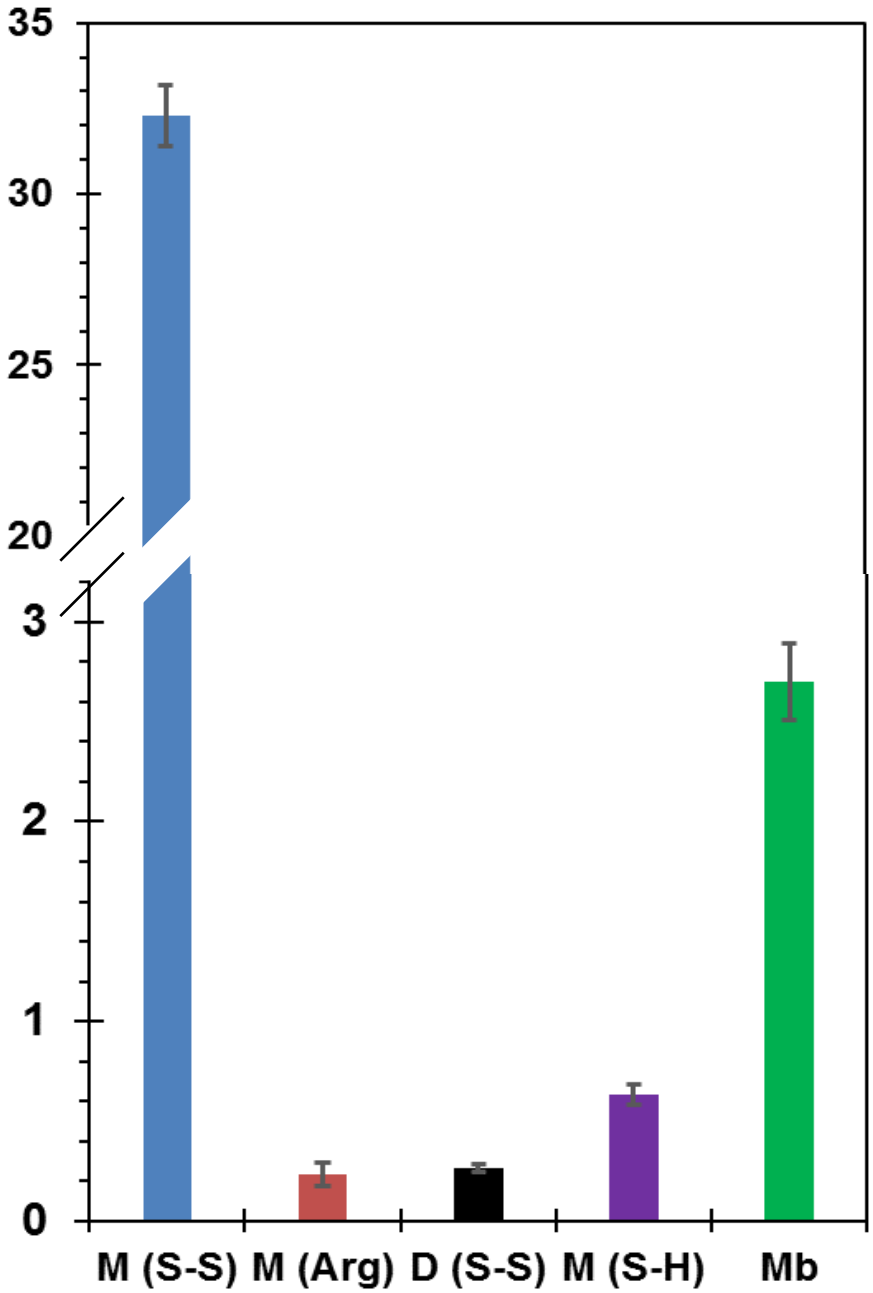

Figure 2.3.3.9. Second order rate constant for the nitrite reductase activity of various forms of cytoglobin. M(S-S); monomer with intramolecular disulfide bond, M (Arg); monomer with no disulfide bond, D(S-S); dimer with intermolecular disufide bond, M(S-H); TCEP reduced monomer with free sulhydryl and Mb; myoglobin.

2.3.4 Effect of disulfide on nitric oxide dioxygenase activity and heme iron coordination

The reaction of NO with oxyferrous Cygb in the monomer$_{S\text{-}S}$ form of the protein is shown in Figures 2.3.4.1 and 2.3.4.2. The reaction of the other forms of the protein exhibited identical optical changes. The initial spectrum, taken <2ms post-mixing, is typical of a mixed spin ferric Cygb with the heme iron partially hexacoordinate but primarily pentacoordinate. There was no evidence of the original pre-reaction oxyferrous Cygb, meaning that the reaction is essentially complete in the ~1.5 ms dead time of the stopped-flow, even at low NO concentration (10 μM). Therefore, the half-time of the reaction of NO with oxyferrous Cygb must be considerably below 1 ms, making the second order reaction greater than 10^8 $M^{-1}s^{-1}$, but likely less than 10^9 $M^{-1}s^{-1}$ due to diffusion rate limits. The end spectrum is that of the ferric protein with hexacoordinate heme iron. Therefore, the kinetics observed (200-400 s^{-1}) is likely that of distal histidine binding, i.e. the relaxation of the protein from pentacoordinate to hexacoordinate state following dissociation of the nitrate product. Figure 2.3.4.3 shows the observed rate constants for the reaction of NO with oxyferrous Cygb at 80 μM NO. With all forms of the protein (monomer$_{S\text{-}S}$, monomer$_{S\text{-}H}$ and dimer$_{S\text{-}S}$ and C38R/C83R mutant) the rate constants of reaction are quite close, ranging from 200 to 400 s^{-1}. The observed rate contents are largely independent of NO concentration (Figure 2.3.4.4), with dimer$_{S\text{-}S}$ slowest at 218 ± 18 s^{-1}, followed by the monomer$_{S\text{-}S}$ 241 ± 35 s^{-1}, monomer$_{S\text{-}H}$, 320 ± 26 s^{-1} and C38R/C83R 393 ± 47 s^{-1}.

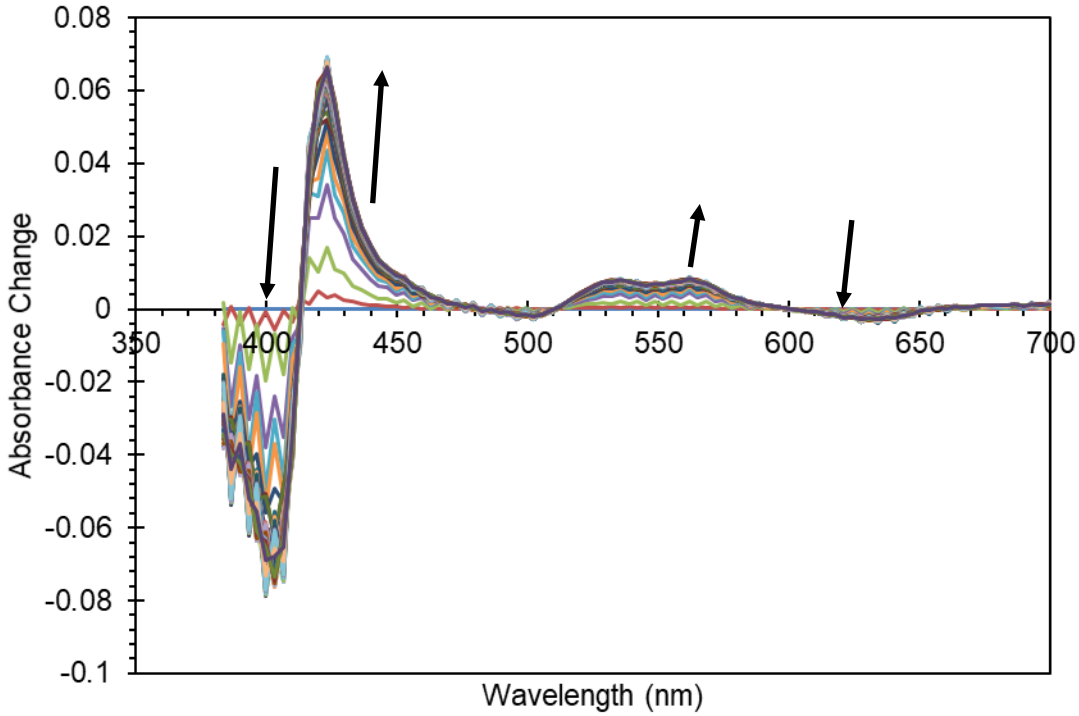

Figure 2.3.4.1 Optical changes of oxyferrous monomeric Cygb with intramolecular disulfide with NO. Protein (5 μM) in 50 mM sodium phosphate buffer pH 7.4 was rapidly mixed with NO (80 μM), each time point is 1.2 ms. Initial spectrum (~1.2 ms) was used as blank.

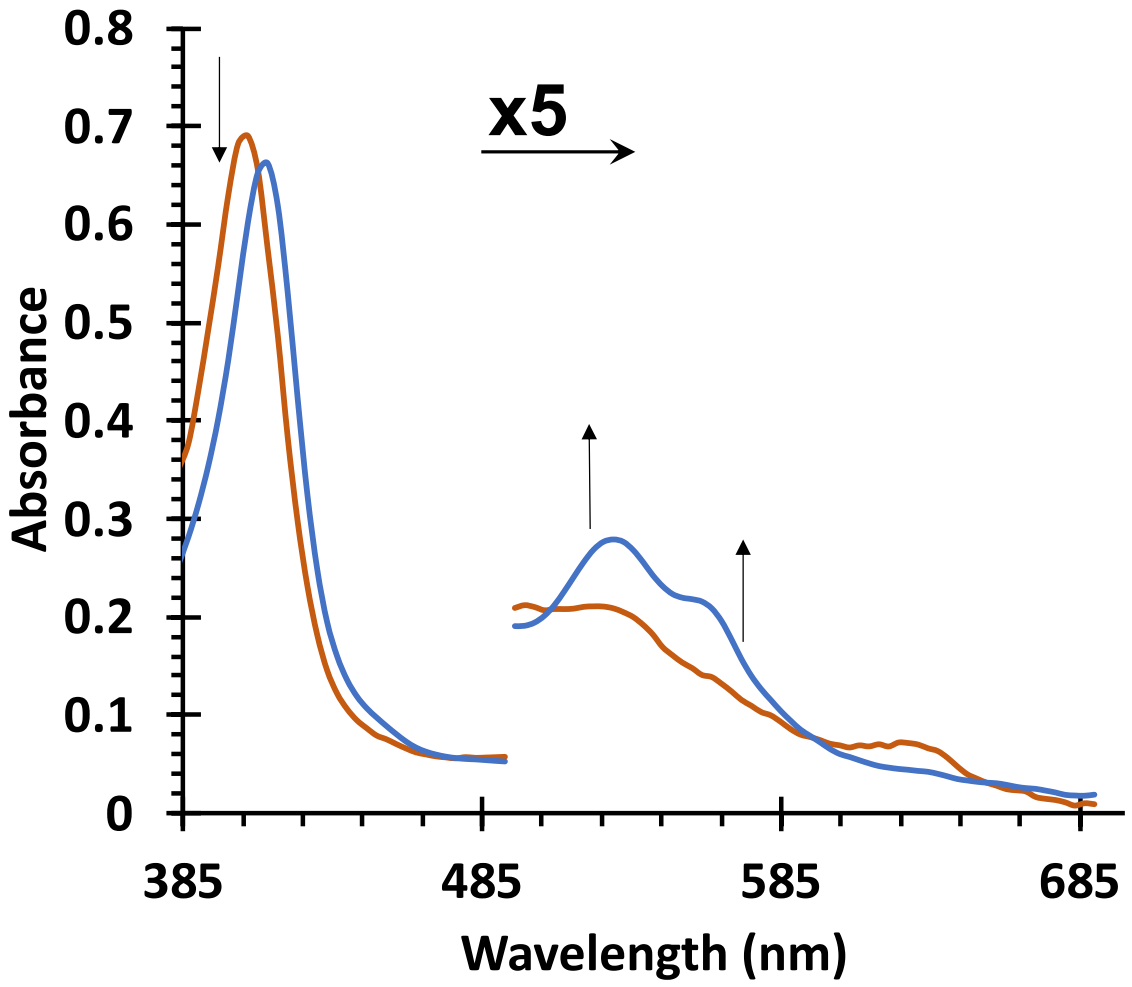

Figure 2.3.4.2 Initial and final spectra of cytoglobin following mixing with NO as fitted globally for a single pseudo-first order transition. Initial spectrum (~1.5 ms following mixing, red line) is primarily that of pentacoordinate ferric Cygb. Final spectrum (50 ms following mixing, blue line) is that of hexacoordinate ferric Cygb. Initial and final spectra were determined from global fit using Applied Photophysics Pro-Kineticist II software.

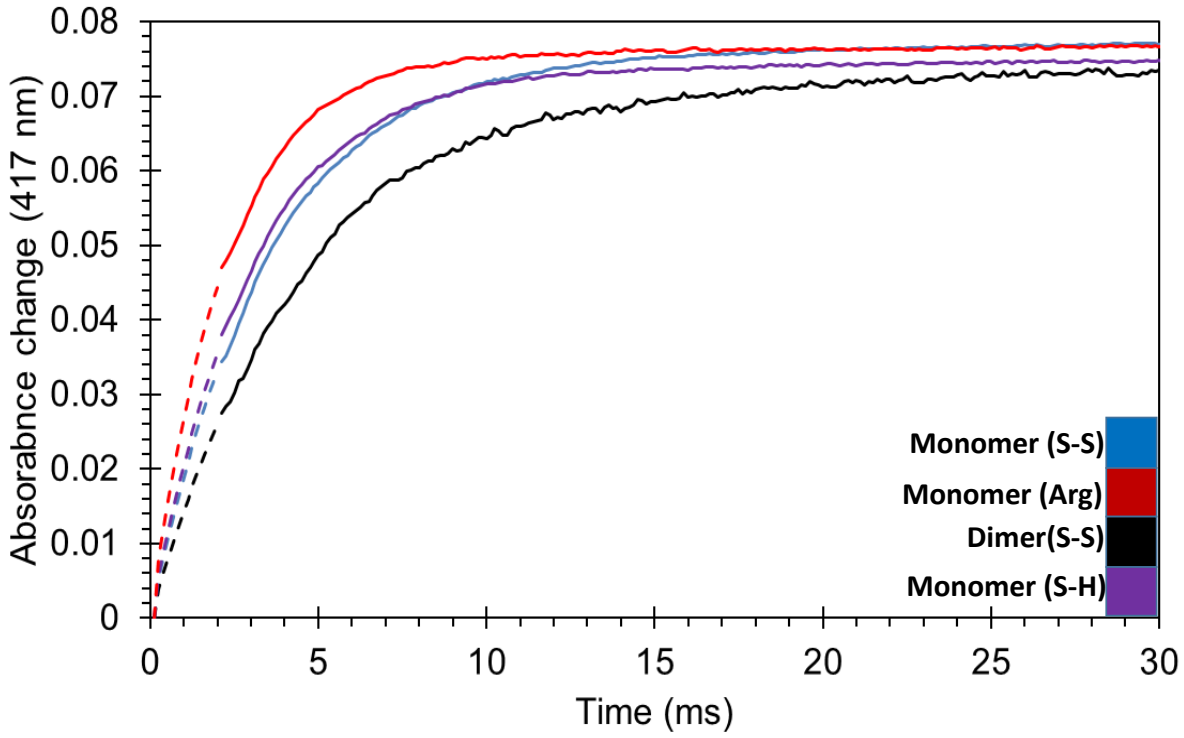

Figure 2.3.4.3 Time course of the nitrite reductase activity of cytoglobin at 417 nm as a function of cysteine oxidation states. Time courses shown are monomeric Cygb with intramolecular disulfide (blue), monomeric Cygb double mutant C38R/C83R (red) and dimeric Cygb with intermolecular disulfide (black) and TCEP reduced Cygb (purple). Time courses within the deadtime of instrument (<2 ms, dashed lines) were constructed using single exponential fits to the data. Reaction was carried with nitrite (3mM) and deoxyferrous Cygb (5 μM) in 100 mM sodium phosphate buffer pH 7.4 at 37 ºC.

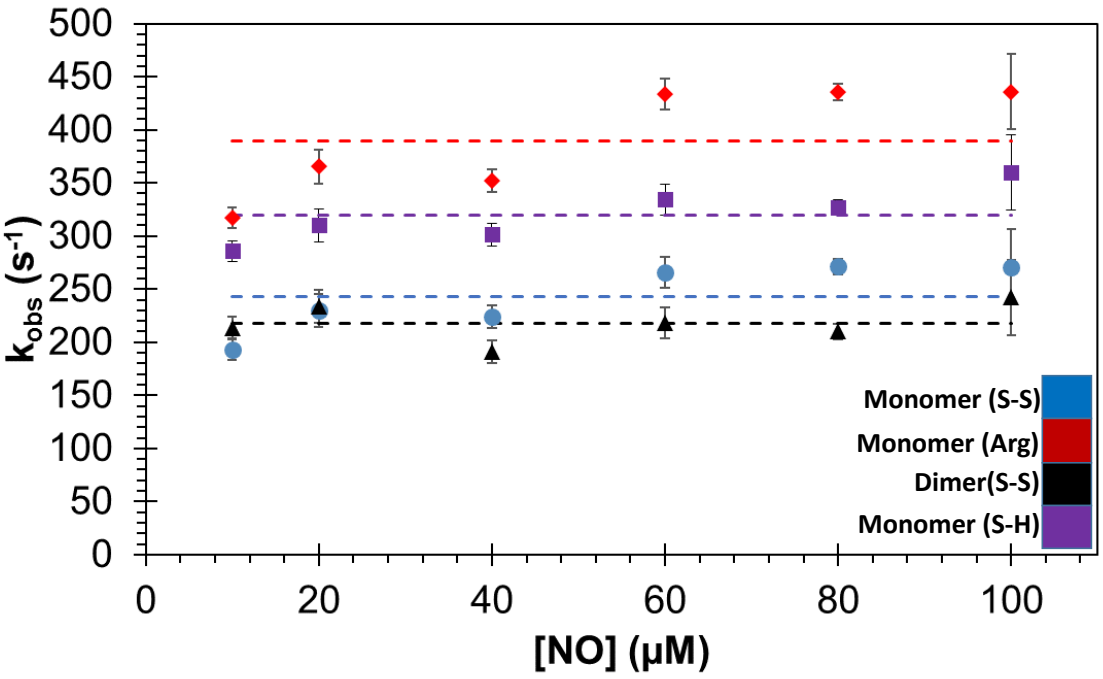

Figure 2.3.4.4 Observed rates of optical changes following mixing are essentially NO concentration independent. Monomeric Cygb with intramolecular disulfide (blue), monomeric Cygb double mutant C38R/C83R (red) and dimeric Cygb with intermolecular disulfide (black) and TCEP reduced Cygb (purple).

2.4. Discussion

Previous reports on the NiR activity of Cygb have not taken the into account monomeric and dimeric forms of the protein and type cysteine interactions (intramolecular, intermolecular. Or free sulfhydryl). The study presented here shows that the monomer$_{S\text{-}S}$ form of the protein exhibits NiR activity far higher than that of the other forms of the protein, dimer$_{S\text{-}S}$ and monomer$_{S\text{-}H}$. The published Cygb second order rate constant of NiR activity (0.14 $M^{-1}s^{-1}$) most closely correlates with our measurement of dimer$_{S\text{-}S}$ or monomer$_{S\text{-}H}$ forms of the protein (0.26 and 0.63 $M^{-1}s^{-1}$ respectively); thus, it was likely a protein in the dimer$_{S\text{-}S}$ or/and monomer$_{S\text{-}H}$ form of the protein that was used in previous studies on NiR activity. Mutation of the cysteines slows the NiR activity further, probably due to an influence on the arginine residue on the nearby distal histidine. It is unclear whether the dimeric form of the protein has physiological relevance *in vivo*. The micromolar concentration of the protein in cells (Li et al., 2012b, Schmidt et al., 2004b) may yield monomeric protein rather than the dimer, but this has not been confirmed. Nonetheless, the monomeric forms of the protein, either with free sulfhydryl or intramolecular disulfide bond, are the likely form of the protein in the cytosol of cells and hence it is important to characterize the activities of both forms of the protein.

The NiR activity of the monomer$_{S\text{-}S}$ form of Cygb is higher than that of other similar globins (Table 2.4.1). The allosteric state of human hemoglobin $\alpha_2\beta_2$ tetramer have a significant effect on the NiR activity of erythrocyte Hb, the T state showing a 50-fold lower NiR activity (0.12 $M^{-1}s^{1}$) than the R state Hb (6 $M^{-1}s^{1}$) (Table 2.4.1) (Huang et al., 2005). This closely resembles the effect of the oxidation state of the cysteines in the monomeric protein, it too showing a 50-fold change in NiR activity. Cygb also has reported allosteric properties of O_2 binding (Fago et al., 2004), but this relates only to the dimeric protein and cannot account for the observations of the high NiR activity exhibited by the monomer$_{S\text{-}S}$ protein. The NiR rates observed on the monomer$_{S\text{-}S}$ in this study can likely be explained by the intramolecular disulfide having an impact on the NiR activity, and this lies partially effect on this bond on heme iron coordination. We have previously shown

that the intramolecular disulfide enhances the distal histidine dissociation rate by over 1000-fold (Beckerson et al., 2015a). Furthermore, the NiR activity of Ngb is enhanced 2000-fold with distal histidine mutation to generate a 5-coordinate geometry (Tiso et al., 2011a). Therefore, the more pentacoordinate-like geometry of the Cygb with intramolecular disulfide is likely to enhance NiR activity.

To our knowledge, the NiR activity of human Cygb with intramolecular disulfide is higher than that reported of any member of the hemoglobin superfamily in vertebrates to date. A recent report shows a high NiR activity of globin X from zebrafish (*Danio rerio*) at 26.7 ± 2.0 $M^{-1}s^{-1}$ (Corti et al., 2016b). Globin X is a hexacoordinate globin that can be found in the blood of fish, amphibians and reptiles (Droge and Makalowski, 2011). Concentrations of globin X *in vivo* are typically in the micromolar range, similar to cellular concentrations of Cygb (Fago, 2004), thus the oxygen carrying capacity of globin X in the blood is limited, suggesting a different role for this protein. The high NiR activity of globin X comes close to our reported value, although performed at higher temperatures, illustrating the biological relevance of ancient globins as important NiR enzymes (Corti et al., 2016b). A recent finding with zebrafish Cygb observed low rates of NiR activity with Cygb2 (0.31 $M^{-1}s^{-1}$, 25 °C), but much high rates with Cygb1 (14.6 $M^{-1}s^{-1}$, 25 °C) (Corti et al., 2016a). Interestingly, neither isoform of Cygb in zebrafish have the two cysteines to form intramolecular disulphides observed in human Cygb (Cygb2 has C38 only), although other cysteine residues are present but are unlikely to be in positions to for intramolecular disulfide bonds. However, the different sequence identity of Cygb1 results in a pentacoordinate protein, whereas Cygb2 is hexacoordinate (Corti et al., 2016a). This is consistent with the general observations that pentacoordinate and pentacoordinate-like globins have enhanced NiR activity in comparison to their hexacoordinate counterparts and supports our proposal that the higher NiR activity of $monomer_{S\text{-}S}$ Cygb is, at least in part, due to the more pentacoordinate-like nature of this form of the protein. This hypothesis is further explored though site directed mutation in Chapter 3.

Protein	k_{NR} ($M^{-1}s^{-1}$)	Temperature (ºC)	Reference
Cytoglobin$_{S\text{-}S}$ (monomer)	32.3	25	This work
Zebrafish Cytoglobin 1	14.6 28.6	25 37	Corti et al. Nitric Oxide. 2016; 53: 22-34.
Zebrafish Globin X	26.7	37	Corti et al. Proc. Natl. Acad. Sci. 2015; 113:8538-8543.
Hemoglobin R state	6.0	25	Huang et al. J. Clin. Invest. 2005;115:2099–2107.
Equine Myoglobin	2.9 2.7	25 25	Li et al. J. Biol. Chem. 2012;287:36623–36633. This work
Cytoglobin$_{S\text{-}H}$	0.63	25	This work
Zebrafish Cytoglobin 2	0.31	25	Corti et al. Nitric Oxide. 2016; 53: 22-34.
Cytoglobin$_{S\text{-}S}$ (Dimer)	0.26	25	This work
Cytoglobin (unknown cysteine oxidation)	0.40	25	Corti et al. Nitric Oxide. 2016; 53: 22-34.

	0.14 0		Li et al. J. Biol. Chem. 2012;287:36623–36633. Peterson et al. J. Inorg. Biochem. 2008:102,1777-1782.
Hemoglobin T state	0.12	25	Huang et al. J. Clin. Invest. 2005;115:2099–2107.
Neuroglobin$_{S\text{-}S}$	0.12	25	Tiso et al. J. Biol. Chem. 2011;286:18277–18289.
Neuroglobin$_{S\text{-}H}$	0.062	25	Tiso et al. J. Biol. Chem. 2011;286:18277–18289.

Table 2.4.1. Nitrite reductase activity of various members of the hemoglobin family. All are human globins unless otherwise stated.

The observed kinetics following the NOD activity of Cygb are largely independent of NO concentration (Figure 2.3.4.4). This is due to the NO-independent relaxation of the pentacoordinate ferric Cygb to hexacoordinate, resulting from binding of the distal histidine (H81) to the space vacated by the nitrate product. The rate of distal histidine binding appears to be largely independent of the oxidation state of the cysteines. As one of these cysteines (C83) is close to the distal histidine one might expect some influence on histidine binding, but the influence of the cysteine appears to be minimal with only a factor of two separating the slowest and fastest rates. This is keeping with previous observations that the intramolecular disulfide only affects the histidine on-rate (k_H) by <2 fold following CO photo-dissociation (Beckerson et al., 2015a). The true reaction of NO with oxyferrous Cygb is faster than that observable by stopped-flow and is thus close to the diffusion rate limit. Any effects of the oxidation state of the cysteines on this reaction must be lie between these upper and lower rate limits and is therefore limited.

Previous observations of Ngb also report an NO concentration-independent maximal rate (Table 2.4.2) with the reaction between NO and oxyferrous Ngb too quick to be observed (Brunori et al., 2005a). This was interpreted as the initial species observed being ferrous-peroxynitrite, with the Soret maximum at 407-408 nm. This intermediate then decayed in a first order process to ferric Ngb consistent with a dissociation of the peroxynitrite leaving as nitrate. However, the spectra observed for the Cygb intermediate in Figure 2.3.4.1 and 2.3.4.2 is more consistent with a predominantly high spin ferric Cygb than peroxynitrite or nitrate bound ferric heme iron, with the observed rate of 200-400 s^{-1} that of distal histidine binding. Either way, the true NOD activity of Cygb cannot be ascertained by the methods employed here, but the data does suggest that the NOD activity of Cygb is inherently faster than that measured by NO depletion kinetics that requires Cygb redox cycling (Gardner et al., 2010, Zhou et al., 2017).

Protein	k_{NOD} ($M^{-1}s^{-1}$)	Temperature	Reference
Hemoglobin N (*M. tuberculosis*)	$7.5x10^{8}$	23 °C	Ouellet et al. 2002 Proc. Natl. Acad. Sci. U. S. A. 99, 5902-5907
Neuroglobin	$>7x10^{7}$ 90 s^{-1} (maximal k) 300 s^{-1} (maximal k)	5 °C 5 °C 20 °C	Brunori et al. (2005) Proc. Natl. Acad. Sci. U. S. A. 102, 8483-8488
Myoglobin (Equine)	$3.4x10^{7}$	20 °C	Eich et al. 1996 Biochemistry. 35, 6976-6983
Cytoglobin	$3x10^{7}$ (by NO consumption) 200-400 s^{-1} (maximal k)*	20 °C 20 °C	Gardner et al. 2010 J. Biol. Chem. 285, 23850-23857 This work.

Table 2.4.2. Nitric oxide dioxygenase activity of various members of the hemoglobin superfamily. All are human globins unless otherwise stated. * The k_{NOD} for cytoglobin measured here was distal histidine binding and did not represent true NOD activity, here we estimated at $>1x10^{8}$ $M^{-1}s^{-1}$.

From the data presented here, the NiR activity of Cygb may have a more important biological role than previously understood. Although more studies are required to explore the role of NiR activity in cells, we can speculate that the NO generating activity of Cygb can be controlled through the oxidation of the surface exposed cysteines, enhancing NO production under conditions such as oxidative stress. Recently Cygb has been found to be co-localised with nNOS in various areas of the mouse brain, expressed in the cytoplasm of neurons (Reuss et al., 2016) and downregulation of Cygb prevents angiotensin-mediated hypertension (Liu et al., 2017a). This illustrates the proposition that Cygb, like Ngb, is involved in NO homeostasis. Cygb has been noted to protect hypoxic tumors against oxidative stress (Bholah et al., 2015, Oleksiewicz et al., 2013), particularly against the effects of cancer therapies such as chemotherapy and radiotherapy (Oleksiewicz et al., 2013, Shivapurkar et al., 2008). It has also been previously suggested that Cygb regulates the levels of NO under hypoxic conditions has been suggested to indirectly regulate vascular tone in tissues under hypoxia by inducing vasodilation through cessation of NO scavenging, thereby alleviating the oxygen deficiency stress (Bholah et al., 2015). Our data supports these propositions, suggesting a role that can potentially unify the observed effects of the protein *in vitro* with the suggested roles of the protein *in vivo*.

Generation or exposure of cysteines to NO can promote S-nitrosylation. The S-nitrosylation of vertebrate Hb via beta-Cys93 has been reported contribute to blood pressure regulation and hence oxygen delivery (Frehm et al., 2004, Jia et al., 1996, Luchsinger et al., 2003, Zhang and Hogg, 2004). S-nitrosothiol formation in Ngb was observed following the reaction with nitrite, with considerably smaller fractions of S-nitrosylation observed with Cygb (Petersen et al., 2008). However, as no Cygb-dependent NiR activity was observed in the study, in contrast to ours and other studies, the level of S-nitrosylation as a function of cysteine oxidation, and its potential consequences on Cygb catalytic activities, may need reappraisal.

The role of Cygb in NO homeostasis is illustrated in Figure 2.4.1. Cygb can, under conditions of normoxia, regulate NO through dioxygenase activity as previously suggested (Bholah et al.,

2015). Under conditions of hypoxia, NO can be generated by NiR activity. However, under oxidative conditions the NiR activity of Cygb is significantly enhanced, upregulating NO generation to a point that it may be physiologically significant. Our data, together with that of others, suggests that cysteine oxidation is crucial in modulating the redox chemistry of the protein, potentially acting as a redox switch. Under conditions of hypoxia-induced oxidative stress conditions may favour depletion of antioxidants such as glutathione and hence promotion of cysteine oxidation leading to an enhanced Cygb generation of NO in the presence of nitrite. The consequences of this for cell biochemistry is a complex issue due to the diverse NO cell signaling pathways. However, it is of note that the expression mechanism of induction of Cygb is HIF-1alpha dependent, with high specificity and sensitivity of its induction by hypoxia (Fordel et al., 2004). Ngb on the other hand, is less influenced by hypoxia.{Zhang, 2014 #288}.

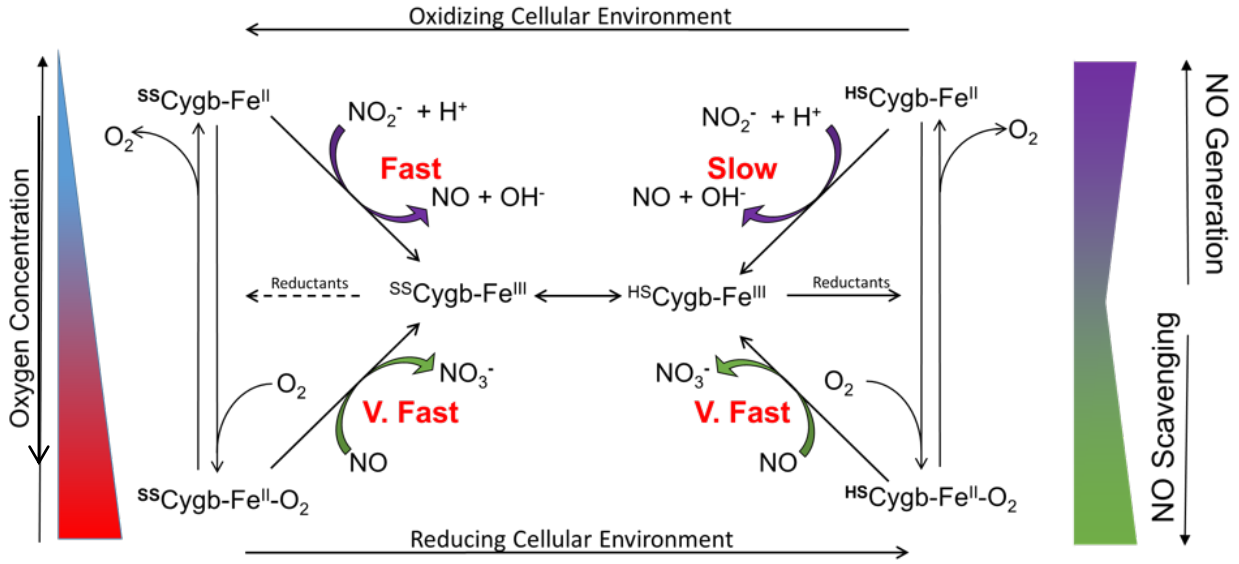

Figure 2.4.1 Cytoglobin-mediated control of NO homeostasis. NO homeostasis is controlled by the redox environment of the cell in addition to oxygen concentration. Under a normoxic cellular environment the cytoglobin sulfhydryl oxidation state does not influence the NO scavenging capability of cytoglobin. However, under hypoxic conditions the NO generating capacity of cytoglobin from nitrite is highly influenced by the oxidation state of its surface-exposed cysteine, which in turn is linked to the redox environment of the cell.

Chapter Three

Modulating the function of cytoglobin through point mutation to control nitric oxide dioxygenase, nitrite reductase and oxidative reactions.

3.1 Introduction

Cytoglobin (Cygb) is a low abundance hexacoordinate globin found in all tissues of vertebrates (Burmester, 2002). Despite extensive effort to assign a biological role to Cygb the function of this protein still not clearly understood (Hankeln et al., 2005). However, the proposed physiological roles of Cygb include scavenging nitric oxide (NO) (Liu, 2012, Reeder, 2017) scavenging of reactive oxygen species (Ostoji, 2008, McRonald, 2012) lipid peroxidation (Reeder, 2011, Ascenzi, 2013, Tejero, 2016) and nitrite reductase activity (NiR) (Reeder, 2017, Li, 2012). Observations that Cygb gene expression is up regulated in response to cellular hypoxia/ischemia (Emara, 2010, Shaw, 2009, Avivi, 2010) infer a potential role in either oxygen sensing (i.e. O_2 homeostasis) or NO homeostasis. It has been proposed that Cygb functions as a regulator of intracellular O_2 homeostasis by acting as a redox-sensitive anti-oxidative protein in hepatic stellate cells (Yoshizato, 2016). However, it has also been proposed that Cygb is involved in NO homeostasis via the generation of NO in hypoxic conditions through its NiR activity and scavenging NO in normoxic conditions through the nitric oxide dioxygenase (NOD) activity.

As a result of its NO scavenging capability, Cygb could provide cytoprotective support for NO sensitive enzymes, like those proposed for myoglobin (Mb) and neuroglobin (Ngb). It has been shown that Mb and Ngb can protect terminal oxidases in the electron transport chain (Halligan, 2009, Fang, 2011), and regulate the blood flow to hypoxic tissues in the vasculature by vasodilation through NO production (Liu, 2012, Liu, 2013) A recent report proposed that Cygb plays a significant role in regulating vascular tone through NO scavenging in the vasculature (Liu, 2017, Lilly et al., 2018). A knockout of Cygb lengthens NO decay which leads to low blood pressure. Down regulation of Cygb also led to inhibition of angiotensin-mediated hypertension highlighting the relevance of Cygb NO homeostasis in regulating vascular tone with implications for role during hypoxic/ischemic insults (Totzeck et al., 2012). The co-localisation of Cygb with neuronal NO-synthase (Reuss, 2016) as well as the implication of

NO metabolism by Cygb in fibrogenesis (Van Thuy et al., 2017) also links Cygb to NO metabolism(Gardner, 2010). The NiR mediated NO generation by Cygb in anaerobic conditions, and oxygen-dependent NO consumption, suggests a potential regulatory role of Cygb in response to oxidative stress (Liu, 2012, Li, 2012, Petersen, 2008) The NiR and NOD activities performed by ferrous Cygb, oxidizes the Cygb to ferric. Therefore, for these activities to be physiologically relevant Cygb will need a rapid cellular reduction system to recycle the ferrous form. This proposition is supported by the observation that Cygb is rapidly reduced by cellular reductants like Cytochrome b5 and ascorbate (Gardner, 2010).

As expressed recombinantly in *E. coli*, depending on the redox state of the cysteines Cygb can be produced in three states (Lechauve, 2010). These states are (i) a monomer with oxidized cysteines forming an intramolecular disulfide bond (monomer$_{\mathbf{S\text{-}S}}$) (Lechauve, 2010) (ii) a monomer with reduced cysteines, i.e. free sulfhydryl with (monomer$_{\mathbf{S\text{-}H}}$),(de Sanctis et al., 2004a) or (iii) a homodimer (dimer$_{\mathbf{S\text{-}S}}$) with the two pairs of cysteines forming two intermolecular disulphide bonds (Cys38-Cys83 and Cys 83-Cys38)(Makino, 2006) (Figure 3.1.1).Crystal structures of Cygb are available as either a dimer$_{S\text{-}S}$ or a monomer$_{S\text{-}H}$ (de Sanctis et al., 2004c, Makino, 2006) However, the crystal structure of the monomer$_{S\text{-}S}$ is not available. The state of oligomerization *in vivo* is unknown. However, Cygb is likely to exist as a monomer *in vivo* due to the low levels of expression (Lechauve, 2010).

In monomeric Cygb, due to the proximity of Cys83 to the heme iron distal histidine on helix E, the presence of an intramolecular disulfide bond creates a compact structure changing the equilibrium of the distal histidine - heme iron ligation, through an increase in distal histidine off rate from 0.17 s^{-1} to 109 s^{-1} (Beckerson, 2015a). Thus, the protein is more pentacoordinate-like compared to the protein in the absence of this disulfide bond. The difference in structural configuration due to the redox state of the cysteines creates a cysteine redox state-dependent modulation of the binding or/and reactivity with exogenous ligands such as CO and NO (Beckerson, 2015b). The presence of the intramolecular disulfide bond in the monomer$_{S\text{-}S}$ switches ligand migration pathway of CO (Astudillo, 2013) and lipid-induced changes in coordination (Reeder, 2017, Reeder, 2011). As discussed in chapter 2, the monomer$_{S\text{-}S}$ form

of the protein also enhances the nitrite reductase (NiR) activity of Cygb over 50 fold from that of the $monomer_{S\text{-}H}$ and $dimer_{S\text{-}S}$ but a minimal influence on NOD activity (Reeder and Ukeri, 2018). Hence the physiological role of Cygb is likely to be influenced on its oligomeric and disulfide state *in vivo* (i.e. $monomer_{(s\text{-}s)}$,$monomer_{(s\text{-}h)}$ and $dimer_{S\text{-}S}$)(Beckerson, 2015b).

Targeted mutagenesis of residues in the distal pocket of Mb, hemoglobin (Hb) and Ngb have been shown to specifically modulate either the NIR or/and NOD activities (Tejero, 2015, Birukou, 2011, Varnado, 2013). The NIR activity of Ngb was increased ~2000 times by mutation of the distal histidine (His64) to an alanine (Tejero, 2015). Bimolecular ligands like NO have been shown to migrate to the distal coordination site of Hb through the rear of the heme pocket, to access the central iron. The distal histidine acts like a gate rotating out of place to enable bimolecular ligands ligate to the central heme iron (Birukou, 2011). This mechanism can be impeded by removing the space at the rear of the heme pocket with large hydrophobic residues such as phenylalanine or tryptophan, hampering access the distal coordination site. Mutation of neighbouring residues of the distal histidine such as Leu(B10) to tryptophan was effective in hampering in the NOD activity of Hb and Mb without significant impacting on the binding of CO or O_2 (Birukou, 2011, Scott, 2001).

In this chapter the effect of specific point mutations on the ligand binding properties of Cygb and potential physiological reactivities are examined. The mutations described above were mapped to Cygb with the aim of modulating the NiR or NOD activity. Mutations that can impact one or more specific function(s) of Cygb may be utilized, though cell-based studies in determining the contribution of specific activities to cellular response to oxidative stress, potentially leading to a greater understanding of the role of Cygb in cancer therapy resistance.

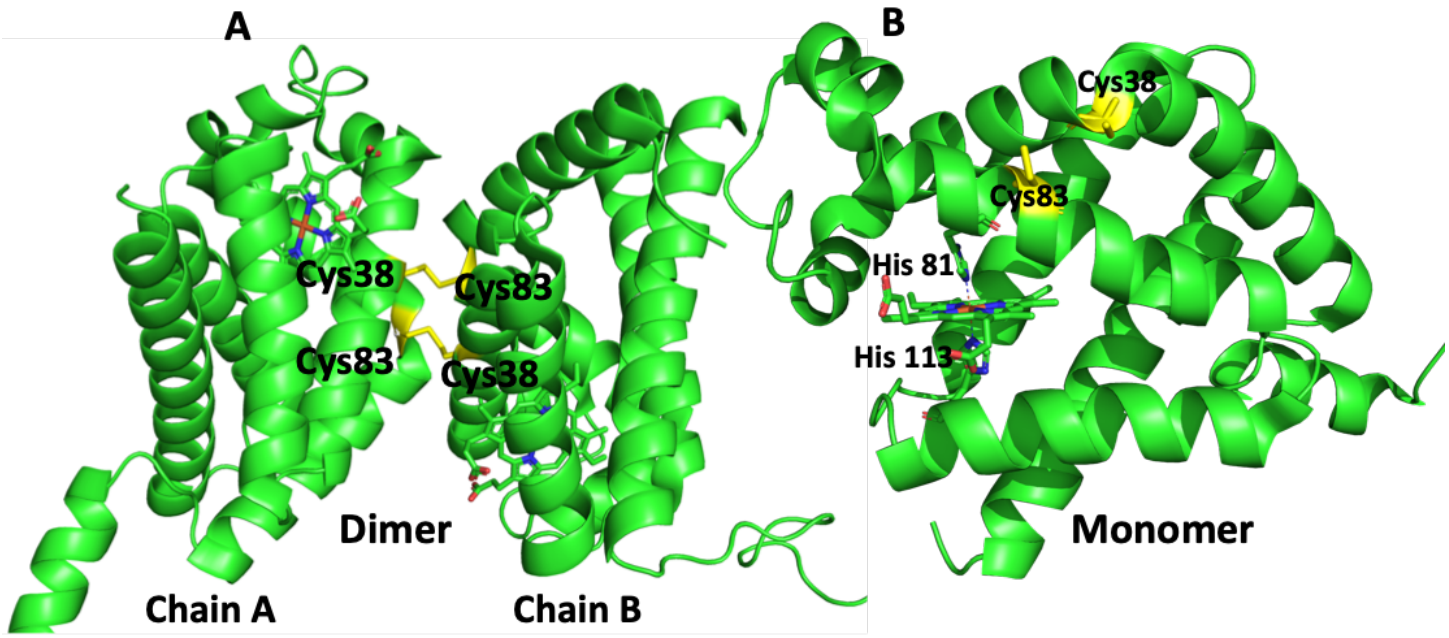

Figure 3.1.1. Crystal structure of Cygb PDB ID: 2DC3 generated by pyMol molecular graphics software. Monomeric Cygb (A), Dimeric Cygb (B), Cygb possesses an hexacoordinate structure, in which the sixth coordination site is occupied by a distal histidine (His81) in the absence of external ligands. (A) shows the dimeric structure of Cygb via the formation of an intermolecular sulphide bond between two monomeric subunits. (B) displays the structure monomeric Cygb with two free cysteines.

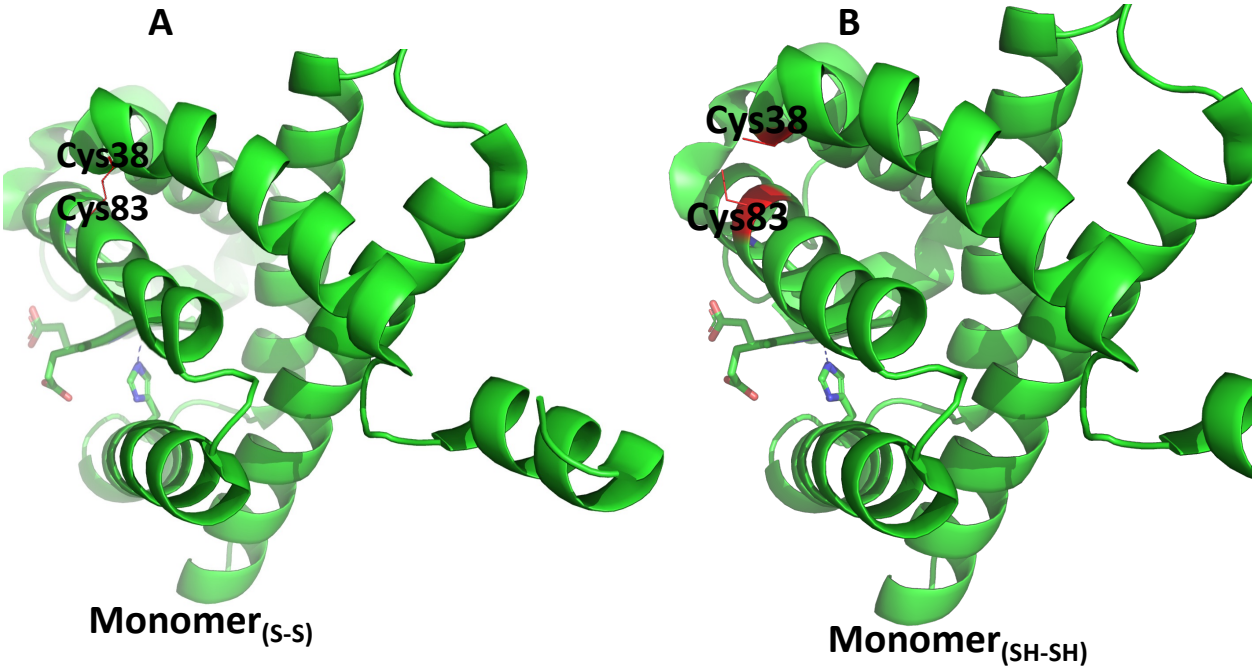

Figure 3.1.2 Monomeric Cygb with and without the intramolecular sulphide bond. (A) The position and formation of an intramolecular disulphide bond (generated *in silico*) in monomeric Cygb. (B) Monomeric Cygb with free sulfhydryl.

3.2 MATERIALS AND METHODS

3.2.1 Materials

Materials such as Proli-NONOate, CO, *pfu* Turbo, DNTP mix, DMSO, phosphate buffers and TCEP are described in section 2.2.1.

3.2.2 Recombinant human cytoglobin expression and purification.

Cygb plasmid was designed from a pET28a backbone with Cygb gene added as an insert and expressed BL21DE3 *E. coli* cells cultured in Luria Bertani media as previously described in section 2.2.2 and (Reeder and Ukeri, 2018)

3.2.3 Site-directed mutagenesis of human cytoglobin.

Cygb mutants where generated by site-directed mutagenesis using a modified Agilent quikchange II protocol on Cygb pET28a plasmid previously described in Chapter 2.2.2. Mutagenesis generated the following mutations and the following primers for C38S, H81A, L46F, and L46W mutants as listed below:

Mutant	Primer
Leu 46 Phe	Forward: 5' GAAGACGTAGGTGTGGCAATTTTCG**TTC**GTTTCTTCGTTAACTTC 3' Reverse: 5' GAAGTTAACGAAGAAACGAACGAAA**ATT**GCCACACCTACGTCTTC 3'
Leu 46 Trp	Forward: 5'GACGTAGGTGTGGCAATT**TGG**GTTCGTTTCTTCGTTAAC 3' Reverse: 5'GTTAACGAAGAAACGAAC**CCA**AATTGCCACACCTACGTC 3'
His 81 Ala	Forward: 5' CTCCGCAGCTGCGTAAA**GCC**GCATGTCGTGTGATG 3' Reverse: 5' CATCACACGACATGCGG**CTT**TACGCAGCTGCGGAG 3'
Cys 38 Ser	Forward: 5' CTGTACGCGAAC**AGC**GAAGACGTAGG 3' Reverse: 5' CCTACGTCTTCG**CTG**TTCGCGTACAG 3'
Cys 83 Ser	Forward: 5' CGTAAACACGCA**TCT**CGTGTGATGGGTG 3' Reverse: 5' CACCCATCACAC**GAG**ATGCGTGTTTACG 3'

Table 3.2.3.1 list of primers employed in site directed mutagenesis of cytoglobin. Table Shows targeted residues and primers used to generate mutant proteins.

3.2.4 Nitric oxide dioxygenase activity.

The NOD activity was initiated by reacting oxyferrous Cygb with nitric oxide at micromolar concentrations. The NOD activity was initiated at 10 °C by 1:1 rapid mixing of 10 μM oxyferrous Cygb (5 μM after mixing) and NO (20-800 μM) using an Applied Photophysics SX-20 stopped-flow spectrophotometer followed by measurement of changes in optical spectra (350-700nm) as described in chapter 2.2.3.

3.2.5 Nitric oxide binding.

The transition of deoxyferrous from hexacoordinated distal histidine bound species, to NO bound species was detected using an Applied Photophysics SX20 stopped-flow spectrophotometer. Degassed sodium phosphate buffer (0.1M, pH 7.4) was prepared using a custom degassing equipment and a tonometer using repeated cycles of partial evacuation using a vacuum pump followed by purging with argon gas. Deoxy Cygb (10 μM) was prepared through degassing via cycles of partial evacuation and argon gas purge with a custom set up that was linked to a vacuum pump and an argon gas supply. Partially deoxygenated protein was transferred to 10 ml glass syringes, Cygb was made ferrous and trace oxygen removed by addition of a minimum amount of dithionite. Proli-NONOate was transferred to 10 ml glass syringes with degassed buffer. Deoxyferrous Cygb (5 μM) after mixing) was rapidly combined (1:1) with NO (20-800 μM) by stopped-flow at 20 °C.

3.2.6 Nitrite reductase activity.

The NiR activity was monitored by reacting 5 μM Cygb with sodium nitrite (0 – 20 mM), in 0.1 M sodium phosphate buffer pH 7.4, in the presence of ~5 mM sodium dithionite which was added preceding the reaction. Optical changes were measured using an Agilent 8453 diode array spectrophotometer fitted with multi-cell carriage and temperature control. The nitrite reductase activity of the H81A mutant was measured using the Applied Photophysics SX-20 stopped flow spectrophotometer due to the more rapid activity. Kinetics was obtained from time courses at (416-429nm) using the least squares methods with Microsoft Excel.

3.3 Results

As shown in chapter 2, deoxy Cygb reacts with nitrite to generate NO and ferric Cygb. Here mutations that have shown to affect the NiR activity in other globins such as Ngb (Tejero, 2015) (Tejero ., 2015) have been mapped onto the equivalent position on Cygb as shown in Figure 3.3.1. In addition, mutations that are known to affect the NOD activity of Mb and Hb (Scott, Gibson and Olson, 2001; Varnado ., 2013) have also been mapped onto Cygb. This was accomplished using molecular graphics software (Deepview version 4.1.0) where the structures were aligned Figure 3.3.2 – 3.3.3. These include H81A, equivalent to H64A in Ngb, which has been reported to enhance the NiR activity of Ngb by over 2000-fold (Tiso ., 2011). Additionally, L46F and L45W, equivalent to L29F and L29W in Hb and L29F - L29W in Mb and Hb (Scott, Gibson and Olson, 2001; Varnado ., 2013), have been shown to decrease the NOD activity by over 10 fold in Mb/Hb due to the NO accessing the oxygen though the rear of the heme pocket as described in the introduction.

We have previously examined the effect of the oxidation state of cysteine on the NiR and NOD activities of Cygb (Chapter 2, also Reeder and Ukeri, 2018). Cysteine mutation to arginine was used to prevent dimerization of the Cygb by electrostatic interactions. However, it is plausible that changing cysteine to arginine affects the interaction of NO with Cygb. Therefore here we explore the effects of the mutation of cysteine to serine, both neutral molecules of the same size, in the NO binding, NiR and NOD activities.

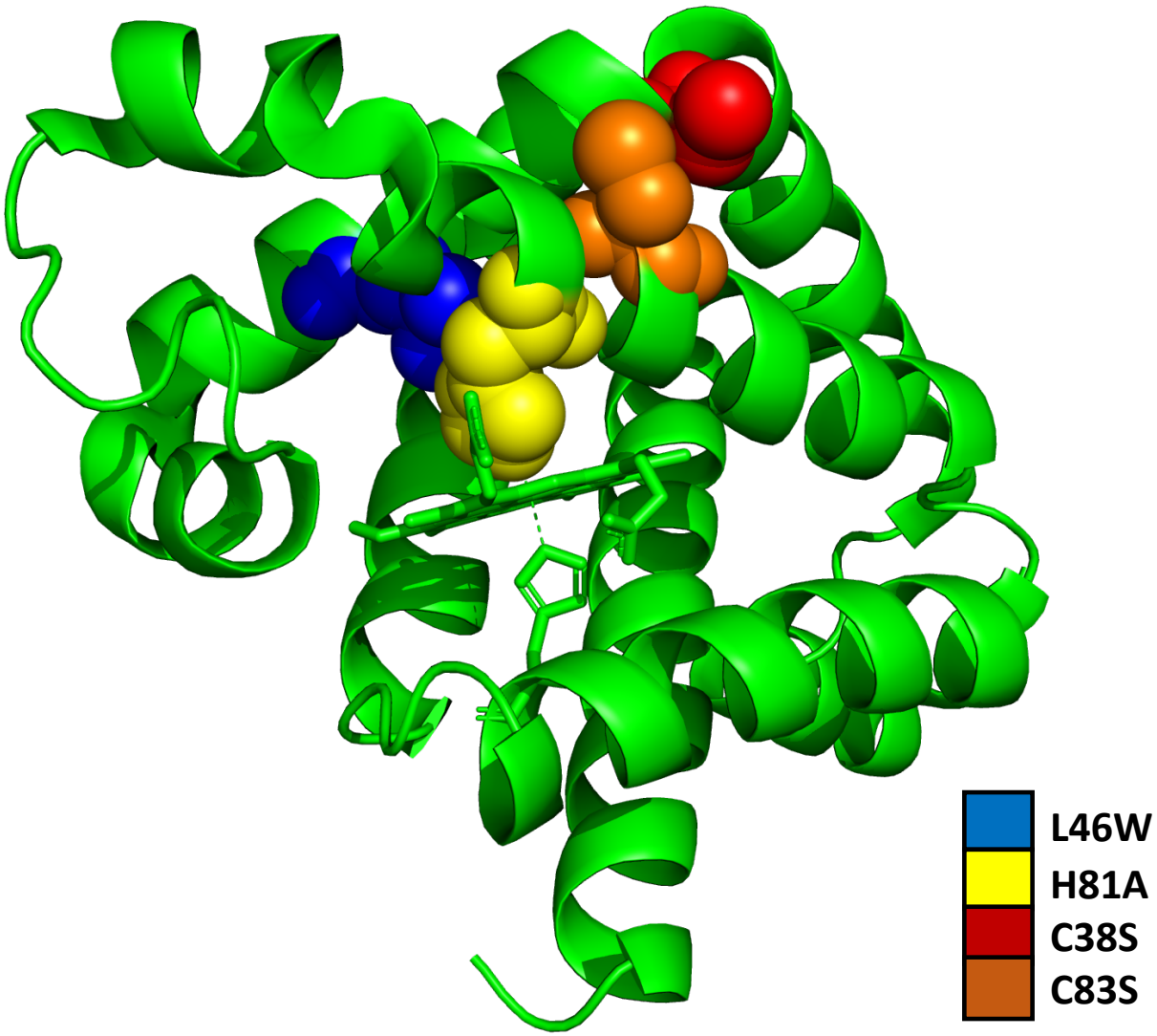

Figure 3.3.1. Positions of targeted site mutations on Cytoglobin. The PDB used was 2DC3. The proximal histidine and heme are shown as stick (Cyan). The targets for the mutations are in spacefill and are L46 (Blue), C38/C83 (Red/Orange) and H81 (Yellow)

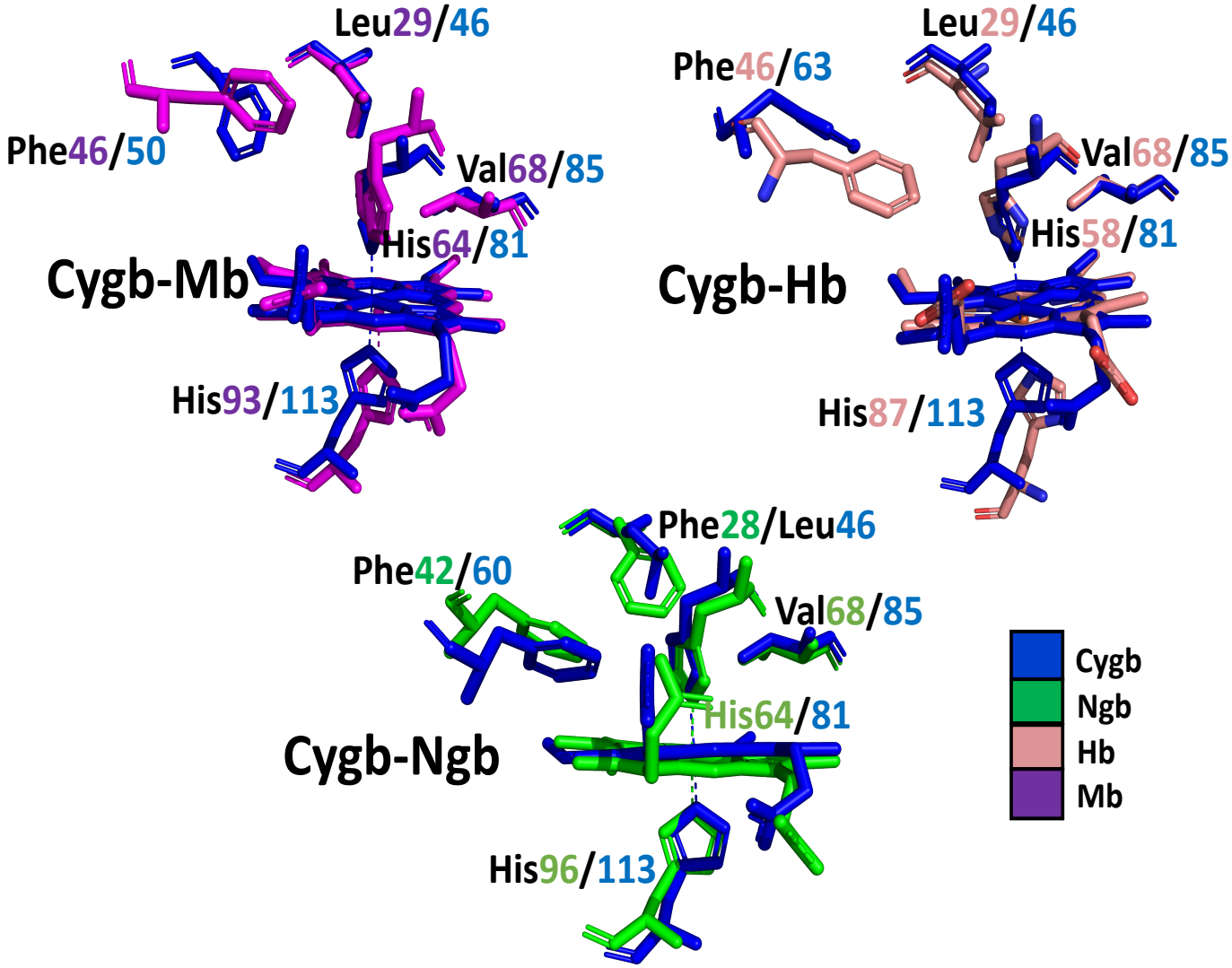

Figure 3.3.2 Identification of target for point mutation on cytoglobin. Cygb was aligned to Mb (Cygb-Mb), Hb (Cygb-Hb) and Ngb (Cygb-Ngb). Targets for point mutation on Cygb were selected by structural alignment of Cygb to Mb Hb and Ngb. Residues already known to degrade or enhance NOD and NiR activities with mapped to Cygb and equivalent residues selected.

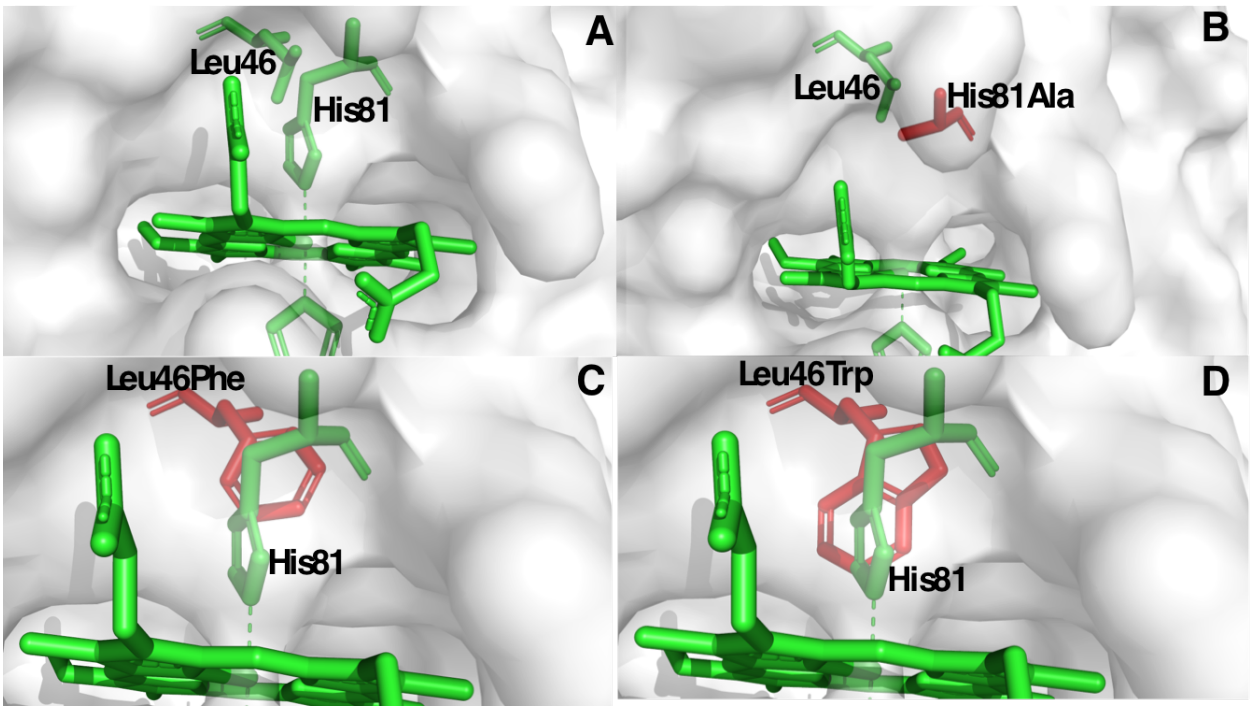

Figure 3.3.3. Showing in silico mutation of targeted sites in cytoglobin. This figure illustrates the impact of mutation on the ligand migration to the central heme iron of Cygb, WT Cygb (A) showing targeted distal residue, mutation of distal histidine to alanine (B), mutation of leucine to phenylalanine (C), mutation of leucine to tryptophan (D). Depending on the side chain of mutant residue the size of the distal binding pocket of reduced or enlarged affecting ligand migration the sixth coordination side.

3.3.1 Effect of mutation on nitric oxide binding.

The optical changes of the binding of NO to deoxyferrous WT Cygb is shown in Figure 3.3.1.1A. WT Cygb in the deoxyferrous form is hexacoordinate with a proximal and distal histidine ligated to the heme iron (His-Fe-His). This is exhibited in the two sharp deoxyferrous peaks in the visible region of the spectrum at 530 and 560 nm, indicative of hexacoordinated globins like Ngb (Dewilde, 2001) and other heme proteins such as cytochrome c (Butt and Keilin, 1962). The optical changes of NO binding shifts the Soret from 429 to 419 nm (Basu et al., 2008) and is accompanied with a less defined visible region, typical of the NO bound ferrous protein (Bonaventura, 2013). The optical changes of the L46F mutant exhibits an identical deoxyferrous and ferrous-NO spectrum to the WT protein (Figure 3.3.1.1B). In Figure 3.3.1.1C the C38S/C83S deoxyferrous spectrum is once again essentially identical to the WT protein. The ferrous-NO species is very similar to the WT NO bound protein. However, there is a small peak at 560 nm in all three proteins (WT, C38S/C83S and L46F) which is greater in the C38S/C83S mutation. This peak is at the same position as the alpha band (560 nm) of the deoxyferrous protein. Hence an explanation is a subpopulation of the protein retains the histidine in the distal position. In Figure 3.3.1.1D, the L46W mutation changes the deoxyferrous spectrum so that the two α and β peaks in the visible region are less prominent and more like a pentacoordinate protein such as Mb and the 560 nm band in the NO-bound species is much less prominent. Finally, the H81A mutation creates a typically pentacoordinate deoxyferrous spectrum as expected with this mutation Figure 3.3.1.1E. The NO-bound species is quite different compared with the other mutations and WT protein with peaks in the visible region at 545 and 580 nm with no 560 nm band. This is very similar to NO-bound Mb Figure 3.3.1.1F.

The kinetics of NO binding to deoxyferrrous protein as a function of NO concentration is shown in Figure 3.3.1.2. NO binding to cytoglobin was a biphasic process, showing a fast and slow kinetic component (Figure 3.2.1.2A). Previous studies examining the binding of CO to Cygb also shows a biphasic binding process (Beckerson, 2015a). This was identified to result from

a heterogenous population of monomeric species with the majority of the protein having a intramolecular disulfide bond (fast kinetics) and small subpopulation of a monomer with free sulfhydryl's (relatively slow kinetics) (Lechauve, 2010). The biphasic binding of NO to WT Cygb can also be assigned to this heterogenous population of cysteine oxidation states. The elimination of the dicysteines by a reductant (TCEP) eliminated the fast component of the reaction simplifying the reaction to monophasic kinetics. Figure 3.3.1.2B . Additionally, the C38S/C83S mutation shows a monophasic NO binding (not shown) with a slow rate (0.2 s^{-1}), Figure 3.3.1.2C. For the WT Cygb the rapid kinetics of NO binding assigned to the monomer with intramolecular disulfide bond, is essentially concentration independent over the concentrations of NO used. Additionally, the L46F and C38S/C83S are also NO concentration independent. The k_{obs} of NO binding is 12, 13 and 0.3 s^{-1} for WT, L46F and C38S/C83S respectively which closely follows the the distal histidine off rate for the protein with an intramolecular disulfide bond for WT and L46F and the distal histidine off rate for the free sulfhydryl for the C38S/C83S. However, the L46W and H81A mutants show concentration dependence that is linear with respect to the NO concentration Figure 3.3.1.3C and 3.3.1.3D. NO binding to the L46W and H81A mutants were rapid in comparison to the WT and exhibited a second other rate constant of 1.6 x 10^5 $M^{-1}s^{-1}$ and 6.6 x 10^6 $M^{-1}s^{-1}$ $\pm$ for L46W and H81A respectively.

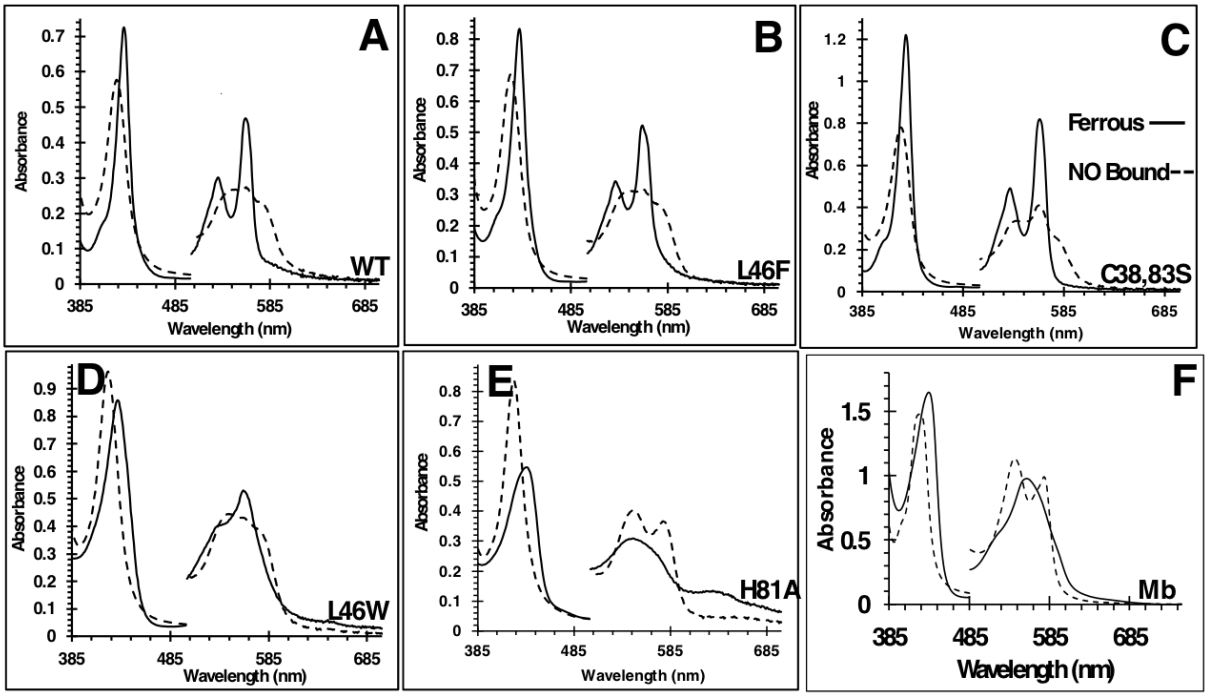

Figure 3.3.1.1 Initial (——) and final (-----) spectrum depicting deoxyferrous and NO bound (800 μM) cytoglobin for wild type (A), C38S/C83S (B), L46F (C,) L46W (D) H81A (E) and Mb (F). These spectra display the spectra characteristics of deoxyferrous and NO bound species in mutant and wild-type proteins. Initial spectrum represents species in which the sixth coordination site is occupied by the endogenous ligand, while the final spectrum represent species in the sixth coordination site is occupied by NO. Mb was added for comparison.

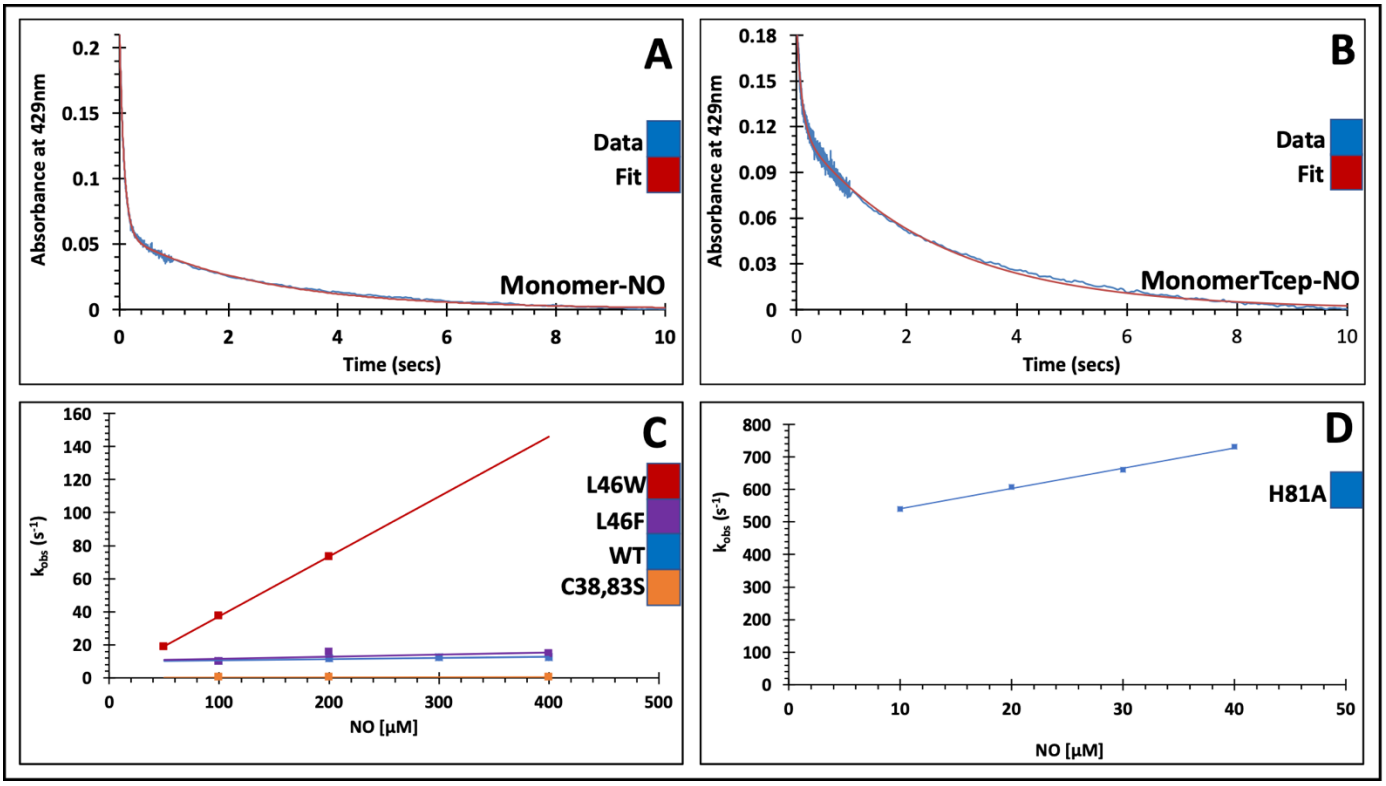

Figure 3.3.1.2 The effects of specific mutations on the kinetics of NO binding in monomeric cytoglobin. (A) Biphasic kinetic time course illustrated by monomeric WT Cygb with predominantly fast rate of NO binding. (B) TCEP reduced disulfides increase the amplitude of the slow NO binding . (C and D) The effect of mutations on the NO binding kinetics of specific muations as a function of NO concentration. WT Cygb (blue) and L46F (purple) Cygb exhibit a rate constant of ~10 s^{-1} that is NO concentration independent. The C38S mutant showed a much lower rate constant of 0.2 s^{-1}, also NO concentration independent. The L46W mutant showed concentration dependent NO binding with a second order rate constant of 3.64 x 10 $M^{-1}s^{-1}$. For H81A (panel D) some concentration dependence on NO binding was observed but was much more rapid compared to the other forms of the protein.

3.3.2 Effect of mutation on the nitrite reductase activity.

The reaction of deoxyferrous Cygb with nitrite in the presence of a small excess of dithionite leads to the consumption of nitrite by the deoxyferrous species and generation of ferrous NO-bound protein (chapter 2 section 2.3.3). The optical spectrum in the Soret region is shifted from 429 to 422 nm during the reaction depicting the transition from deoxy to NO-bound form (chapter 2, Figure 2.3.3.2). This transition is also accompanied by a decrease in intensity of the alpha and beta peaks in the visible region. The NiR activity of monomeric Cygb with an $monomer_{S\text{-}S}$ showed biphasic kinetics with fast and slow phases fitted to a double exponential function (Chapter 2, Figure 2.3.3.5). A comparative study of rate constants of the different forms of Cygb ($monomer_{S\text{-}S}$, $monomer_{S\text{-}H}$, $dimer_{S\text{-}H}$, see chapter 2, section *2.3.3* including a double cysteine mutant had assigned the fast phase to the $monomer_{s\text{-}s}$, and the slow phase to the $dimer_{S\text{-}H}$ or $monomer_{S\text{-}H}$. This study also confirms that Cygb monomer, as prepared following expression, has mixted cysteine oxidation. Here the dimeric protein was removed by gel filtration leaving $monomer_{S\text{-}H}$ with free sulfhydryl and $monomer_{S\text{-}S}$ with an intramolecular disulfide with the latter making up ~85% of the protein, similar to that observed with NO binding (chapter 2, Figure 2.3.3.5). The observed second-order rate constant of the NiR activity of WT $monomer_{s\text{-}s}$ as a function of nitrite concentration was 30 $M^{-1}s^{-1}$ (Table 3.3.2.1), essentially identical to that found previously (chapter 2 section 2.3.3), (Reeder and Ukeri, 2017). Mutation of additional residues had profound effect on the NiR activity of Cygb with the H81A and the L46W having the most impact on nitrite dependent generation of NO, the impact of the L46F was an intermediate between the C38S mutation and the WT see table 3.3.2.1. Replacement of the distal histidine by alanine led to ~40 fold increase in the NiR activity, which was in agreement with previous work, removal of the distal histidine disrupts the gating mechanism in the distal pocket, reducing steric hindrance for ligand accessibility (Tejero, 2015, Birukou et al., 2011). The L46F mutation led to a ~2 fold decrease in activity this could due to the smaller phenylalanine side chain creating modest impact on the bulk of distal pocket and equilibrium of the distal histidine. A leucine to phenylalanine mutation on an identical position on myoglobin (L29F) generated similar result on ligand migration to the distal heme pocket, the

minimal effect was reported to be due to smaller the smaller side chain having minimal effect on the bulk of the heme pocket (Scott, 2001). The L46W mutation created ~1000 fold decrease in an activity, previous studies have linked the effect of this mutation on equivalent positions on Mb and Hb to increase in bulk of distal pocket and introduction of steric hindrance(Varnado et al., 2013, Scott et al., 2001). The L46W mutation has also been reported to increase the energy barrier needed for bond formation in the distal coordination site(Scott et al., 2001).

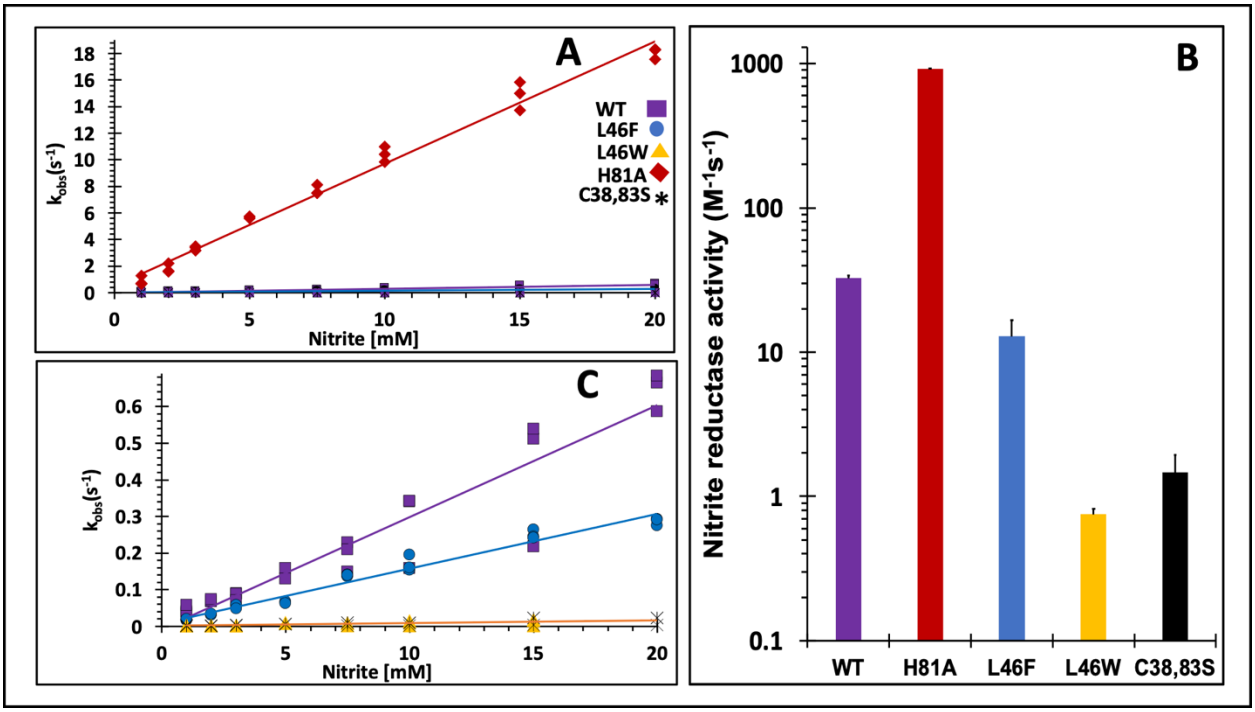

Figure 3.3.2.1 Effect of mutations on the rate constants of the nitrite reductase activity of cytoglobin. (A) The rate constants for the formation of ferrous NO from the reaction of Cygb and nitrite and the effect of mutations on the reaction. WT (■), H81A (◆), L46F (■) and L46W (▲) C38S/C83S (∗). (C) Expanded view of (A), not including H81A mutation. (B) Second order rate constants of NiR in a log scale.

Second order rate constant of the NiR and NOD activity		
Protein	k_{NiR} ($M^{-1}s^{-1}$)	k_{NOD} ($M^{-1}s^{-1}$)
CygbWT	30	>1 x 10^8 ($250s^{-1}$ maximal k)
CygbH81A	1170	-
CygbL46F	15	>1 x 10^8 ($250s^{-1}$ maximal k)
CygbL46W	0.2	1.6 x 10^5
CygbC38S,C83S	0.2	-
CygbC38R,C83R	0.2	>1 x 10^8 ($465s^{-1}$ maximal k)

Table 3.3.2.1. Table shows the second order rate constant of the NiR and NOD activity WT and mutant cytoglobin. This table illustrates the effect of mutagenesis on enzymatic activity of Cygb. The H81A mutation was successful in modulating the NiR activity, increasing it ~40 fold compared to WT protein, with other mutations lowering the activity similar to that of the disulfide reduced protein. The NOD activity is not significantly affected by any of the mutations (with some effect on maximal rate), apart from L46W which shows at least a 1000 fold decrease in NOD activity, but not the L46F mutation.

3.3.3 Effect of mutation on nitric oxide dioxygenase activity

The reaction NO with oxyferrous Cygb can be seen in Figure 3.3.3.1. Here the NO reacts with the oxygen bound to Cygb to generate nitrate (via peroxynitrite) and ferric Cygb (equation 1). The issue with monitoring this reaction is that it is typically very fast with rate constants reported using other globins typically > $1x10^8$ $M^{-1}s^{-1}$ (Gardner, 2005). The initial WT Cygb spectrum immediately following NO addition to oxyferrous Cygb (~1.2 ms) is not that of the oxyferrous species but that of a mainly pentacoordinate ferric Cygb with the final spectra that of the hexacoordinate ferric protein (Figure 3.3.3.1A, upper panel). Therefore, the optical changes observed are typical of the ferric protein relaxing from a pentacoordinate to a hexacoordinate state with the NOD reaction being completly missed within the dead time of the stopped flow. The kinetics of this relaxation is 183-270 s^{-1} fitting to a hyperbola (Figure 3.3.3.1A, lower panel).

For the L46W and C38S/C83S mutations the optical changes and kinetics were essentially identical to that of the WT protein (Figures 3.3.3.1B and 3.3.3.1C). However, the L46W mutant (Figure 3.3.3.1D) shows a concentration-dependent reaction of oxyferrous to the ferric protein is observed, so that the spectrum of the protein immediately following NO addition is still predominantly that of the oxyferrous proteins (Figure 3.3.3.1D, upper panel). The observed rate constant ranged from 3.5 - 22.5 s^{-1} (10-120 μM NO) with a second-order rate constant of $1.6x10^3$ M^1s^1. This value represents a true NOD rate constant for the protein due to the slow rate which can be detected by stopped-flow.

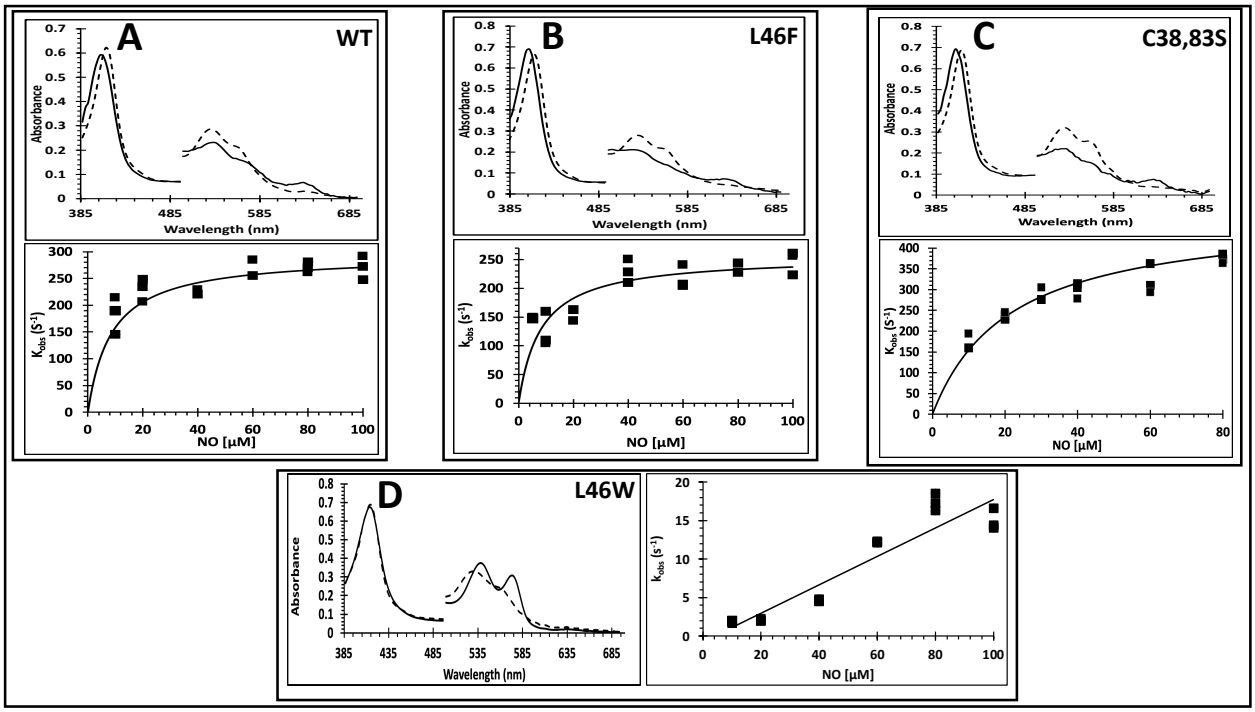

Figure 3.3.3.1. Effect of point mutations of nitric oxide dioxygenase activity of cytoglobin. (A), Change in optical spectra of WT Cygb following addition of NO (20 μM) to oxyferrous protein (5 μM). The first recorded spectrum at ~1.2 ms (solid line) showed ferric Cygb rather than oxyferrous Cygb in a mainly pentacoordinate state. The final spectrum is that of the ferric protein in a hexacoordinate form (dashed line). Lower panel: The kinetics of WT Cygb as a function of [NO] fitted to a hyperbola. (B) Changes in spectra and kinetics for L46F mutation showing similar changes and activity as that of the WT. (C) Changes in spectra and kinetics for C38S/C83S mutation also showing similar changes and activity as that of the WT. (D) Changes in spectra and kinetics for L46W mutation showing that the initial spectrum is primarily still oxyferrous with a significantly decreased rate of oxidation to the ferric protein without exhibiting the pentacoordinate form. All reactions were at 20 °C in 100 mM sodium phosphate pH 7.4.

3.4 Discussion

The NiR activity of WT cytoglobin was successfully decreased by targeting the cysteines (C38S/C83S), which has been earlier reported (via TCEP reduction or by C38R/C83R mutation) to modulate the distal histidine, affecting binding of external ligand to distal pocket (see Chapter 2, section 2.3.3 and (Reeder and Ukeri, 2017). This was in agreement with our current work a ~160 fold decrease was observed in the rate of reaction as a result of point mutant on cysteine. As for the previous study, we assign this effect to a decrease in off rate resulting from a more relaxed endogenous distal histidine(Zhou et al., 2017). The effect of cysteine mutation on the NO binding to deoxyferrous cytoglobin was also observed, with NO having difficulty coordinating to distal binding site due to a more relaxed protein.

Replacement of the distal histidine by a smaller ligand (H81A), led to rapid biochemical activity in cytoglobin supporting gating effect of distal histidines on hexacoordinate globin, a property reported in myoglobin and hemoglobin, in the histidine modulate binding of external ligand to the distal site (Olson et al., 1988). Removal of this histidine reduces steric hindrance leading rapid ligand binding to the distal site, the distal ligand is known to modulate ligand entry to distal coordinate site in hemoglobins (Birukou, Schweers and Olson, 2010). However, introducing large residues to by points mutation on residues bordering the distal histidine led to decrease activity in relation to size of residue. The L46F residue led to decrease in activity but not as much as the larger L46W see table 3.3.2.1.

The effect of mutation on ligand migration at the distal pocket of myoglobin have been studied by Olson et al. While the histidine gating mechanism is primary route for ligand entry to the active site of the protein, secondary pockets and alternative cavities play an important role in ligand coordinated to to the central heme iron, these site also enable ligand achieve conformation needed to bond to protein (Scott, Gibson and Olson, 2001). In these studies Olson et al were able to attenuate ligand entry the L29W mutation in myoglobin similar to results achieved in present study.

At higher [NO] the number is not the maximum velocity of the reaction (as given by the Michaelis Menten equation) but the k_{on} of the distal histidine. At lower [NO] the lack of NO is having an impact of the NOD reaction, although this is unclear as to the mechanism of action. In previous studies on the NOD activity of globins, it is often reported that rates of NOD are of the order of a few hundred per second (Brunori et al., 2005). Here we show that this is not the true NOD activity but merely the settling of the heme pocket geometry. Although Hb is initially pentacoordinate, some change in heme pocket geometry cannot be ruled out as these studies typically use single wavelength measurements. This may cast doubt on the interpretation of the results in the literature (Gardner, 2005).

Previous work looked the impact of the L29F and L29W (reflected as L46F and L46W on Cygb see figure 3.3.2), mutation on ligand migration in myoglobin, the L29F mutation had minimal impact on ligand entry to myoglobin in contrast with L29W mutation which markedly affected ligand migration the reason for this was increasing the energy barrier making bond formation more difficult (Scott, Gibson and Olson, 2001). The NO binding data (Figure 3.3.1.2) shows that the L46W changes the NO binding, increasing the rate (but not as fast as the H81A) and makes the rate not dependent on the slow off rate for the distal histidine. This may mean that the distal histidine off rate is increased by the L46W mutation, further experiments may reveal this. However, the suppressed NOD activity of the L46W may not be a reflection of this change in histidine off rate as the Cys mutations (or TCEP reduction) also changes the histidine off rate (Beckerson, Reeder and Wilson, 2015) but does not alter the NOD, only the NiR (the same happens with the L46W and L46F mutations (see Figure 3.3.2.1).

These mutations create specific changes in the potential physiological activities of Cygb suggested throughout the literature. Although more work needs to be done to examine the effect of these mutations on other potential functions, oxygen binding affinity (Ostojic et al.,

2006), peroxidase activity (Beckerson et al., 2015), particularly with lipids (Reeder, Svistunenko and Wilson, 2011), this work provides an pathway to examine the effect of these mutations in cell lines. For example, it is believed that Cygb plays a role in NO homeostasis and that this may be linked to the protection by Cygb of certain cancers, particularly hypoxic ones(Shaw et al., 2009). Measuring the cytoprotective effect of upregulated (or in this case induced) mutant Cygb expression in cancer cell lines (be the muations enhance or suppress specific activities) may inform on the potential mechanism of their protective effect in vivo. NO homeostasis also plays an important role in cancer pathology(Choudhari et al., 2013), attenuating the NOD and NiR activity of Cygb by mutagenesis could serve therapeutic frame work to help sensitise tumours to oxidative stress (McRonald, Risk and Hodges, 2012).

Chapter 4

Probing the heme pocket of Cygb through photolysis of the ferrous NO complex: The effects of an intramolecular disulfide bond.

4.1 Introduction

Cytoglobin (Cygb) is a vertebrate hemoglobin the functions of which are not fully understood (Burmester et al., 2002). Cygb hexacoordinate member of the human globins which also includes neuroglobin (Ngb) and androglobin (Adgb) (Burmester et al., 2000c, Burmester et al., 2002) (Hoogewijs et al., 2012). Expression studies have shown ubiquitous expression of Cygb with presence identified in a wide array of tissues (Shigematsu et al., 2008a). Cygb is a low expression protein with concentration estimated to be 5μM in smooth muscle cells (Zweier and Ilangovan, 2020).

Cygb and the new additions to the human globin family (including Ngb) are hexacoordinated (De Sanctis et al., 2004b), having an intrinsic ligand occupying the sixth coordination site of the heme iron in the distal pocket (De Sanctis et al., 2004b). This differs from other members of the human hemoglobin family (hemoglobin and myoglobin) which have the sixth coordination site vacant in the absence of external ligand (pentacoordinate) (Uppal et al., 2016).

Cygb has a distal histidine (His81) which occupies the sixth coordination site of the iron. Therefore, the binding of external ligands have to displace the endogenous distal histidine to access the heme iron distal site (Sawai et al., 2005, Sawai et al., 2003, Beckerson et al., 2015b). This leads to competitive ligand binding between exogenous and endogenous ligands (Trent et al., 2001).

Cygb have been reported to confer cancer therapy resistance (Chakraborty et al., 2014, Fang et al., 2011), and play a role as a tumour suppressor gene (Zhang et al., 2019, Rowland et al., 2019). Other proposed physiological functions of Cygb includes collagen synthesis (Schmidt et al., 2004a), lipid peroxidase activity (Beckerson et al., 2015c, Tejero et al., 2016b), peroxidase activity (Li et al., 2007), oxygen sensing (Schmidt et al., 2005, Ostojić et al., 2006), scavenging of reactive oxygen species and nitrogen species (McRonald et al., 2012, Singh et al., 2014, Wen et al., 2017). Cygb has been suggested to be an NO dioxygenase and nitrite

reductase (Halligan et al., 2009b, Li et al., 2012a, Zweier and Ilangovan, 2020), consumption of NO has been observed to be in a oxygen dependent manner (Liu et al.), and generation of NO from nitrite is relatively rapid with a second order rate constant of ~30 $M^{-1}s^{-1}$ making Cygb the fastest nitrite reductase among mammalian globins (Reeder and Ukeri, 2017). The role of NO homeostasis is thought to be a regulatory mechanism to protect tissues against hypoxia (Avivi et al., 2010, Liu et al., 2013, Zhang et al., 2017). Hence it been proposed that Cygb functions as a nitrite reductase (NiR) hypoxic tissues generating NO and NO dioxygenase (NOD) In normoxic tissues consuming NO, the NiR and NOD may function as a signaling route to vasodilatation through NO production, and vasoconstriction through NO consumption (Liu et al., 2012a, Liu et al., 2017b). This strongly suggests the role Cygb in relation to NO homeostasis (Reeder and Ukeri, 2017, Zweier and Ilangovan, 2020) and is explored in chapters 2 and 3.

Cygb has two surface exposed cysteines capable of forming a disulfide bond (Sugimoto et al., 2004), due to positioning of the cysteines on Cygb adjacent to each other on the E and B helices (B2 and E9) a disulfide bond can be formed within a monomeric subunit (intramolecular) or two bonds can be formed between two monomeric units (intermolecular) (Lechauve et al., 2010).

Depending on the oxidation state of the cysteines, as expressed recombinantly in *E. coli,* Cygb has been observed as monomer with intramolecular disulfide bond, monomer with free sulfhydryl groups, dimer with intermolecular disulfide bond (Lechauve et al., 2010, Beckerson et al., 2015b, Beckerson et al., 2015f). The oxidation state of the cysteines and the oligomeric state of Cygb *in vivo* is currently unknown, however, due to its low cellular concentration and the generally reductive state of the cytoplasm the protein may be monomeric with free sulfhydryl, and disulfide bond formation occurring upon an oxidative insult (Cumming et al., 2004, Backer et al., 2018).

The distal histidine is located on the E helix of this protein (Makino et al., 2006b), the formation of an intramolecular disulfide bond, is thought to create compact structure in which the distal histidine is pushed away from the heme iron in the distal pocket making it more accessible to

external ligands, the lack of the disulfide bond creates a more relaxed structure, in which the distal histidine is closer to the distal coordination site making it less accessible to exogenous ligands (Lechauve et al., 2010; Tsujino et al., 2014). As discussed in chapter 2, the intramolecular disulfide bond in the monomeric protein extensively alters the distal histidine off rate, hence altering the hexacoorrdinate-pentacoordinate equilibrium and binding exogenous ligands (Beckerson et al., 2015b, Reeder and Ukeri, 2017). Flash technique is widely used to examine rapid ligand binding properties, especially those of bimolecular photo-labile ligands like NO and CO (Hoffmant and Gibsont, 1978, Kobayashi et al., 1982, Hargrove, 2000). The same technique has been applied to probe ligand binding properties of hexacoordinated like rice hemoglobin (Trent et al., 2001).

In this chapter the effect on cysteines on recombination kinetics of CO and NO with Cygb have been explored. Previous reports have shown that the formation of intramolecular disulphide bond in monomeric cytoglobin, favours the pentacoordinate conformation, leading to rapid ligand (CO, nitrite), binding kinetics in Cygb populations with this bond (Beckerson et al., 2015b). Other studies have reported cysteine dependent heterogeneity on the binding migration pathway of Cygb, introduced to Cygb populations as a result of the redox states of the cysteine residues (Astudillo et al., 2013a). Here we probe the effect of disulfides and ligand migration pathway, using recombination kinetics of NO following femtosecond and nanosecond laser flash photolysis, along with stopped-flow binding kinetics of NO and CO, examining the effect of the cysteine redox state of Cygb on the ligand binding and recombination kinetics.

4.2 Materials and Methods

4.2.1 Nitric oxide binding

The binding of NO to deoxyferrous Cygb was followed using an Applied Photophysics SX20 stopped flow spectrophotometer fitted with a diode array. Degassed sodium phosphate buffer (100 mM, pH 7.4) was prepared as described above. Buffer was transferred anaerobically to

volumetric flasks (10 ml) that were pre-purged with argon. Using a Hamilton syringe stock concentrated solutions of monomer and dimer Cygb were added in 10ml volumetric flasks to give a final of concentration 10 μM. Degassed protein was transferred anaerobically to 5ml glass syringes, minimum (μM range) sodium dithionite was introduced into glass syringes to reduce the protein and to remove trace oxygen. Dithionite can slowly reduce disulfides as shown in section 2.3.3. Here dithionite was added immediately prior to data collection on the stopped-flow was within minutes to ensure that degradation of disulfides in monomer samples was minimized. The optical spectrum was measured by diode array spectroscopy to ensure protein was fully in the deoxyferrous form.

Stock proli-NONOate was prepared to a 40 mM stock solution from the crystalline solid, in sodium hydroxide (25 mM) to prevent degradation and purged with argon to remove bulk oxygen molecules from solution, however trace oxygen still remains in solution. Stock proli-NONOate solution was mixed with degassed buffer to make NO concentrations of 40-320 μM (20 – 160 μM after mixing). Deoxyferrous protein was rapidly mixed with NO in a 1:1 ration using the stopped-flow and optical spectra monitored between 350 and 750 nm.

4.2.2 Nitric oxide binding via nanosecond flash photolysis

NO was dissociated from ferrous Cygb by laser flash photolysis using an Applied Photophysics LKS80 laser flash spectrophotometer. The rebinding of NO to Cygb following photo-dissociation was monitored optically. Degassed buffer (100 mM sodium phosphate buffer, pH 7.4) was prepared using a tonometer and a vacuum pump connected to a glass tap via a custom setup that allowed for repeated degassing cycles and purging with argon. The degassed buffer was transferred anaerobically to a 10ml glass syringe.

Using a Hamilton syringe a concentrated stock solution of monomeric or dimeric Cygb was diluted to a glass syringe with degassed buffer giving a final cytoglobin concentration of 10 μM. Sodium ascorbate (10 mM final concentration) and ascorbate oxidase (0.5 U final concentration) were used to reduce the protein, to remove trace oxygen and also preserve the

integrity of the disulfide bonds during the course of the experiment. A cuvette, sealed using a rubber suba-seal septa, was purged with argon and the protein was transferred anaerobically from the syringe. The spectrum was collected to ensure protein was fully in the deoxyferrous form using an Agilent 8453 diode array spectrophotometer. Stock proli-NONOate solution was mixed with protein to final concentrations of 20 – 160 μM NO, under these conditions proli-NONOate rapidly degrades to generate two molecules of NO. The photo-labile NO-Fe bond was broken by a 10 ns laser pulse at 532 nm and recombination of NO to Cygb was monitored at a single wavelength (averaged over 10 laser flashes). Difference spectra were constructed by repeating the photolysis and monitoring wavelengths between 400 – 450 nm at 5 nm intervals.

4.2.3 Nitric oxide binding via femtosecond flash photolysis

Ultrafast broad-band transient absorption experiments at a 500 Hz repetition rate, were performed as previously described.16 Pump pulses centered at 520 or 570 nm were generated using a home-built, non-collinear optical parametric amplifier, and centered at 390 nm by frequency doubling of the fundamental beam. To ensure sharp cut-offs, the pump pulses were spectrally tailored using suitable interference filters. The sample was mounted in a sample holder thermostated at 8 °C and continuously rastered by a Lissajous scanner. Global analysis of the data in terms of multiexponential functions, and taking into account the dispersion of the probe beam, was performed using Glotaran.17

4.2.4 Modelling of NO binding to monomeric Cytoglobin

Ligand binding modes of NO to monomeric cytoglobin was modelled and calculated using the AutoDock suite (Trott and Olson, 2010). Coordinate file for receptor, was prepared from Cygb structure pdb id: 2DC3, chain b extracted from the dimeric structure and used as file for receptor. The ligand (NO) was obtained from the protein data bank rcsb.org (Berman et al., 2000). A single docking experiment was performed and output file visualised on PyMOL (Schrodinger, 2015).

4.3 Results

4.3.1 Nitric oxide and carbon monoxide binding to cytoglobin by stopped-flow

As previously reported the ligand binding kinetics of Cygb are dependent on whether an intramolecular disulfide bond is present or absent [8,14]. Binding of either CO or NO to hexacoordinate Cygb is rate limited by the dissociation rate constant of the histidine residue occupying the 6th coordination position of the iron (his-off rate constant). This dissociation is relatively rapid (~10 s^{-1}) when the intramolecular bond is present (monomer$_{S\text{-}S}$**)** but much slower (~0.5 s^{-1}) when it is absent as in the (monomer$_{S\text{-}H}$**)** or in the dimer with the intermolecular disulfide bond (dimer$_{S\text{-}S}$**)** (Beckerson et al., 2015b). It has not been proven possible to prepare pure single molecular species lacking intra s-s bond, presumable because sulfhydryl exchange may occur spontaneously in solution (Lechauve et al., 2010). However, it is possible to prepare samples in which the monomer$_{S\text{-}S}$ is either the predominant species or a minor form. This is illustrated in Figure 4.3.1.1 in which CO and NO binding time courses are Fhown in Figure 4.3.1.1 A and B illustrate binding to Cygb samples either primarily monomer$_{(S\text{-}S)}$ or a dimer$_{(S\text{-}S)}$ preparation. Figure 4.3.1.1A shows the time course for NO binding to a monomer$_{(S\text{-}S)}$ preparation and exhibits biphasic kinetics with a large fast phase (~10 s^{-1}), and the slower phase (~0.5 s^{-1}). Figure 4.3.1.1 B shows the comparable data for NO binding to the dimer$_{(S\text{-}S)}$ in which we observe a major slow phase (~0.5 s^{-1}) and a minor faster component (~10 s^{-1}). For the monomeric protein we surmise that the two rates reflect a mixture of components, relating to the presence or absence of the intramolecular disulfide bond (monomer$_{S\text{-}S}$ and monomer$_{S\text{-}H}$ respectively). The dimer also exhibits biphasic binding kinetics, except here there are mainly dimeric species, and a minor fraction (<15 %) of monomer$_{S\text{-}S}$. The reactions for monomer and dimer with CO are given in Figure 4.3.1.1 C and D where the same pattern is observed as seen in Figure 4.3.1.1. A and B and with essentially the same rate constants. Table 4.3.1 reports effect of the disulfide bonds on CO and NO binding on Cygb monomer$_{S\text{-}S}$, monomer$_{S\text{-}H)}$ **or** dimer$_{S\text{-}S}$.

The data provides strong evidence that the rates observed are independent of the nature of the ligands but are rate limited by the His-off rates in the different molecular species.

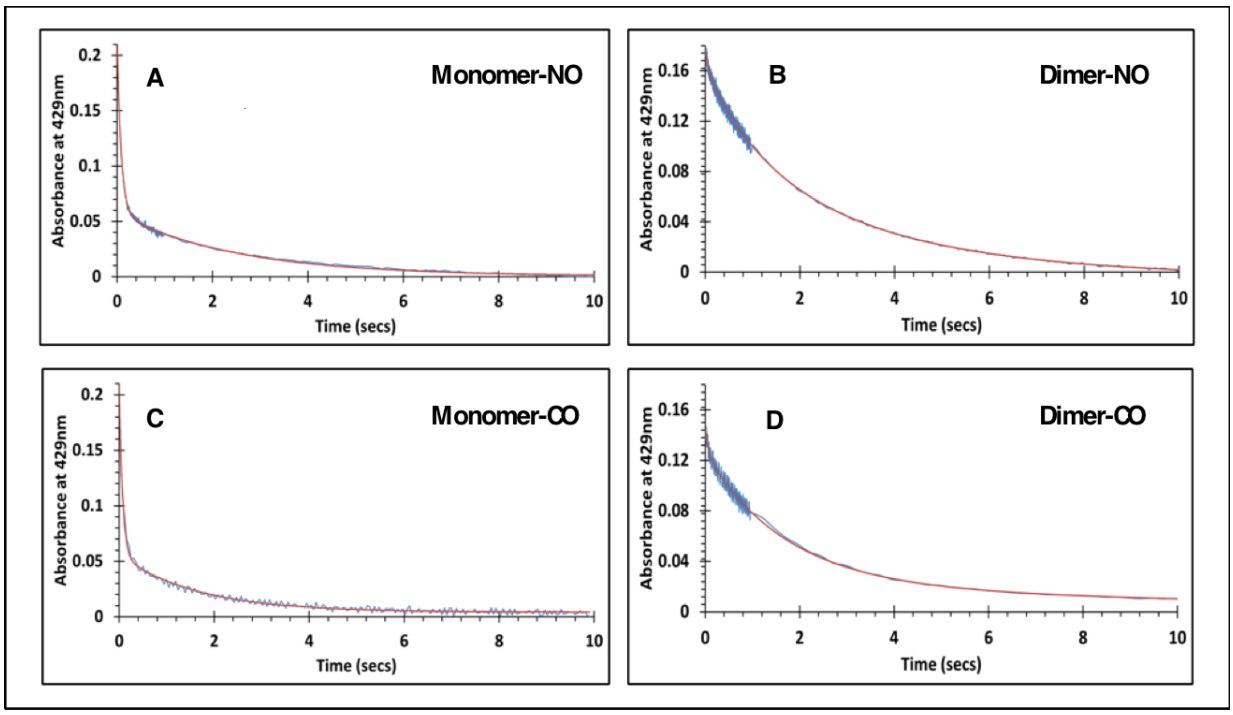

Figure 4.3.1.1. Time courses of NO (20 μM, A and B) and CO (400 μM, C and D) binding to deoxyferrous cytoglobin (5μM) in 100mM sodium phosphate buffer (pH 7.4) at 20 ºC. All time courses were followed at 429nm, showing the loss of the un-ligated deoxyferrous species of either the monomeric (A and C) or dimeric (B and D) protein. The data points are shown in blue and the fits to double exponentials in red. The amplitude and rate constants derived from the fits are given in table 4.3.1.

Protein Preparation	Ligand	Amplitude (Fast)	Amplitude (slow)	Rate constant (fast) s^{-1}	Rate constant (slow) s^{-1}	% Fast	% Slow
Monomer	NO	0.167	0.054	12.0	0.42	73.8	26.2
Monomer	CO	0.158	0.051	15.4	0.61	75.4	24.6
Dimer	NO	0.0163	0.165	12.8	0.55	9.0	91.0
Dimer	CO	0.018	0.126	13.3	0.59	12.9	87.0

Table 4.3.1 Amplitude and rate constants for NO (20 μM) and CO (400 μM) binding to Cygb (5 μM).

Representing predominantly biphasic and predominantly mono-phasic in $monomer_{S\text{-}S}$ and $dimer_{S\text{-}S}$. The amplitudes represent the ratios of $monomer_{S\text{-}S}$ in monomeric Cygb for the fast phase and the $monomer_{S\text{-}H}$ and $dimeric_{S\text{-}S}$ Cygb for the slow phase. Data calculated from the time courses seen in figure 4.3.1.1. n=3.

4.3.2 Nanosecond laser photolysis of cytoglobin monomer and nitric oxide.

The NO-bound ferrous Cygb forms of the protein containing either predominantly monomer$_{S\text{-}S}$ or molecular forms lacking the intramolecular disulfide bond i.e. monomer$_{S\text{-}H}$ and the dimer$_{S\text{-}S}$ were further investigated by laser flash photolysis (10 ns light pulse, this section) or by ultrafast laser photolysis (4 fs light pulse, section 4.3.3). Conventional laser photolysis employing a 10 ns pulse reports on rebinding of NO to the heme from bulk solution while the ultra-fast pulse allows the study of geminate recombination from within the heme pocket.

At high NO concentrations (80-160μM) recombination of NO from bulk solution followed a single exponential time course for over 90% of the total amplitude change. The amplitude of this signal monitored as a function of wavelength was used to construct the spectrum for NO binding and this is shown in Figure 4.3.2.1 where (after normalization - see legend) it is compared with the difference spectrum of deoxy Cygb ***minus*** NO adduct taken by a scanning spectrophotometer. It is clear from this comparison that these two spectra are very different in peak position, with the peak and trough being ~10 and 6 nm different respectively. Also shown is the deoxy minus NO adduct difference spectrum obtained using the His81Ala mutant, taken by a scanning spectrophotometer, in which the sixth coordination position of the deoxy form is vacant. Comparison of the kinetic spectrum of the WT and that of the static spectrum of the mutant shows that these are more closely similar. We interpret this to mean that the fast phase of the recombination, seen in conventional nanosecond laser flash photolysis and at high [NO], reports binding of NO to the penta-coordinate heme unperturbed by the intrinsic histidine ligand i.e. rebinding of NO occurs before the distal histidine residue has time to rebind to the heme.

At low NO concentrations (~20 μM) the time course for NO recombination following photolysis was biphasic (Figure 4.3.2.2). At some wavelengths (e.g. 425 nm) the fast and slow phases made differing and/or opposite spectral contributions to the overall absorbance change (Figure 4.3.2.2 inset). The total amplitude of the absorbance change, i.e. including both phases, is shown in Figure 4.3.2.2 (red line), where it is seen to differ from the spectrum collected at the higher NO concentration (blue line). This is to be expected given the slow phase now makes

a spectral contribution. The amplitude of the faster phase, monitored as a function of wavelength, exhibited the same spectral distribution as the fast phase (Figure 4.3.2.1, discussed above) identified with NO binding to the penta-coordinate heme. The spectrum associated with the slow phase was determined by obtaining the difference spectrum between the total absorbance change and that of the fast phase. This spectrum is given in Figure 4.3.2.2 (purple line) where it is comparable in shape with that obtained of the WT protein statically (i.e. hexacoordinate ferrous form minus the NO adduct, green line). It is apparent that the two spectra are more closely similar indicating that the slow phase reports NO binding to the hexacoordinate species resulting by the initial out-competing of the histidine rebinding to the heme following photolysis.

The interpretation of the data given above is consistent with data on CO binding to Cygb and with the literature on ligand binding to hexacoordinate heme proteins (Smagghe et al., 2006, Beckerson et al., 2015b, Beckerson et al., 2015). A model that describes the reactions is given in Figure 4.3.2.3. Prior to flash photolysis Cygb exists in the NO-bound ferrous state. Laser photolysis leads to the formation of pentacoordinate ferrous species. Following photolysis this species may either rebind NO to form the NO complex or may bind distal histidine to form the low spin hexacoordinate (His-Fe-His) species. At high NO concentrations rebinding, to form the NO adduct, out-competes His binding while at low concentrations NO binds more slowly and His binding effectively competes.

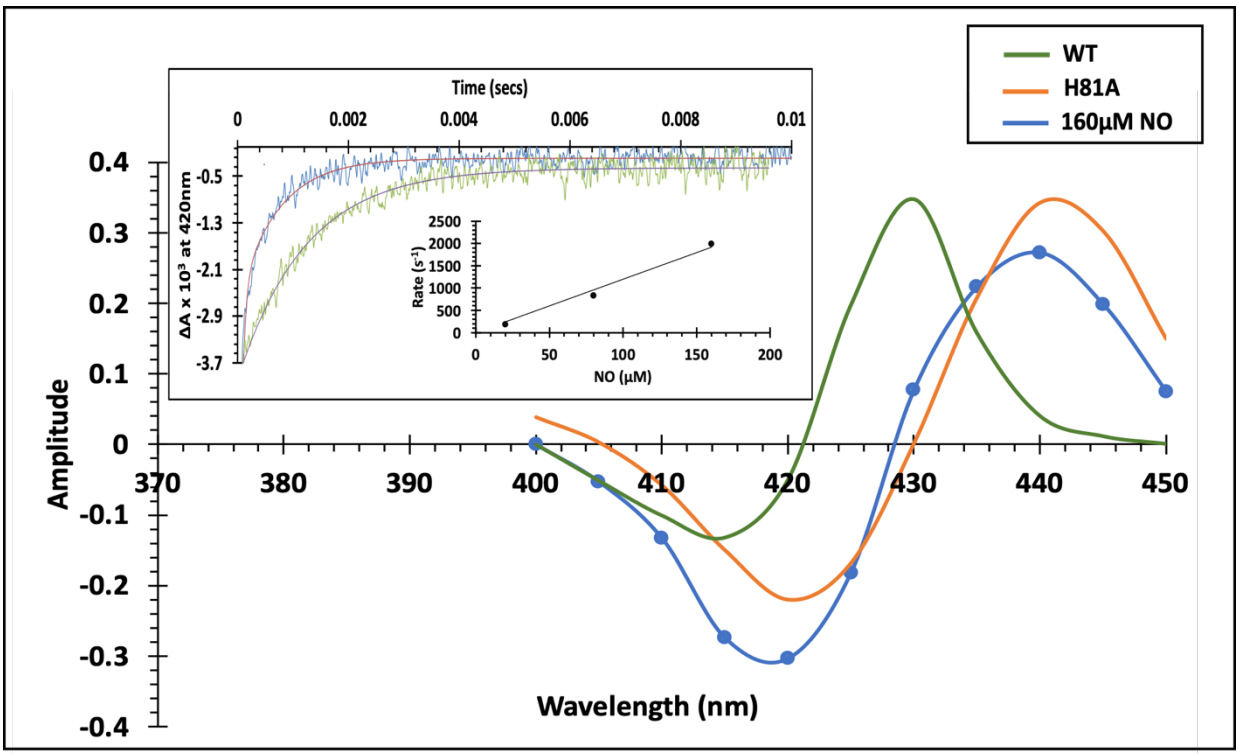

Figure 4.3.2.1 High concentration nitric oxide recombination to pentacoordinate cytoglobin. Comparison of the static difference spectra (Fe^{2+} minus Fe^{2+}-NO) for WT $monomer_{S\text{-}S}$ Cygb taken by scanning spectrophotometer (green line) and the His81Ala variant (orange line) is compared to the kinetic difference spectrum (Fe^{2+} minus Fe^{2+}-NO) for WT $monomer_{S\text{-}S}$ constructed from the amplitude of kinetic traces following photolysis at the indicated wavelengths (blue line). NO concentration was 160 µM in 100 mM sodium phosphate buffer pH 7.4 at 20 ºC. The kinetic difference spectrum has been multiplied by a factor of 70 to make comparison clearer. The inset illustrates kinetics traces collected at 420nm from WT protein and at NO concentration of 80 µM (green) or 160 µM (blue).

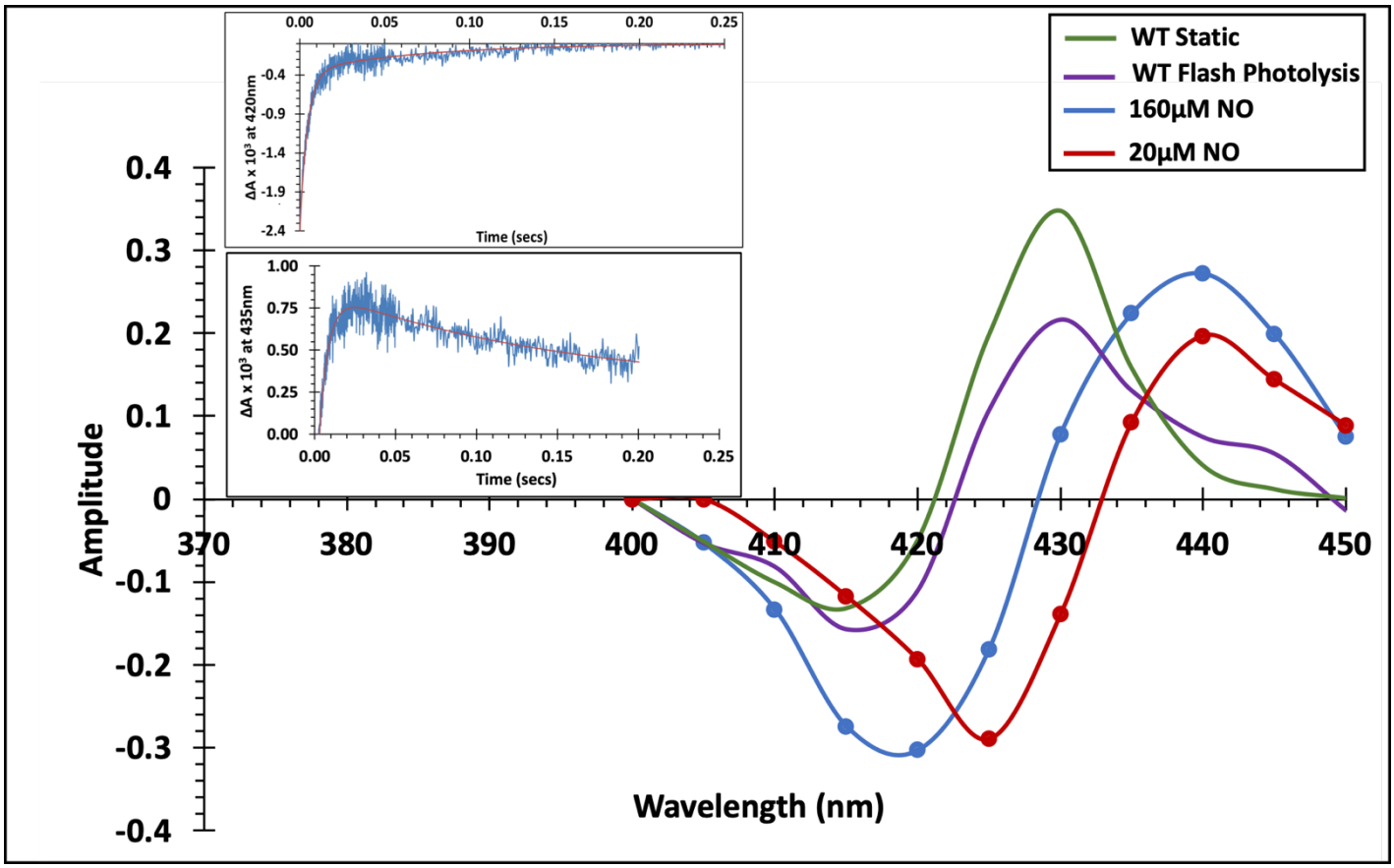

Figure 4.3.2.2 Low concentration nitric oxide recombination to a mixture of pentacoordinate and hexacoordinate cytoglobin. Comparison of the static difference spectra (Fe^{2+} minus Fe^{2+}-NO) for WT $monomer_{S\text{-}S}$ Cygb (green line) with the kinetic difference spectrum (Fe^{2+} minus Fe^{2+}-NO) constructed from the total amplitudes of kinetic traces (slow + fast) following photolysis at the indicated wavelengths at 160 µM NO (blue line), 20 µM NO (red line) and the kinetic difference spectrum constructed from the amplitudes of slow phase at 20 µM NO (purple line). The kinetic difference spectra was multiplied by a factor 70 to make comparison clearer. The inset illustrates kinetics traces collected at 420 nm and 435 nm at 20 µM NO.

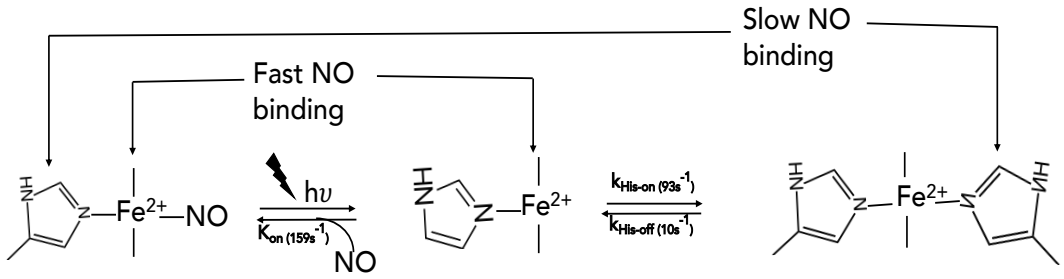

Figure 4.3.2.3. Model for NO recombination to monomeric cytoglobin at following laser flash photolysis. This model illustrates rapid NO migration to the distal coordination site high NO concentration (160μM) or relaxation the distal histidine and subsequent displacement by NO at low NO concentration (20μM) after dissociation of ligands by photolysis.

4.3.3 Laser photolysis of the NO adduct of the ferrous dimer$_{(S\text{-}S)}$ cytoglobin

The dimer$_{S\text{-}S}$ of Cygb behaved in a very similar way to the monomer$_{S\text{-}S}$ described in section 4.3.2. At high NO concentrations the time course for NO rebinding was essentially monophasic with a pseudo-first order rate constant dependent on the NO concentration. At lower NO concentrations a slower phase became apparent. Figure 4.3.3.1 shows a comparison of the difference spectrum associated with NO binding to the pentacoordinate ferrous forms. The spectra for the two forms (monomer$_{S\text{-}S}$ and dimer$_{S\text{-}S}$) are identical both in size and shape thus indicating that the fraction of photo-dissociated NO escaping into bulk solution is the same for both protein forms.

The amplitudes of these fast phases suggest that only ~3-4% of the photo-dissociated NO escapes the heme pocket. This low apparent quantum yield (ϕ =0.03) is within the range typically found for NO photo-dissociation and implies that there must be a large geminate combination process in which photo-dissociated NO recombines with the heme from within the heme pocket and in the ps-ns time range.

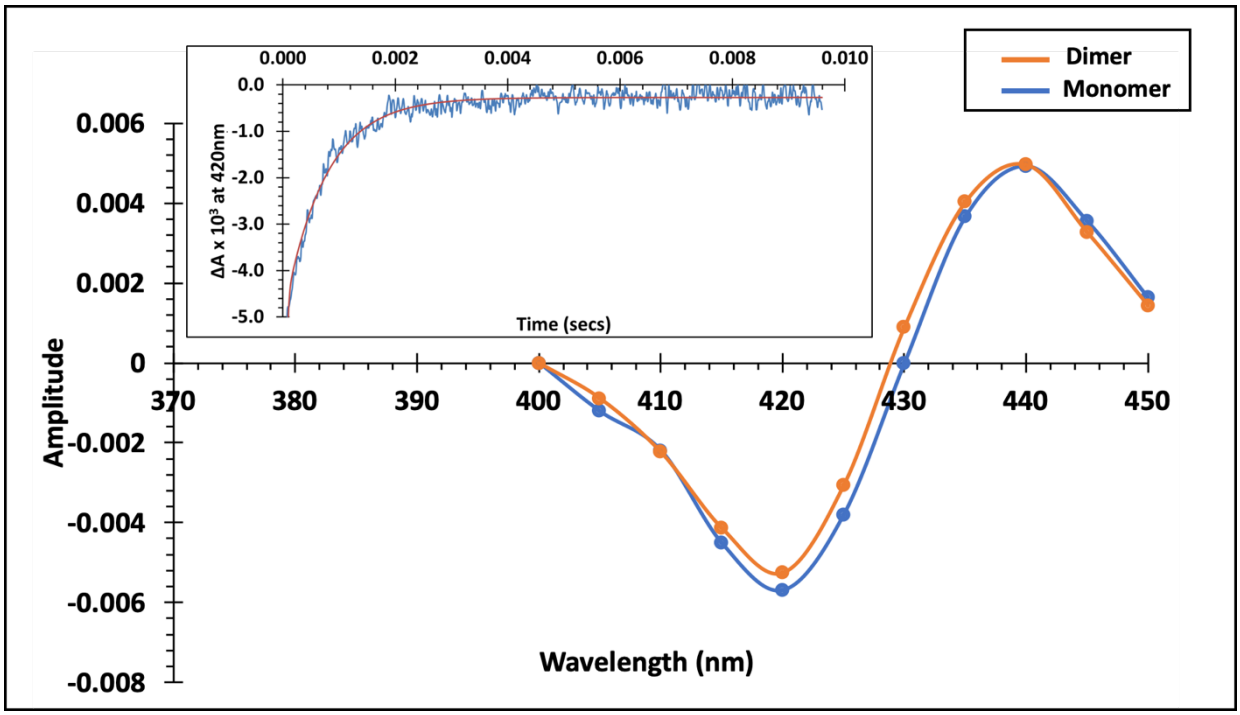

Figure 4.3.3.1 *Spectra comparison of NO recombination after dissociation of NO bound monomer and dimer by flash photolysis.* This figure illustrates the similarity between NO recombination of Cygb monomer and dimer after flash photolysis. This can be observed by the similarity of each difference spectra component obtained from the monomer and dimer after dissociation of NO (120μM) by flash photolysis and subsequent recombination. The inset illustrates kinetics traces collected at 420 nm and is identical to the recombination kinetics of monomeric Cygb at high concentration (80μM & 160μM).

4.3.4 Ultrafast femtosecond laser photolysis of cytoglobin and nitric oxide.

In order to explore the postulated geminate recombination, we undertook a series of ultrafast laser photolysis experiments on the NO recombination of Cygb. The kinetics of the NO rebinding to the different Cygb variants following photolysis where in all cases similar and fitting to sum of exponential gave similar time constants and amplitudes for the spectral transitions. However, the fraction that escapes the bulk (constant phase) differs. In the dimer$_{S-S}$ and monomer$_{S-H}$ it is ~3.5% (± 0.5%), in monomer$_{S-S}$ it is 0.6%, virtually zero within experimental error. The monomer$_{S-S}$ has a substantially larger-amplitude for the ~60 ps phase than the other variants (monomer$_{S-H}$ or dimer$_{S-S}$), suggesting that ligand escape from the heme pocket may occur on this timescale in the other variants. Altogether the results indicate that the presence of the intramolecular disulfide bridge between Cys 38 and 83 prohibits virtually any escape of NO from the heme pocket.

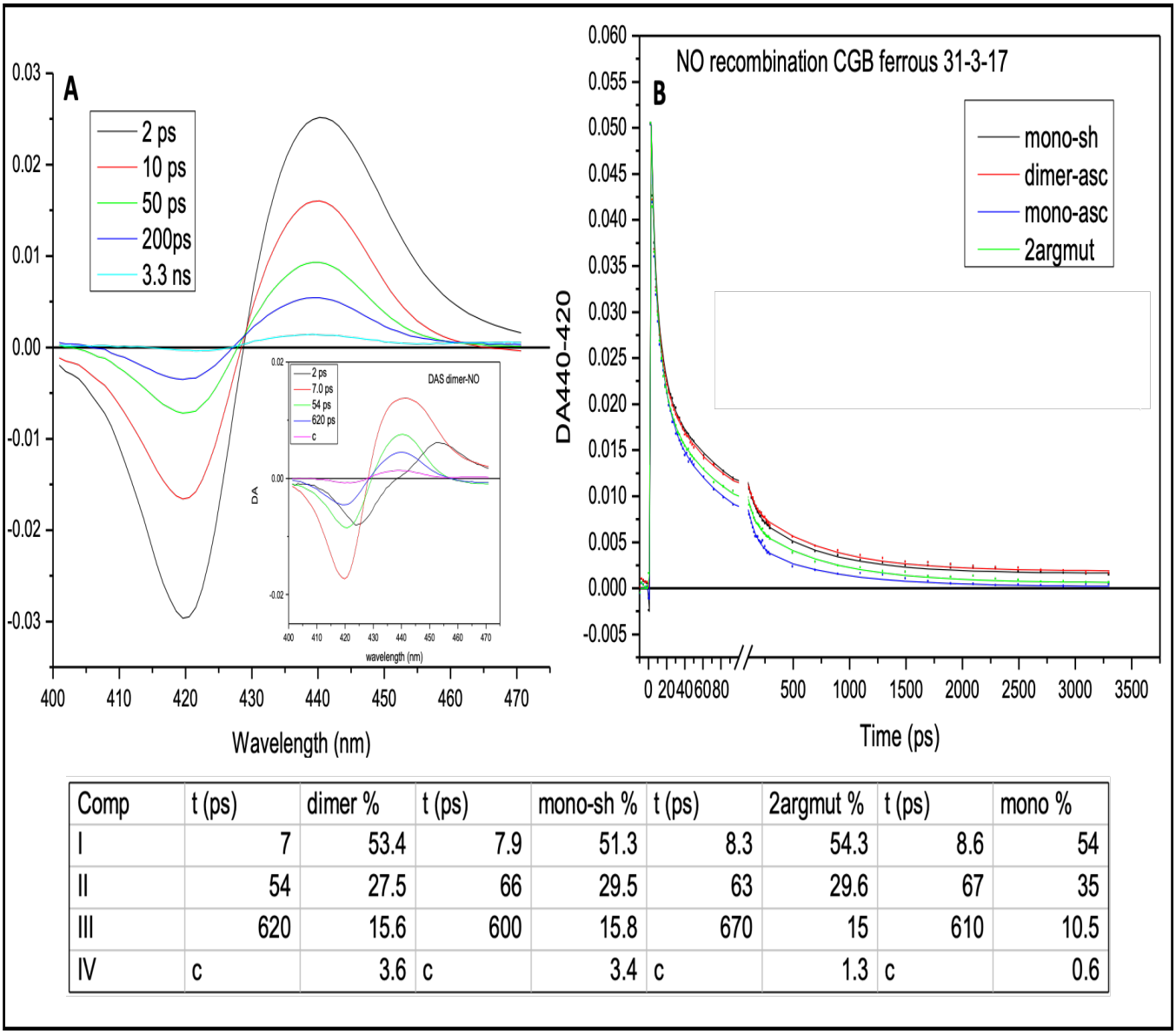

Comp	t (ps)	dimer %	t (ps)	mono-sh %	t (ps)	2argmut %	t (ps)	mono %
I	7	53.4	7.9	51.3	8.3	54.3	8.6	54
II	54	27.5	66	29.5	63	29.6	67	35
III	620	15.6	600	15.8	670	15	610	10.5
IV	c	3.6	c	3.4	c	1.3	c	0.6

Figure 4.3.4.1. Optical changes and kinetics of geminate NO recombination to cytoglobin. (A) The difference spectra (ferrous-NO bound as baseline) consist of a red-shift corresponding to the 5-coordinate minus 6-coordinate NO- bound forms. At short delay times (a few ps) the spectra are more redshifted, presumably due to heating(B) The observed decay as NO recombines with Cygb (monomer$_{(S-S)}$, black line; dimer$_{(S-S)}$ red line, monomer$_{(S-H)}$, blue line and a double mutant (cys38arg/cys83arg), green line) is highly multiphasic, and accounts for ~97% of the amplitude change on the timescale up to 3.5 ns, the rest attributed to NO escaping into the bulk solution. Satisfactory fitting of the data requires 5 components, with time constants of ~2 ps (presumably mostly cooling, see different decay associated spectrum, Inset to (A)), 7 ps, 50 ps, 600 ps and >>4 ns.

4.4 Discussion

Laser flash photolysis have been previously applied ligand binding dynamics studies of CO to hexacoordinate like rice non-symbiotic hemoglobin, in the case of the this globin biphasic recombination kinetics was reported, involving a fast and slow phases linked to an open (penta-like) and closed (hexa-like) conformation (Trent et al., 2001). Similar studies have also be carried out on Ngb, another hexacoordinate member of the human globin family, following photo-dissociation of CO from Ngb by flash photolysis. Four kinetic features were observed, a rapid geminate phase, and extremely fast bimolecular phase, endogenous ligand binding and displacement of endogenous ligand by exogenous ligand (Kriegl et al., 2002). Earlier work probing the recombination kinetics of CO to cytoglobin reported similar kinetics observed in Ngb, at high CO concentration kinetic features represented rapid geminate phase followed by relaxation of intrinsic histidine, at low CO concentration a bimolecular phase and displacement of intrinsic ligand (Beckerson et al., 2015b). The Cytoglobin study mentioned above also looked at how intramolecular disulphide bond formation on monomeric populations, affected recombination kinetics, protein populations with intramolecular disulphide bonds were reported to have alterations on the equilibrium of the distal ligand, shifting the protein to a more open conformation, favouring ligand ligation to the central heme iron (Beckerson et al., 2015b). Here, in this study, we explore the exit and entry route of ligands to the distal binding pocket using ultrafast and conventional photolysis, coupled with stopped flow spectroscopy.

Comparison of Figure 4.3.3.1 and Figure 4.3.4.1 revealed an interesting discrepancy in the fraction of NO that escapes the bulk from the monomer$_{S\text{-}S}$ and the other variants when measured by either conventional nanosecond or ultrafast laser photolysis. Using nanosecond laser photolysis we see that the dimer$_{S\text{-}S}$ and monomer$_{S\text{-}H}$ release identical fraction to bulk determined by the amplitude of rebinding (Figure 4.3.3.1 and Figure 4.3.3.2). While the ultrafast laser data clearly indicate that the dimer release comprises 3-4% of the total and the monomer$_{S\text{-}S}$ only 0.6% (Figure 4.3.3.3). We may reconcile data by noting that the ultrafast

laser allows data collection only up to 4 ns following pulse while the conventional laser can only commence data collection after the laser pulse which is the order of 10 ns in length. Given this we suggest that there is slower relaxation following photolysis that releases NO to bulk that occupies the time region 4 – 10 ns, a region not observed by ultrafast because it too long and not seen in conventional flash photolysis because it is too short, This relaxation will only occur in monomer$_{S\text{-}S}$ but not the other variations (Hamdane et al., 2003, Astudillo et al., 2013a). Structurally this would imply that the intramolecular disulfide bond alters the exit root for NO such that this ligand explores other regions of the interior of the protein before release to bulk (Tsujino et al., 2014b). Although there are no crystal structures for the Cygb monomer$_{S\text{-}S}$ form, there are structures published for monomer$_{S\text{-}H}$ with xenon binding cavities (de Sanctis et al., 2004c). We have used this to examine the potential pathways for NO geminate recombination.

Figures 4.4.1 and 4.4.2 shows the cavities available in Cygb in grey, the xenon cavity identified by crystallography in green and NO in blue and red. Nine binding modes was predicted using AutoDock suite ligand-docking software, with each binding mode occupying a particular position in the protein cavity. Binding modes 2, 8, 4 overlapped xenon pockets identified by x-ray crystallography. Binding modes 1, 3, 6 were in the heme pockets. Mode 7, 5, 9 while proximal to the xenon pockets seems to be protein cavities potentially providing an exit into bulk solution. Therefore, the photo-dissociated NO would likely occupy these three major areas predicted from the AutoDock of the Xe cavity structure. Hence the germinant recombination of NO would also be predicted to stem from these three major areas within the globin structure. This may explain the three major exponentials observed from the ultrafast spectroscopy (Figure 4.3.4.1). Further investigations used site directed mutagenesis to selectively block or impede these cavities could confirm this hypothesis.

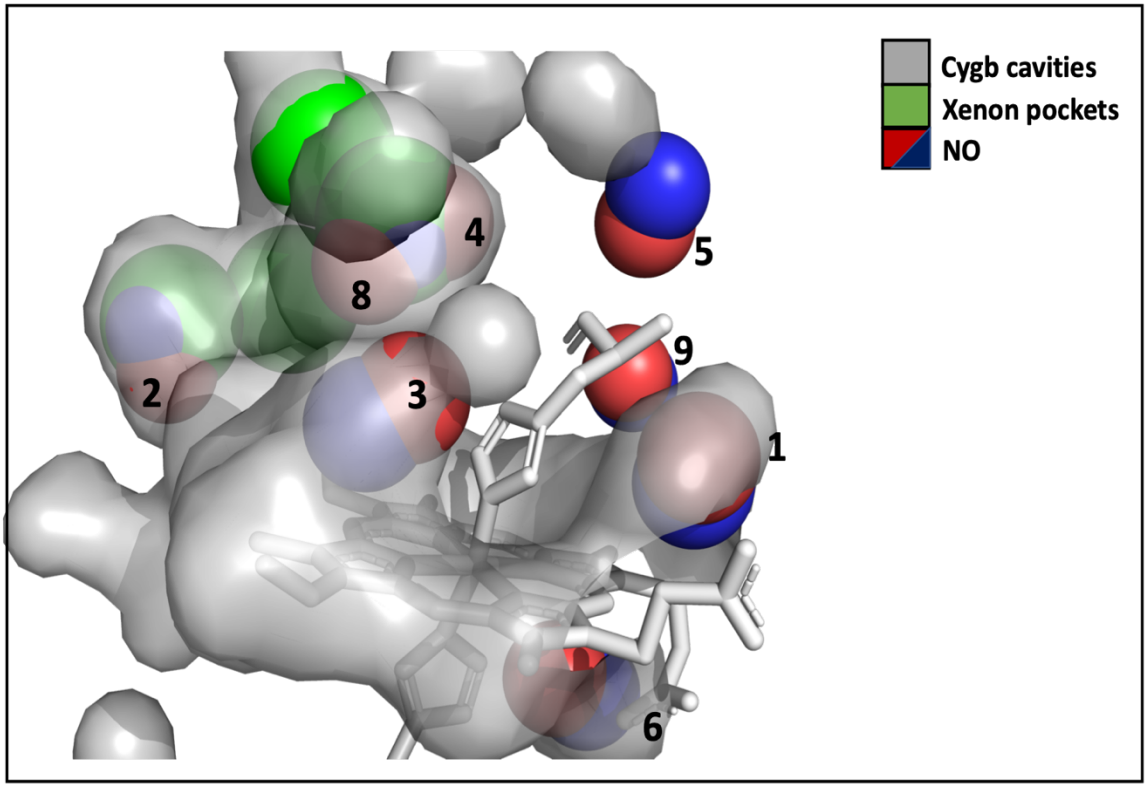

Figure 4.4.1 Protein structure PDB ID:1URY showing cavities in Cygb and predicted NO binding in these cavities. Numbers indicates the potential cavities NO can occupy. AutoDock was used to predict the NO sites.

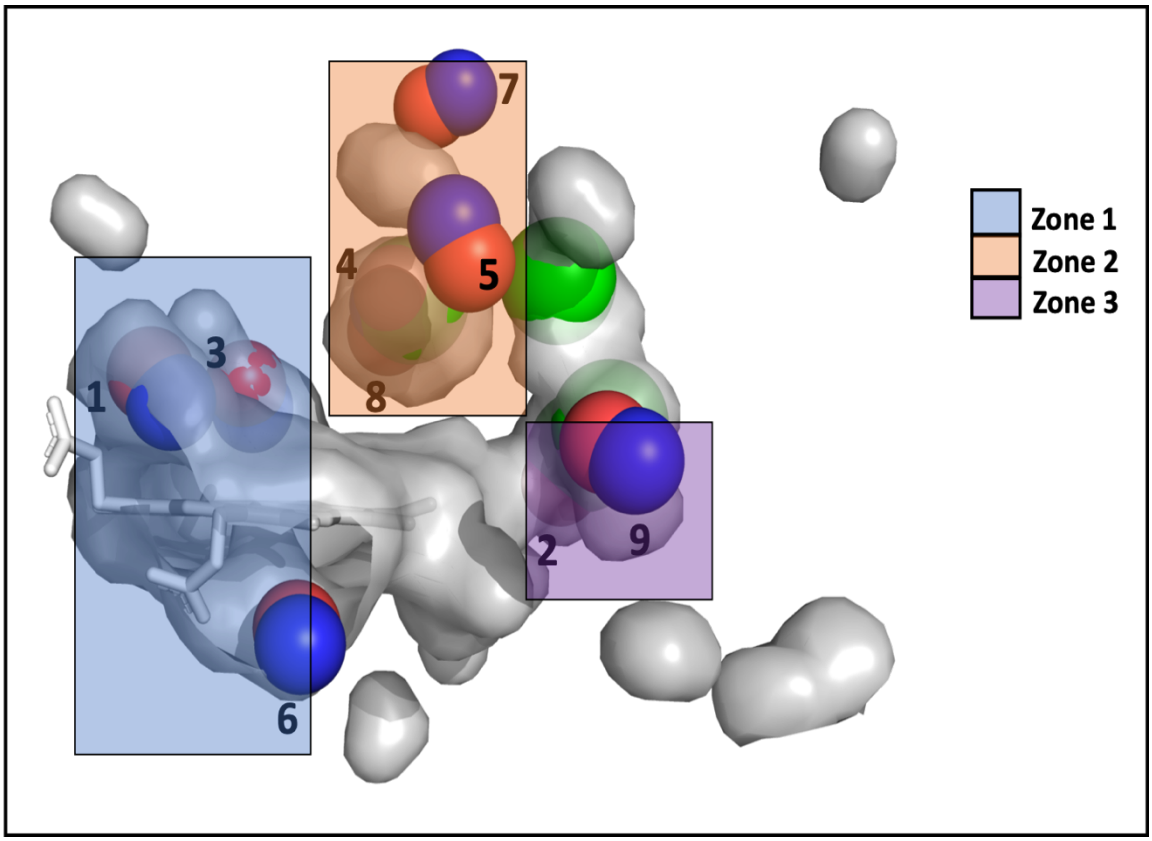

Figure 4.4.2 Predicted pockets occupied by NO using AutoDock suite ligand docking software. Pockets predicted to bind NO were clustered into three zones to fit data observed by ultrafast spectroscopy.

Figure 4.4.3 illustrates a three zone model in which the three different exponential represent different binding sites, at different proximity from the heme iron. Rapid recombination represent a temporary docking site close to distal binging site, and slower recombination a more distant docking site. The proximity of these zones from the distal coordination site and the effect intramolecular disulfide on protein dynamics may account from these three component from ultrafast spectroscopy. A study on the impact of cysteines on CO migration after photo-dissociation, reported different CO migration routes on the $monomer_{S\text{-}S}$ and $monomer_{S\text{-}H}$ form of the protein and alteration of the hydrophobic tunnels on $monomer_{S\text{-}S}$ the form of the protein. This appears to be in agreement with our data. The presence of the intramolecular disulfide bond alters protein dynamics and ligand migration pathway. The ability of this bond form in oxidative environment (De Backer et al., 2018), suggest bonds may serve as redox sensitive switches and signal transducer during oxidative stress (Reeder et al., 2011b).

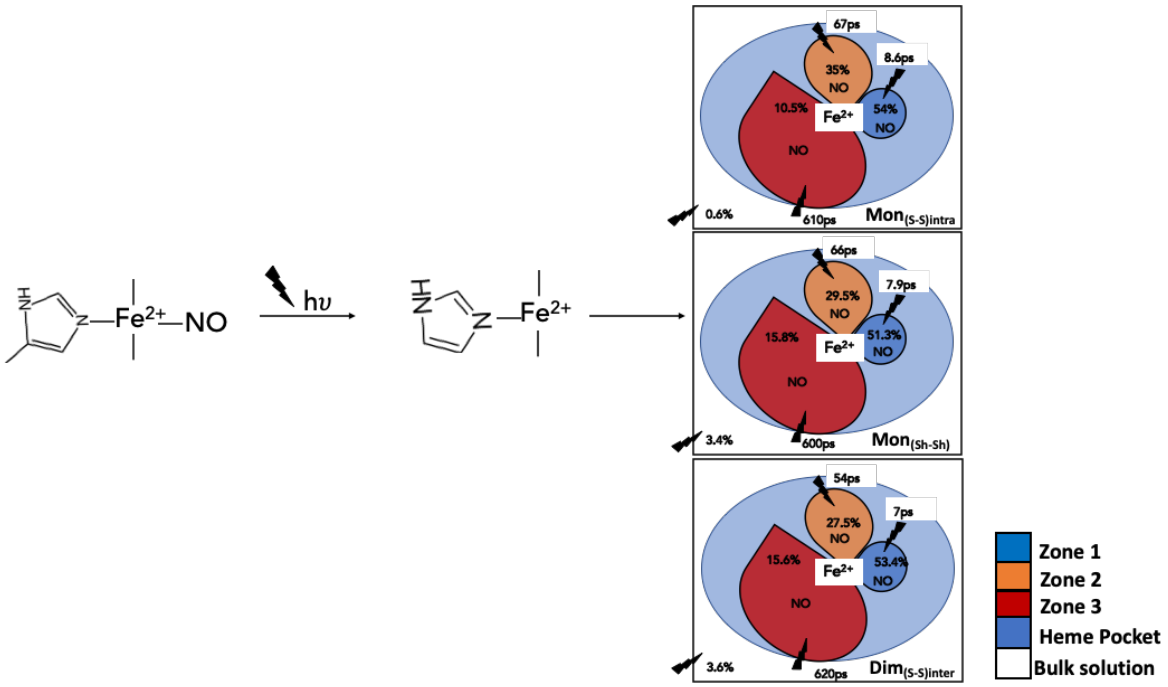

Figure 4.4.3. An illustration of predicted NO recombination ligand migration pathway following flash photolysis. Zone 1 -3 represent predicated regions of occupancy by NO (predicted from the AutoDock, Figures 4.4.1 and 4.4.2), with percentage NO recombination measured by ultrafast photolysis.

Chapter 5

Biochemical and biophysical properties of Androglobin globin domain

5.1 Introduction

Androglobin (Adgb) is newest member of the human globin family, identified as a chimeric protein with a permutated globin domain, Adgb was first discovered in sea urchin, and later found in 30 metazoan taxa along with 22 vertebrates including humans (Hoogewijs et al., 2012). Adgb has 1667 amino in its sequence making it larger than other human globins, which are typically ~120 to 190 amino acids in length, this may suggest a unique role for this globin. Adgb is made of four domains: The N-terminal calpain-like cysteine protease domain is so-called due to its similarity with human calpain-7 (Hoogewijs et al., 2012), see Figure 5.1.1. A circularly permutated globin domain is split in two, sandwiching an internal isoleucine and glutamine (IQ) calmodulin binding motif. A region with no known domain or motive and finally an uncharacterized C terminal domain with an endoplasmic reticulum retention signal. The structure of androglobin is largely unknown, attempts have been to generate possible structure of the globin domain from sequence analysis as seen in Figure 5.1.1 (Hoogewijs, Ebner, et al., 2012)

Very little has been clarified about the characteristics of Adgb. Adgb expression has been associated with post meiotic stages of spermatogenesis with increased expression in fertile males in contrast with infertile male testes, these difference in tissue expression might highlight potential functions of these protein (Hoogewijs, Ebner, et al., 2012). A knockdown experiment in cells showed enhanced apoptosis and repression of proliferation in glioma cell lines due to variations in the levels of several proteins involved in cell proliferation (Huang et al., 2014). The potential physiological roles of the protein are unknown, however, calpains are calcium-activated cysteine proteases. Furthermore, calmodulin (calcium-modulated protein) that is predicted to bind to the IQ binding motif, is also calcium-binding messenger protein. Calcium is also involved in the process of spermatogenesis, with calcium channel blockers used for hypertension treatment often results in reversible male infertility in mice (Lee et al., 2006). Due to difficulty in the purification of the full-length protein as well as the heme domain there is lack of biochemical or biophysical information about Adgb (Bracke et al., 2018). Here

we report stable expression of androglobin globin domain as well as biochemical and biophysical characterization of the globin domain using ligand (nitrite, NO, CO) binding properties, and spectra characteristics of the globin domain. The results show a highly unusual mode of NO binding that may have implications on potential physiological functions.

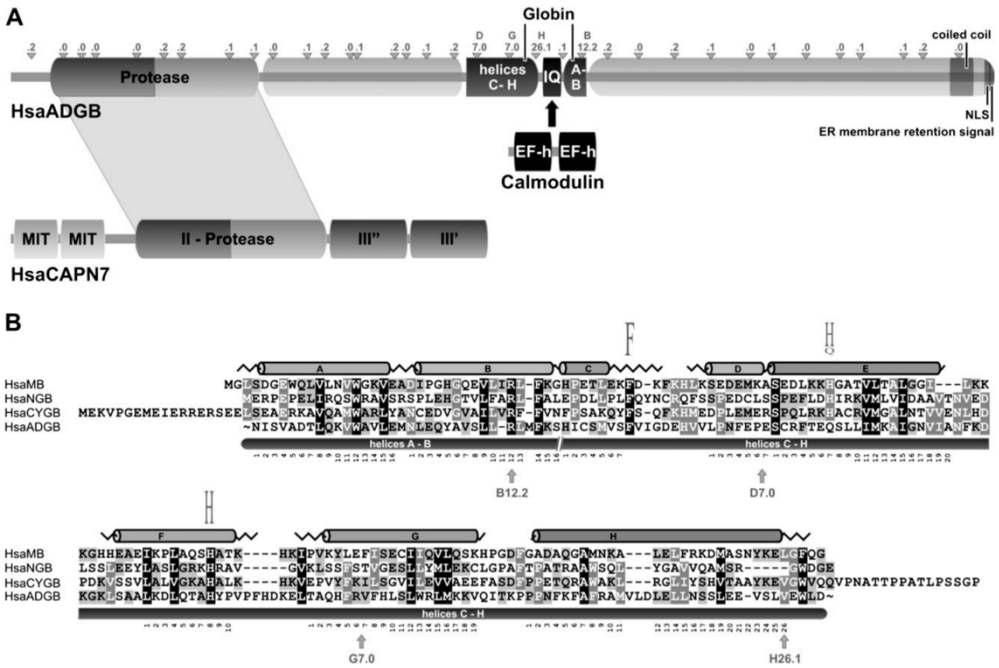

Figure 5.1.1 Androglobin chimeric domain structure as published (Hoogewijs ., 2012).

(A) Adgb Modular domain structure with calpain-like protease domain, permuted globin structure, with IQ motif which may mediate binding to calmodulin in the middle, and candidate nuclear localisation (NLS) and ER membrane retention signal regions, along with microtubule-interacting and trafficking domain (MIT). (B) amino acid sequence alignment of globin region with other hexacoordinate members of the human globin family.

5.2 Materials and Methods

5.2.1 protein engineering purification and expression

The human androglobin globin domain (Adgb-GD) gene was synthesized by Epoch Life Sciences (Texas, USA) . Adgb plasmid was transferred to BL21 DE3 cells by transformation using the heat shock method (42 ºC, 90s). A starter culture was prepared with colonies of transformed BL21 DE3 cells, cultured in solid agar medium containing 50 µg/ml kanamycin sulfate. A distinct colony was placed in a 100 ml Luria Bertani (LB) media containing 50 µg/ml kanamycin sulfate and placed in a shaking incubator at 120 rpm at 37 ºC overnight. Starter culture (20ml), was transferred to four 1.4 L flasks, the optical density of cells was monitored until an optical density of 0.8 -1.0 was reached at 600 nm, at which time protein production was induced using 500 µM Isopropyl ß-D-1thiogalactopyranoside. Aminoleuvelinic acid (250 µM) and 0.1 M ferric citrate were added to facilitate heme production and followed by bubbling with carbon monoxide for 60 s for heme stability. Flasks were sealed using a rubber seal and transferred into a shaking incubator and left overnight at 100 rpm with a temperature of 37 ºC. Cells were harvested by centrifugation (6000 rpm, 4 ºC) for 30 mins. Cells were passed through an Avestin C3 Emulsiflex where cells were lysed and homogenized under pressure (15 -20000 psi), three-cycles. Lysed cells were centrifuged (18000 rpm, 4 ºC, 20 min), supernatant was discarded, and cell pellet recovered due to the formation of exclusion bodies of androglobin. Cell pellet was resolubilized in 20 mM phosphate buffer (wash buffer), containing 0.5 M NaCL, 20 mM imidazole and 1 % sodium dodecyl sulfate (SDS). Resolubilized protein was centrifuged at (18000 rpm at 4 ºC) for 20 mins, and supernatant collected. Supernatant was diluted with wash buffer 1:1 to dilute the concentration of SDS to 0.5 %. Immobilized metal affinity column (IMAC with nickel, 5 ml, GE healthcare) was equilibrated was equilibrated with wash buffer containing 0.5 % SDS. Supernatant was passed through the column with His-tagged protein binding to the column, column was washed with wash buffer containing 0.5 % SDS for 5 min to remove any bacteria proteins or debris. Protein was eluted using sodium phosphate buffer pH 7.4 (elution buffer), containing 0.5 M NaCl, 500 mM imidazole and 0.5% SDS.

Protein was dialyzed and Imidazole a was removed by dialysis, using a dialysis bag with 8 kDa molecular weight cut-off, which was then placed in 5 L containing 1 mM sodium tetraborate buffer, pH 9.5. Dialyzed protein was concentrated using Sartorius Viva-spin 20 centrifugal concentrator with a 3 kDa molecular weight cut off. Dialyzed protein was incubated with heme at concentration of 1:2 protein:heme. Protein was passed through a G25 size exclusion column (5 cm by 1 cm) equilibrated with borax buffer (pH 10.0) to remove excess heme and stored at -80 ºC

5.2.2 Nitrite reductase activity

The nitrite reductase activity of androglobin measured using an Applied Photophysics SX-20 stopped flow spectrophometer. 10 μM protein (diluted to 5μM after mixing) was added to a 10 ml glass syringe. The deoxyferrous form of the protein was obtained by the addition of excess sodium dithionite. Excess dithionite was also added to 10 ml glasses syringe containing sodium phosphate buffer (pH 7.4) and sodium nitrite (2-20 mM before mixing). Protein and sodium nitrite were mixed in a 1:1 ratio and absorbance measured at 385 – 585 nm at an interval of 100 ms.

5.2.3 pH titration of Androglobin

Ferric androglobin (5 μM) was added to a buffer mixture (sodium acetate, sodium tetraborate and sodium dihydrogen orthophosphate, all 5 mM) in a 3 ml cuvette and the pH adjusted to pH 11.0 using sodium hydroxide . HCL (100 μM – 1 M) was titrated in 1 μL aliquots to the protein followed by mixing and measurement of the optical spectra using a Cary 5000 spectrophotometer and pH recorded using a pH meter.

5.2.4 Quantification of free cysteines

Free cysteines in Adgb were quantified using dithiodipyridine assay as described previously (Riener et al., 2002). Protein (5μM) was titrated with sub-stoichiometric (~0.5 μM) aliquots of 4,4’-dithiodipyridine and the absorbance monitored at 324 nm.

5.2.5 Generation of heme domain models and sequence alignment

The model of Adgb heme domain was generated using MODELLER software (Eswar et al., 2003). Adgb sequence used for model was reanalyzed by Brandon Reeder and Chris Reynolds. Neuroglobin (Ngb) sequence was used as a template based on in-house homology studies. Sequence alignment was performed using MUSCLE sequence alignment tool (Edgar, 2004). Protein structures and snapshots were generated using PyMOL molecular graphics system (Schrodinger, 2015).

5.2.6 Electron Paramagnetic Resonance Spectroscopy

Adgb aliquots (80 μM, 250 μl) were placed in Wilmad SQ EPR tubes. Nitric Oxide was added immediately prior to freezing by addition of Proli-Nonoate (1mM, giving 2 mM NO) in 10mM sodium hydroxide. Tubes were flash-frozen in dry-ice-cooled methanol and frozen samples were transferred to liquid nitrogen (77 K). All EPR spectra were measured using a Bruker EMX EPR spectrometer (X-band) equipped with a spherical high-quality Bruker ER 4122 SP9703 resonator and an Oxford Instruments liquid helium system. The modulation frequency was 100kHz. The EPR spectra of the blank samples (frozen water) were subtracted from the EPR spectra of the protein samples using WinEPR v. 2.22 (Bruker Analytik, GmbH) to eliminate the baseline caused by the walls of the resonator, quartz insert or quartz EPR tube.

5.3.1 RESULTS

5.3.1 Modelling of Androglobin globin (Adgb-GD) domain

Earlier studies by Hoogewijs *.,* 2012 demonstrated the presence of A – H helices with a 3/3 globin fold along with conservation of the residues F8 (the proximal histidine) and E7 (normally a distal histidine, but for Adgb this is a glutamine), showing the similarity of the globin domain in androglobin to other known globins like cytoglobin (Cygb), Ngb and Adgb. However, due to difficulty in generating a stable globin domain, there is lack of biophysical and biochemical information about Adgb-GD domain. To successfully produce Adgb-GD recombinantly, amino acid sequence analysis at the University of Essex led to a refinement of the globin domain amino acid sequence. Amino acid sequence analysis, helical analysis and molecular dynamics simulations performed at Essex highlighted possible errors in the assignment to amino acid sequence in the CD region of the globin responsible for in structural instability in Adgb-GD (Figure 5.3.1.1 - 5.3.1.5).

The hydrophobic nature of the conserved residue which Hoogewijs *et a*l made part of the globin fold in the CD region (Figures 5.3.1.1 - 5.3.1.3), made the helical interactions less stable, this observation was made from preliminary investigation of models generated from sequences of Hoogewijs and Essex. This led to changes of residues in the CD region less hydrophobic amino acid residues (Figure 5.3.1.1). Critically, one of the most highly conserved amino acid in globins is the CD1 phenylalanine and is vital for stabilising heme binding (Roesner et al., 2005). In the Hoogewijs sequence alignment, this phenylalanine is assigned to a sequence at the N terminal side of the circularly permuted globin domain (F769). However, in the Essex sequence alignment the CD1 amino acid is a tyrosine towards the C terminal side of the circularly permuted globin domain sequence (Y976). Although highly unusual in mammals, this tyrosine is often observed in the CD1 position in bacteria including truncated globins (Mukai et al., 2002). Modeller (Eswar ., 2003) was further used to generate models using Ngb structure to see how the Hoogewijs- and Essex-derived sequences deviated from each other as a result of the hydrophobic residues. Essex sequence has A – H helices clearly

defined (Figure 5.3.1.4), sequence of Hoogewijs had truncated C and D helices along with a disordered region in the area around the truncated helices, residues responsible for these where the hydrophobic residues (Figure 5.3.1.5).

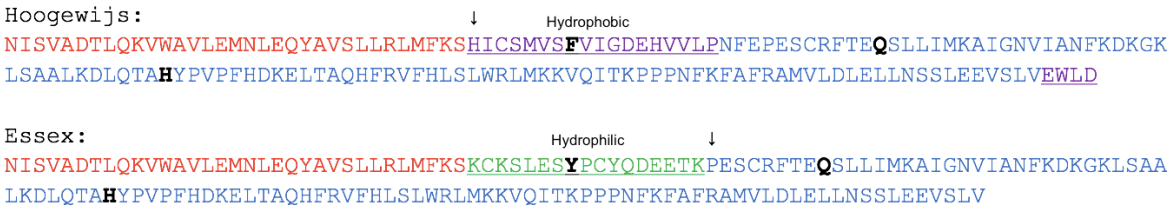

Figure 5.3.1.1 Colour coded sequences of Hoogewijs and Essex showing differences in amino acid residues. In this model of the globin domain, the circular permutation has been removed by splicing the two peptide chains, normally separated by the IQ calmodulin binding domain, together such that the sequence alignment matches non-circularly permuted globins. This division is marked by the arrow. In areas coloured red and blue, the amino acids residues of Essex and Hoogewijs sequences are essentially in agreement. In purple is the hydrophobic CD loop region of the sequence alignment predicted by Hoogewijs . In green is the hydrophilic CD region sequence predicted by Essex. The CD region, from the sequence alignment by the Essex group is hydrophilic, whereas the predicted CD loop region by Hoogewijs is hydrophobic.

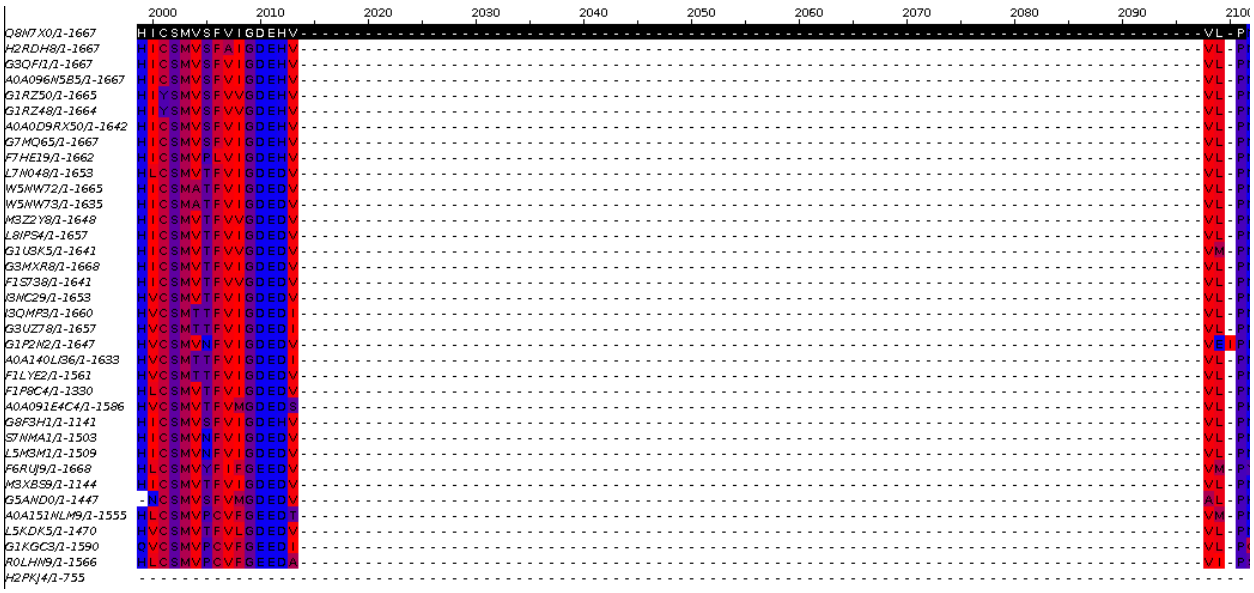

Figure 5.3.1.2 Multiple sequence alignment of the CD loop region of androglobin globin domain by Hoogewijs . The sequence alignment was visualized by Jalview showing hydrophobicity in (red) and hydrophilic residues in (blue) of conserved residues believed to the CD region by Hoogewijs

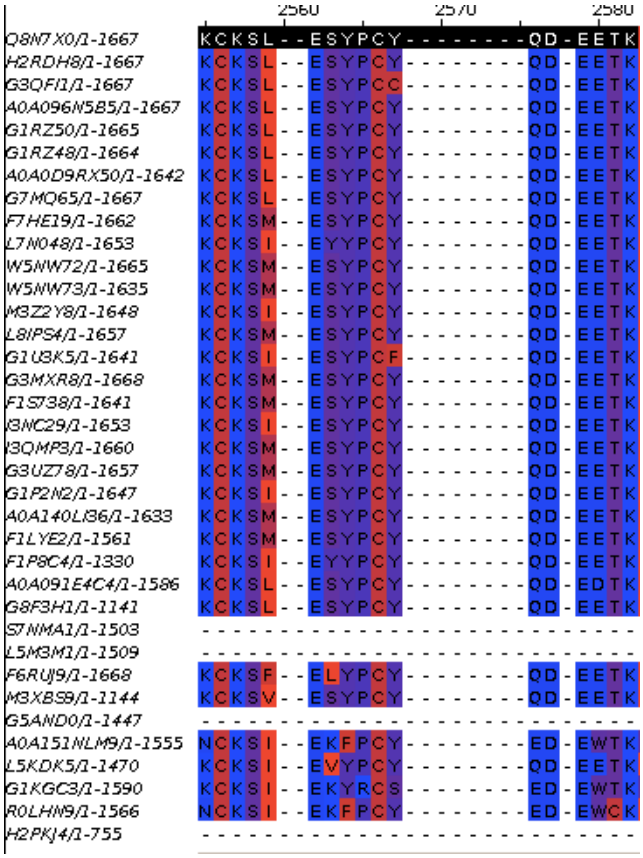

Figure 5.3.1.3. Multiple sequence alignment of the CD loop region of androglobin globin domain by Essex. The sequence alignment was visualized by Jalview showing hydrophobicity in (red) and hydrophilic residues in (blue) of conserved residues believed to the CD region by Essex.

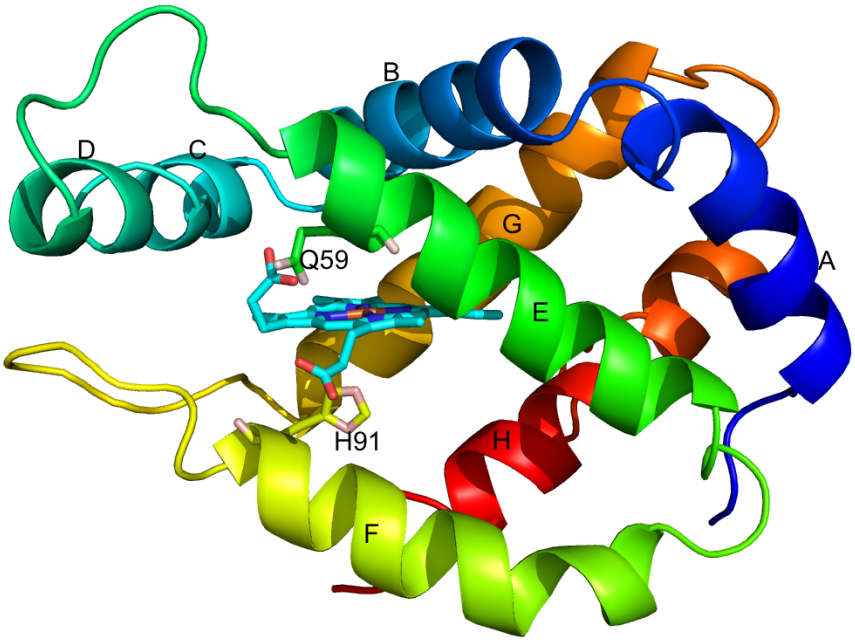

Figure 5.3.1.4. Model of androglobin globin domain (Essex)**.** This model was generated using Modeller software from Essex sequence using neuroglobin as a template showing the distal and proximal coordinated sites, 3/3 globin fold and helices A – H. The proximal histidine (H91) and distal glutamine (Q59) are numbered in accordance with the sequence here, In the full globin sequence they are H823 and Q791 respectively.

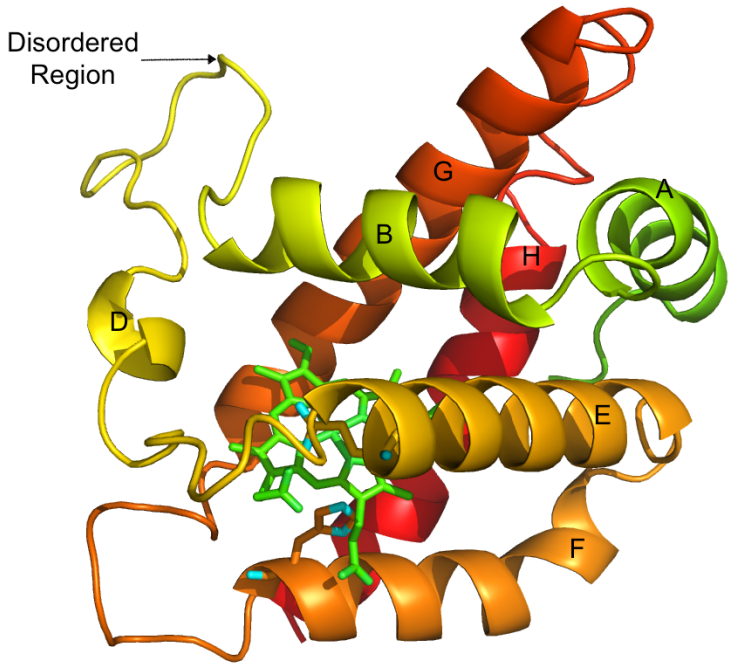

Figure 5.3.1.5. Model of androglobin globin domain highlighting the disordered region (Hoogewijs). This model was generated using Modeller software from Hoogewijs et al sequences showing a disordered region, the region believed to be CD region.

5.3.2 Androglobin globin domain nitrite reductase activity

To examine the ability of androglobin to generate NO, the nitrite reductase activity of androglobin was examined. Like other members of the hemoglobin family Adgb can act as a nitrite reductase (Alayash et al., 2001, Li et al., 2012a, Tiso et al., 2011b). Due to addition of dithionite as reductant in the NiR activity, final reacting protein population is the deoxyferrous NO-bound species, this species represents the end spectrum in this activity.

The nitrite reductase activity of rapid with a rate constant of 40 $M^{-1}s^{-1}$ (Figure 5.3.2.1) exhibiting biphasic kinetics (Figure 5.3.2.1C). The concentration dependence of the fast kinetics on nitrite (Figure 5.3.2.1E) exhibits a high error due to the small amplitude of the optical changes observed in the global fit. The slower rate representing the formation of the deoxyferrous-NO bound species follows a rectangular hyperbola function as a function of nitrite concentration with an apparent K_D of 8.42 ± 0.46 mM NO_2^- and a maximum rate of 2.541 $x10^{-1}$ s^{-1} ± 6.18 $x10^{-4}$ s^{-1}. The effect of reduction of the disulfide bond has a significant effect on the rate of NiR activity (Figure 5.3.2.1 E and F). TCEP reduced free sulfhydryl has a significant effect of the NiR activity of the Adgb decreasing the observed kinetics. The spectrum of the NiR activity suggests a transition from a 6-coordinate ferrous to 5-coordinate ferrous-NO species (Figure 5.3.2.1A and D), inferring a different NO binding mechanism from other members of the human hemoglobin family, possibly via a proximal haem iron NO binding configuration.

.

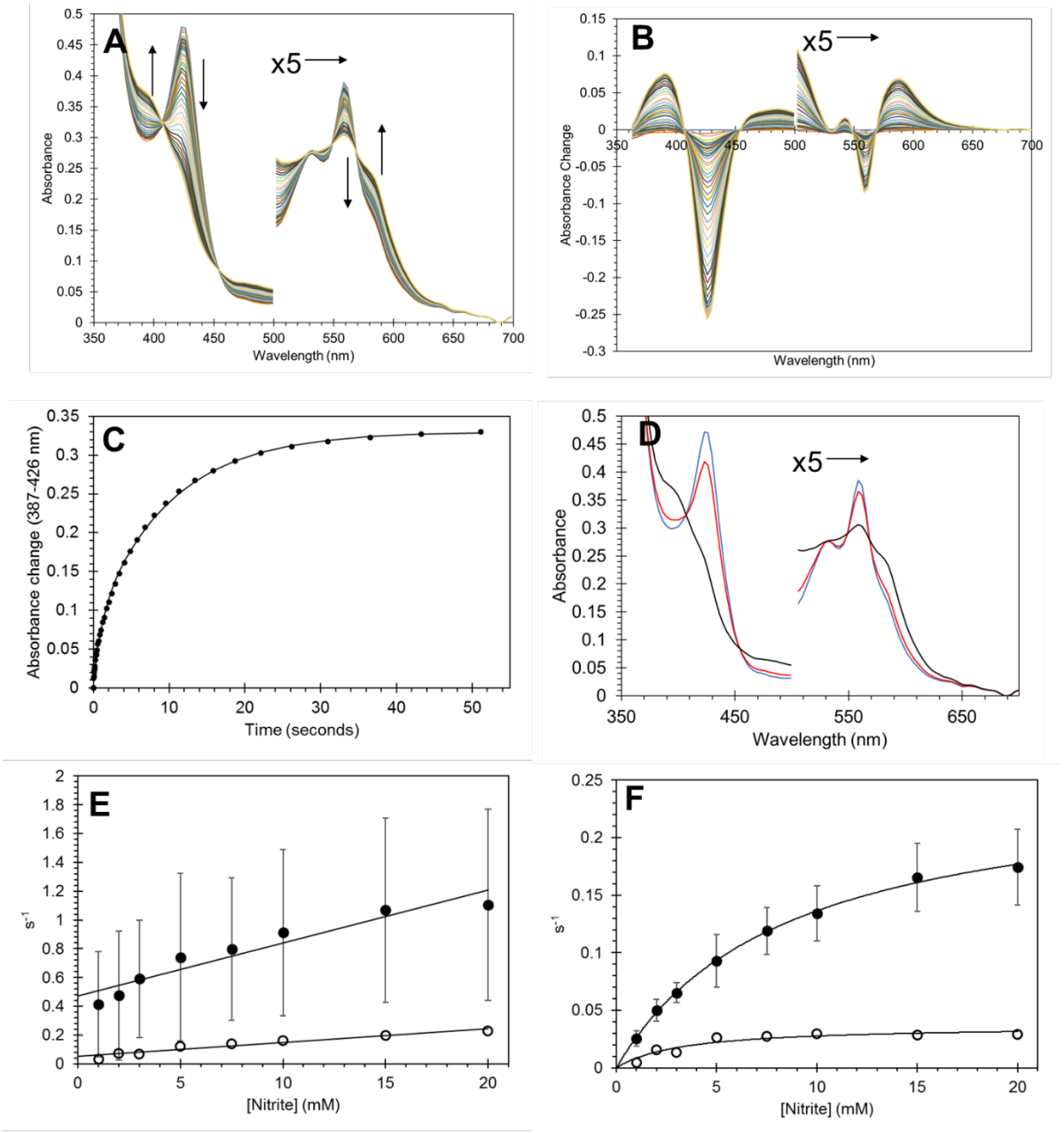

Figure 5.3.2.1. Nitrite reductase activity of Androglobin globin domain. (A) Optical spectra of deoxyferrous Adgb-GD (5 μM) with sodium nitrite (5 mM). (B) Difference spectra with initial ferrous protein set to zero. (C) Time course of Optical changes fitted to a double exponential function (k_1 = 9.25x10^{-1} s^{-1}, k_2= 1.02x10^{-1} s^{-1}. (D) Global fit of initial deoxyferrous protein (blue), intermediate (red) and final ferrous-NO bound spectrum (black). (E and F) The dependence of the rate constants for Adgb-GD nitrite reductase activity. The observed rate constants of the fast (E) and slow (F) phase on the reaction in the presence (●) or absence (by reduction using TCEP, ○) of disulfide bond. n=3.

5.3.3 Nitric oxide binding to ferrous androglobin.

Spectrophotometric investigation and characterization have assigned wavelengths to the spectra properties associated with ferrous, ferrous-NO bound transition of ferric Adgb-GD and the results are presented in Figure 5.3.3.1. The spectrum shifts from 409 nm to 414 nm with the appearance of prominent alpha and beta bands at 565 nm and 532 nm respectively, indicating the binding of NO to the ferric oxidation state. However, on leaving the protein for a few minutes, the optical spectrum slowly changed with a hypsochromic (blue shift) of the Soret peak to 395 nm and a broadening of the visible peaks. The end spectrum was essentially that of ferrous-NO bound to the proximal side. Therefore, the NO is functioning as an auto-reductant, reducing the ferric heme to ferrous. Hence may be a potential mechanism for reduction in vivo albeit a very slow one requiring excess NO.

Preliminary work on the NO binding to Adgb-GD revealed spectra changes which are similar to that observed with hexacoordinate cytochrome c' (Figure 5.3.3.1 and 2). Spectra changes in the Soret region suggests a transition from hexacoordination to pentacoordination, a well characterized behavior in cytochrome c', as a result of NO binding to the proximal side of the heme iron rather than the distal side to give a hexacoordinate form as observed in other globins like cytoglobin (Figure 5.3.3.1).

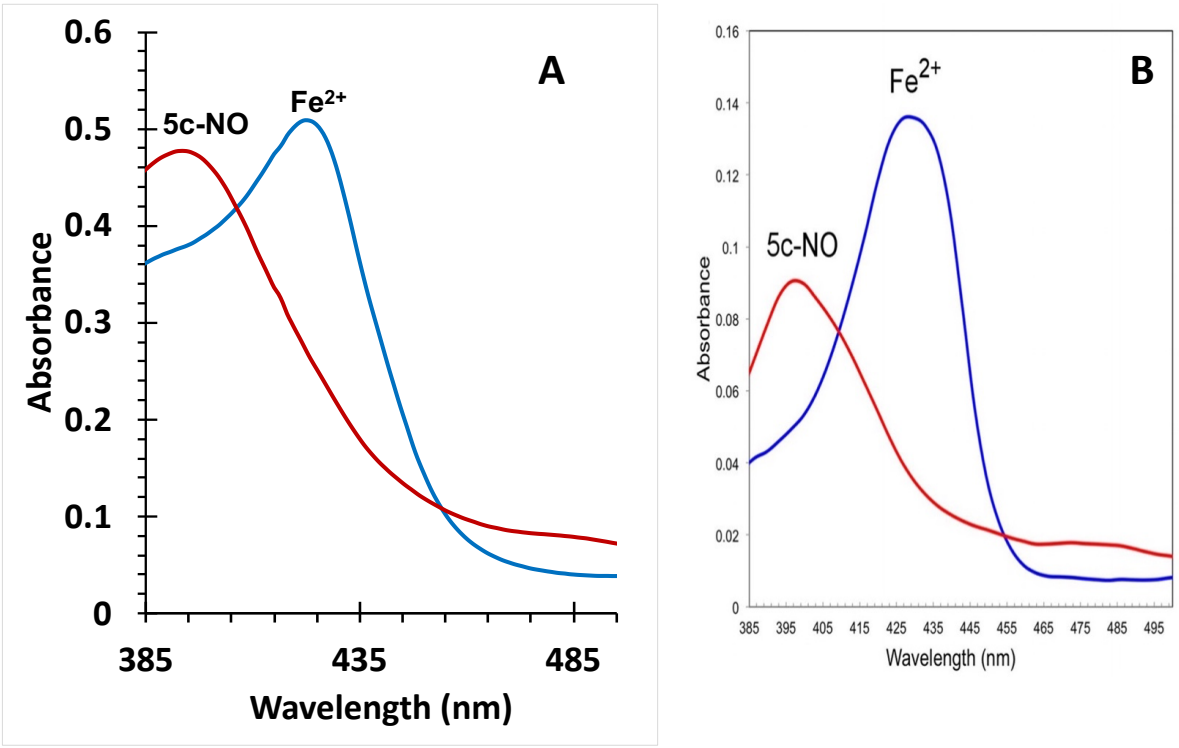

Figure 5.3.3.1. Optical transition of the Androglobin and Cytochrome c' from ferrous to NO-bound.

(A), Binding of NO (200μM) to deoxy-ferrous androglobin (5μM) in 0.1 M sodium phosphate buffer (pH 7.4). **(B),** Optical properties of cytochrome c' from *Shewanella frigidimarina*, showing spectra change from deoxy-ferrous heme iron to a 5-coordinate NO-bound ferrous iron (Manole ., 2015). This shows the Soret spectra characteristics of NO-bound Adgb-GB, with spectral shift of the Soret peak from 426nm (ferrous) to 393nm (NO-bound) is very similar to that of cytochrome c'. Therefore, it is proposed that NO binds to Adgb-GD to for a 5-coordinate heme iron coordinated NO species.

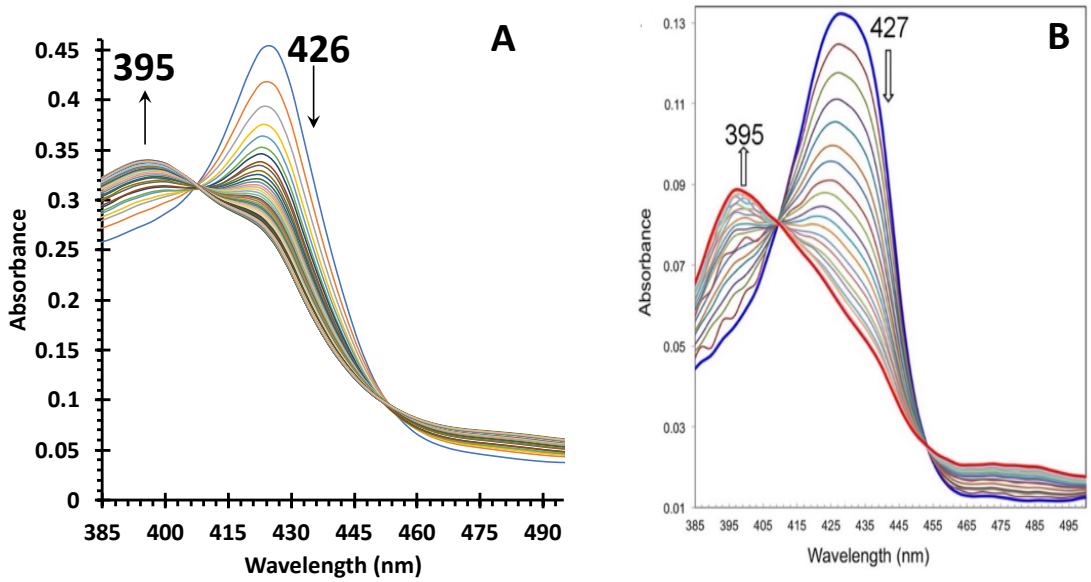

Figure 5.3.3.2. Stopped flow measurement of NO binding to Androglobin and Cytochrome c'. **(A)** Time dependent absorption spectra of Adgb-GD. **(B)** Time dependent absorption spectra of cytochrome c' from *Shewanella frigidimarina* by (Manole et al., 2015). The figure illustrates optical similarity associated with NO-bound ferrous populations of androglobin and cytochrome c' along with the eventual transition to a likely 5-coordinate NO-bound form at 395nm

5.3.4. Visible absorption spectra properties of androglobin

The visible absorption spectra of androglobin was comparatively characterized with pentacoordinate myoglobin and hexacoordinate cytoglobin. The visible absorption spectra of deoxyferrous Adgb-GD (Figure 5.3.4.1), displayed optical properties of at least a partially hexacoordinated globin when compared with deoxyferrous ferrous Mb (Figure 5.3.4.2) and Cygb (Figure 5.3.4.3), with the presence of blue-shift in the 400nm Soret region in contrast with pentacoordinated myoglobin which is red-shifted in that region (Duff, Wittenberg and Hill, 1997; Trent Iii, Watts and Hargrove, 2001). The deoxyferrous state of Adgb-GD also displayed two peaks in the visible region 530nm and 560nm region (Figure 5.3.4.1-3) another property of hexacoordinate globins like Cygb in contrast with penta-coordinate globins like Mb which have broad peaks (Figure 5.3.4.2 and Figure 5.3.4.3) in this region (Arredondo-Peter ., 1997). There was also a difference in the optical transition of the unliganded deoxyferrous Adgb-GD to deoxyferrous-CO bound androglobin (Figure 5.3.4.1).

Binding of CO to deoxyferrous Cygb, and Mb leads to hypochromic changes in the Soret region and visible region (Figure 5.3.4.4C and D). Binding of CO to deoxyferrous Adgb-GD lead to hyperchromic shift in the Soret, α and ß peaks, accompanied by a high spin signal in the 620nm region (Figure 5.3.4.4A). However, spectra properties had striking similarities with the spectrum representing the CO complex of cytochrome c' (Figure 5.3.4.4B).

The extinction coefficient for heme proteins can typically be found by the pyridine-hemochromagen assay (Flink and Watson, 1942) however, HPLC calculates the heme concentration in essentially the same way – by separating the heme from the globin and comparing to samples of known heme concentration. The extinction coefficient for ferric Adgb-GD was calculated to be 100,000 M^{-1} cm^{-1} (per heme) and that of the deoxyferrous androglobin was calculated to be 101, 000 M^{-1} cm^{-1} (Figure 5.3.4.5).

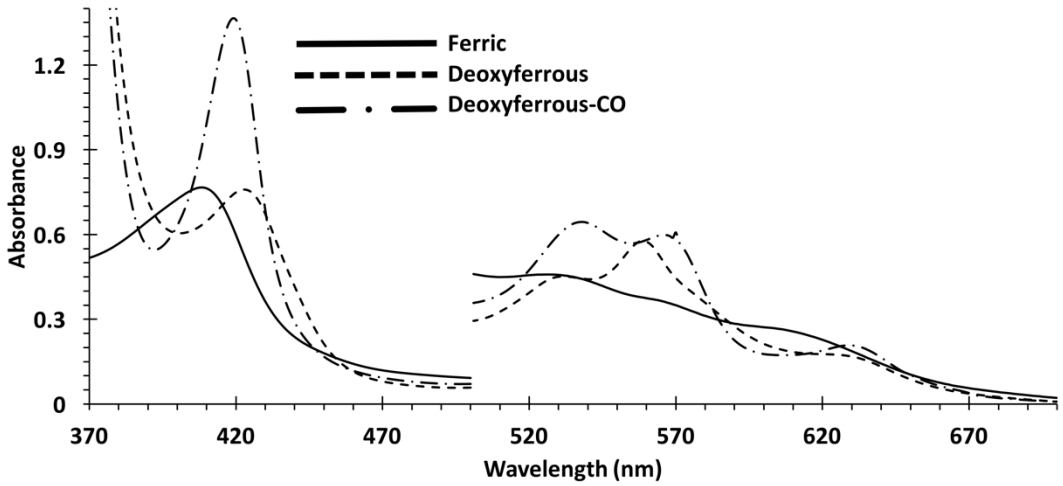

Figure 5.3.4.1. Visible absorption spectra of Androglobin. In bold ferrous-CO bound androglobin, in dashes and dots dithionite reduce deoxyferrous androglobin, in dashed ferric androglobin.

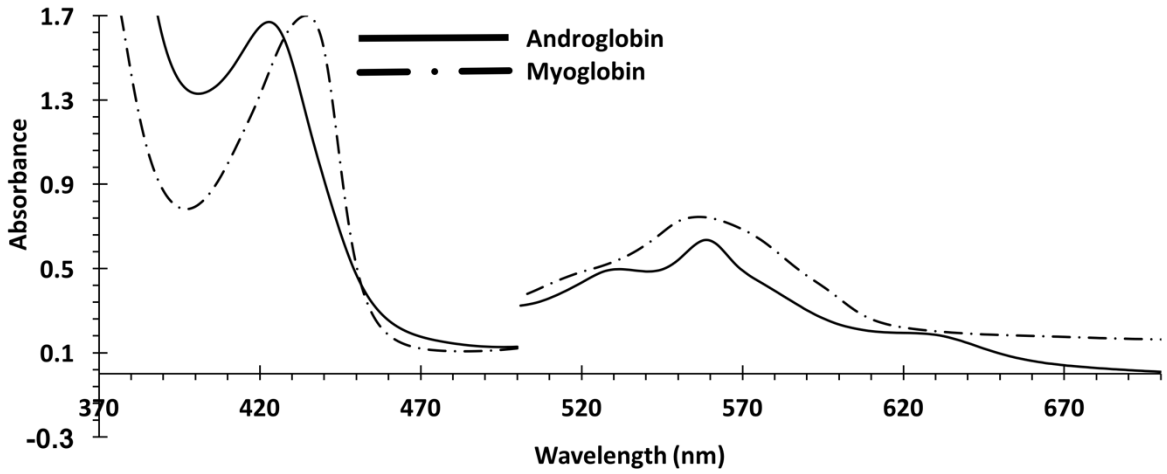

Figure 5.3.4.2. Absorbance spectra of deoxy, ferrous Androglobin and Myoglobin. This figure represents an overlay of human androglobin (bold line), and sperm whale myoglobin (dashed line). The visible region (520nm -700nm) was magnified 5-fold, while penta-coordinate globins like myoglobin have a broad peak in this region in their deoxyferrous form, hexacoordinate globins have split peaks one in the 530nm region, and another in the 560nm region in their deoxyferrous form, this spectra property of androglobin shows it is an hexacoordinate globin.

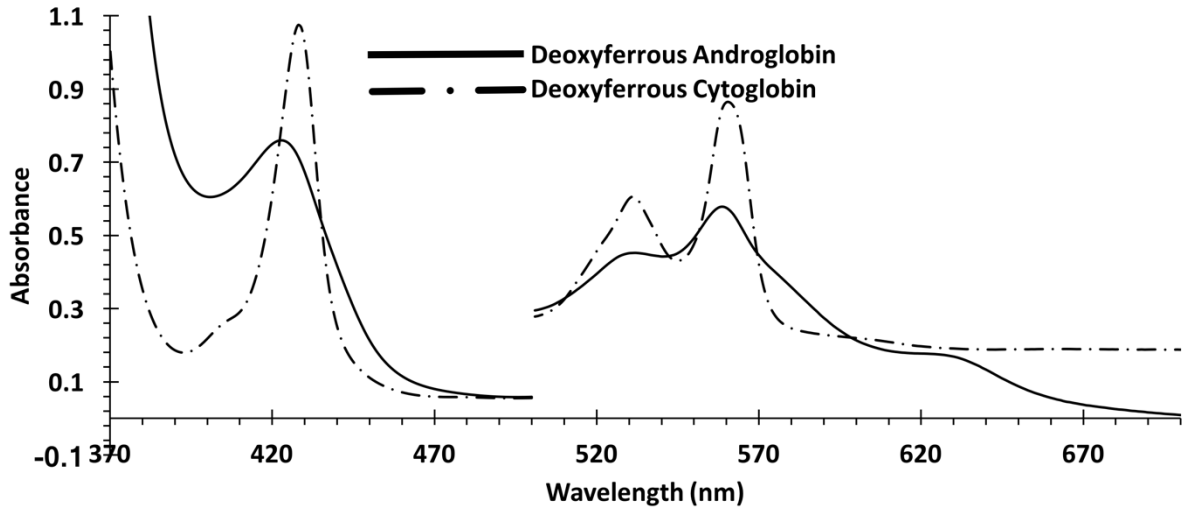

Figure 5.3.4.3. Absorbance spectra of deoxy, ferrous Androglobin and Cytoglobin. This figure represents an overlay of human androglobin (bold line) and neuroglobin (dashed line). A 5-fold of the visible region illustrates the split peaks (530nm and 560nm), a property of hexacoordinated globins. Spectra similarity of androglobin and cytoglobin in the soret and visible region indicates hexacoordination in androglobin.

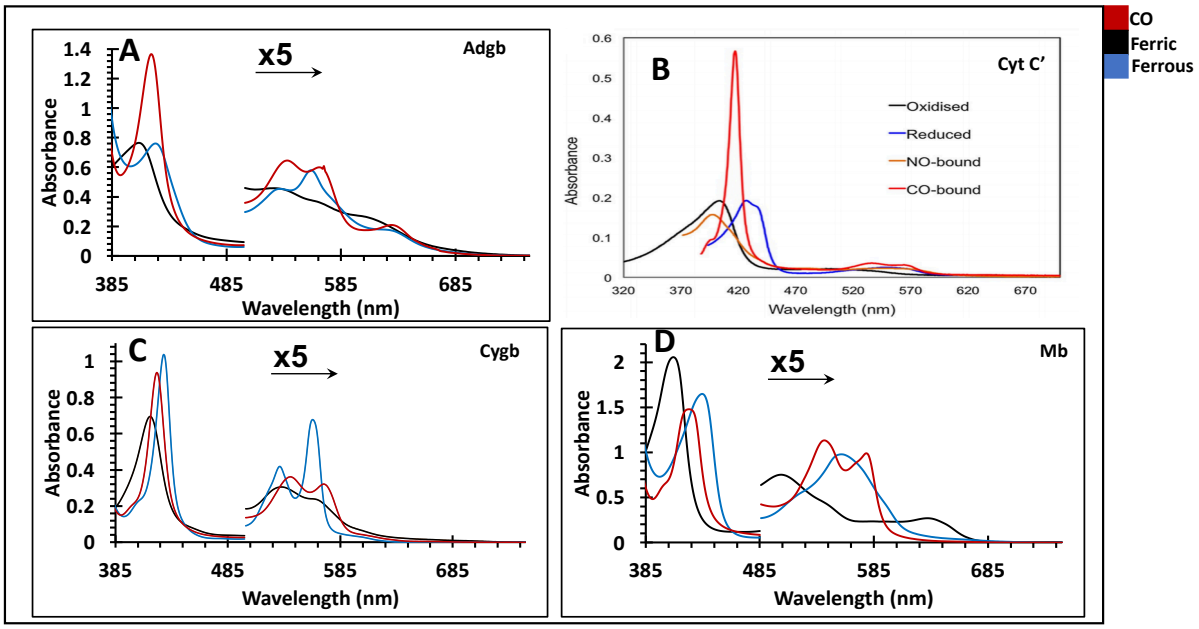

Figure 5.3.4.4 Comparison of the Soret and visible absorption spectra of ferric, deoxyferrous, deoxyferrous-CO bound, human androglobin and cytoglobin, cytochrome c' from Shewanella frigidimarina and horse myoglobin. Visible absorption spectra of Adgb-GD (A), cytochrome c' (reproduced from Manole ., 2015) (B), Cygb (C) and myoglobin (D). In all cases ferric (black), ferrous (blue), and CO-bound (red) are shown.

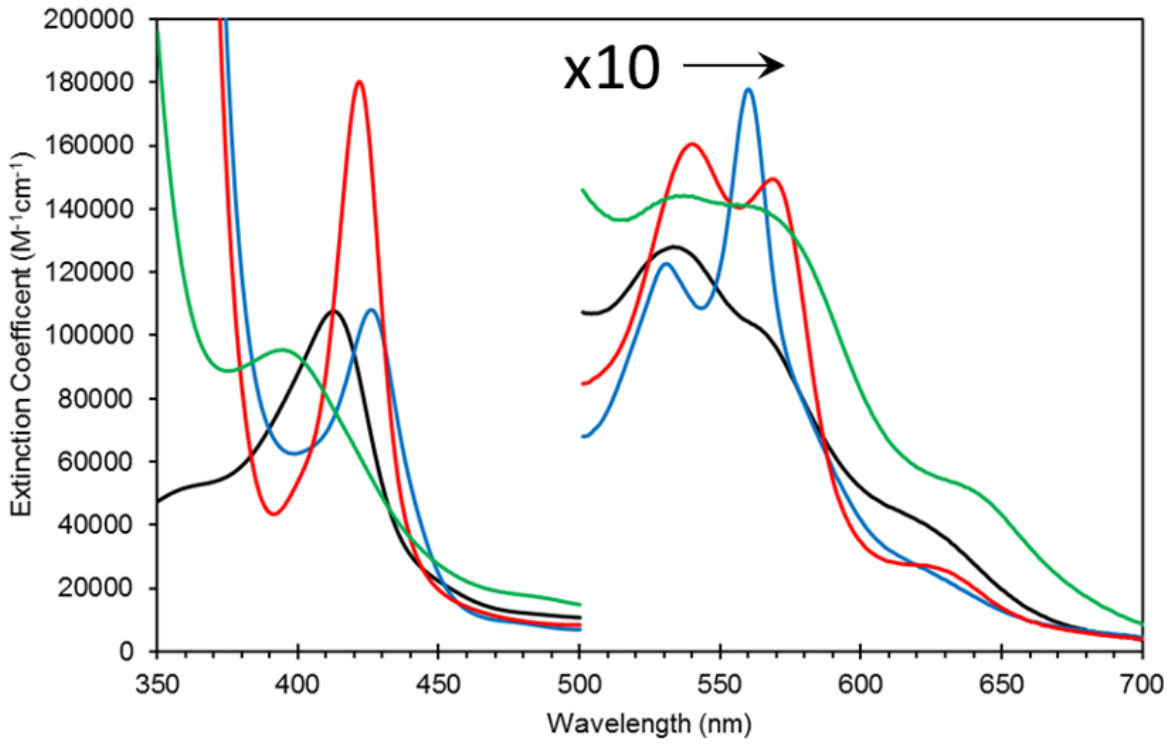

Figure 5.3.4.5. Molar extinction coefficient of androglobin globin domain. Ferric (black line), dithionite reduced ferrous (blue line), reduced ferrous-CO bound (red line) and reduced ferrous-NO bound (green line), as measured by HPLC

5.3.5 pH Titration of Androglobin

The acid/alkaline transition of ferric heme-proteins as a result of ionization of water molecule in the distal pocket of Hb and Mb has been well studied (Brunori ., 1968). The optical transition in ferric heme proteins like Mb (Figure 5.3.5.1B), usually involving a spectra shift from a hydroxide bound (OH-) low spin form at high pH to a high spin water (aqua) heme iron at low pH (Brunori ., 1968). However, this was not this case with Adgb-GD. The pH titration suggests a shift from high spin to low spin, going from high pH to low pH. A 620nm band, typically representive of a high spin species, is seen at pH 11, but disappears at neutral/acidic pH (Figure 5.3.5.1A). There are two possible explanations for this structural change in the Adgb-GD. The transition from high spin state to low spin can be a result of a protonation of an amino acid residue in the distal coordination site, which leads to a structural change resulting in a pentacoordinate to hexacoordinate as pH decreases. An alternative explanation could arise from coordination of a water molecule at high pH, but transitions to a hexacoordiante form at neutral/acidic pH, presumably from the binding of the distal glutamine. Data from pH titration suggests structural transition due to pH titration does not involve binding of OH- under alkaline conditions (as a result of water ionization), but rater structural transition due to pH effects on amino acid residues close to the heme pocket. Crystal structures or resonance raman may elucidate the distal coordination site different pH values. The pH titration curve of Adgb had a pKa of 8.3 (Figure 5.3.5.2).

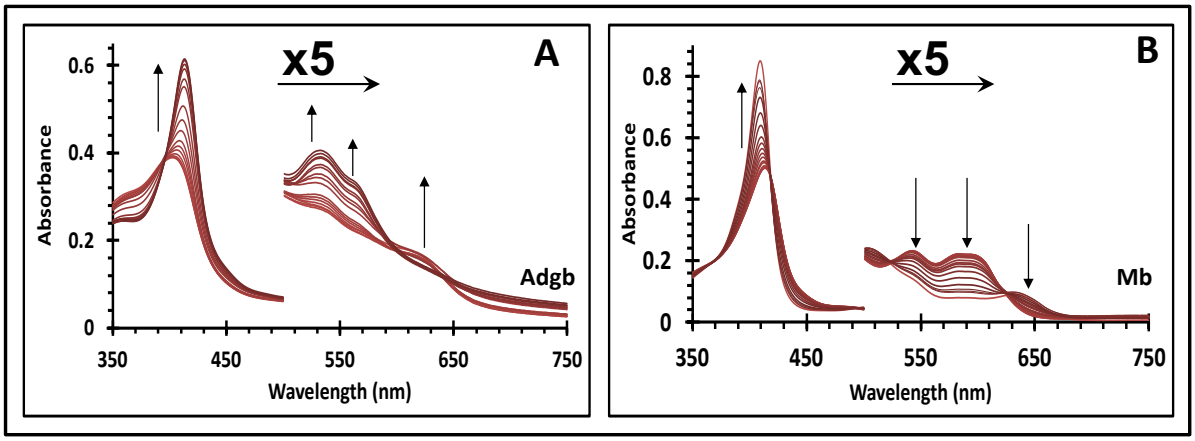

Figure 5.3.5.1 Optical spectra for the acid-alkaline transition of ferric androglobin globin domain and myoglobin. Ferric Adgb-GD and Mb were adjusted to approx. pH 11.0 by addition of buffer (5mM sodium acetate, sodium tetraborate and sodium dihydrogen orthophosphate). Acid (HCl) was titrated into the solution and the pH and optical spectra were recorded. (A) Optical transition induced by pH titration of androglobin from pH 11.0 – 7.4. (B) Optical transition induced by pH titration myoglobin from pH 12.0 – 7.4. Myoglobin had structural transitions typical in ferric hemoglobin due to pH effects, changes observed where that of a high spin heme iron (pH 11.0), transforming to a low spin heme (pH 7.4). Androglobin had the reverse effect, changing from high spin heme at physiological pH to low spin heme at high pH. Arrows represent change in spectra from high to low pH.

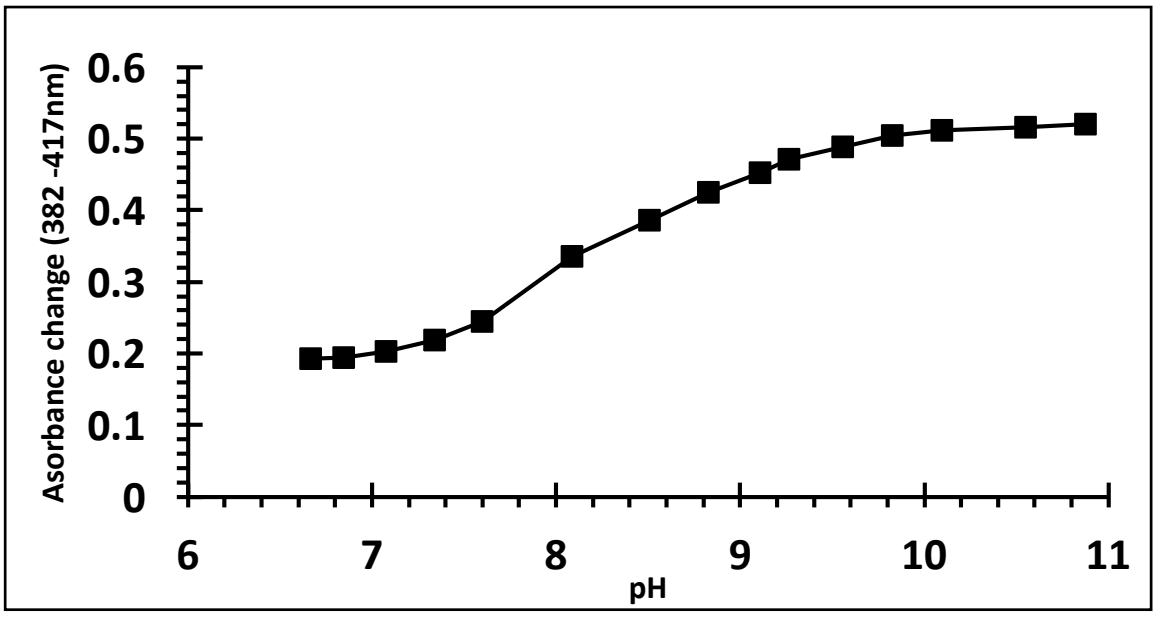

Figure 5.3.5.2. Titration curve for the acid-alkaline transition of ferric androglobin. Absorbance (382-417nm) of 5μM ferric was measured in the 7.4-11.0 pH range using buffer (5mM sodium acetate, sodium tetraborate and sodium dihydrogen orthophosphate). pH changes were made by titration of HCl. The line (equation) represent fit (points) to the Henderson-Hasselbalch equation with a pKa of 8.3.

5.3.6 Quantification of free and disulfide thiols in androglobin globin-domain

Surface exposed cysteines in Adgb-GD where quantified using the dithiopyridine (DTP) assay. This assay makes use of the optical properties of DTP after reaction, when titrated with samples containing thiols. Reaction with thiols leads to chromatic changes that can be measured by colorimetric methods like UV/VIS spectroscopy. At saturated titration point when addition of DTP leads to no further observable optical changes, total absorbance changes measured during titration equals total amount of thiols in samples. This can be used to quantify free thiols, Adgb-GD has 4 cys, 2 are predicted to be surface exposed. Data shows that these 2 cysteines are forming a disulfide bond and that these are in the "CD loop" of the Essex prediction of the structure – hence they could stabilize the protein structure. In Ngb, the loop contains a disulfide bond between Cys46 (C7) and Cys55 (D5), known to stabilise the distal histidine ligation and the redox thermodynamics of ferric Ngb(Bellei et al., 2018, Hamdane et al., 2004) (refs). With our reassignment of the C helix sequence, the CD section of the structure possesses the potential to form a disulfide bond from residues Cys786 and Cys977. Absent in the original sequence alignment, this disulfide could stabilise this crucial juncture of the heme pocket, now the N and C terminal sections of the domain. With four cysteine residues in the protein sequence of the globin domain, we determined how many of those are surface exposed and free to bind dithiodipyridine, or to form a disulfide bond. As shown in Figure 5.3.6.1, there were two (1.9 ± 0.3) free sulfhydryl's per heme detected with the TCEP reduced Adgb-GD, meaning that two of the four cysteines are surface exposed. In the protein as expressed in *E.coli* (without reduction by TCEP), no free cysteines observed. Thus, as expressed, the heme domain possesses a single disulfide bond. From the predicted positions of the cysteines in the model of the protein, only two are predicted to be both surface exposed and close enough to form an intramolecular disulfide, that of Cys 786 and 977 in the "CD loop" region of the protein. Intermolecular disulfides were ruled out based on the observation that the protein is expressed as a monomer as assessed by gel filtration chromatography.

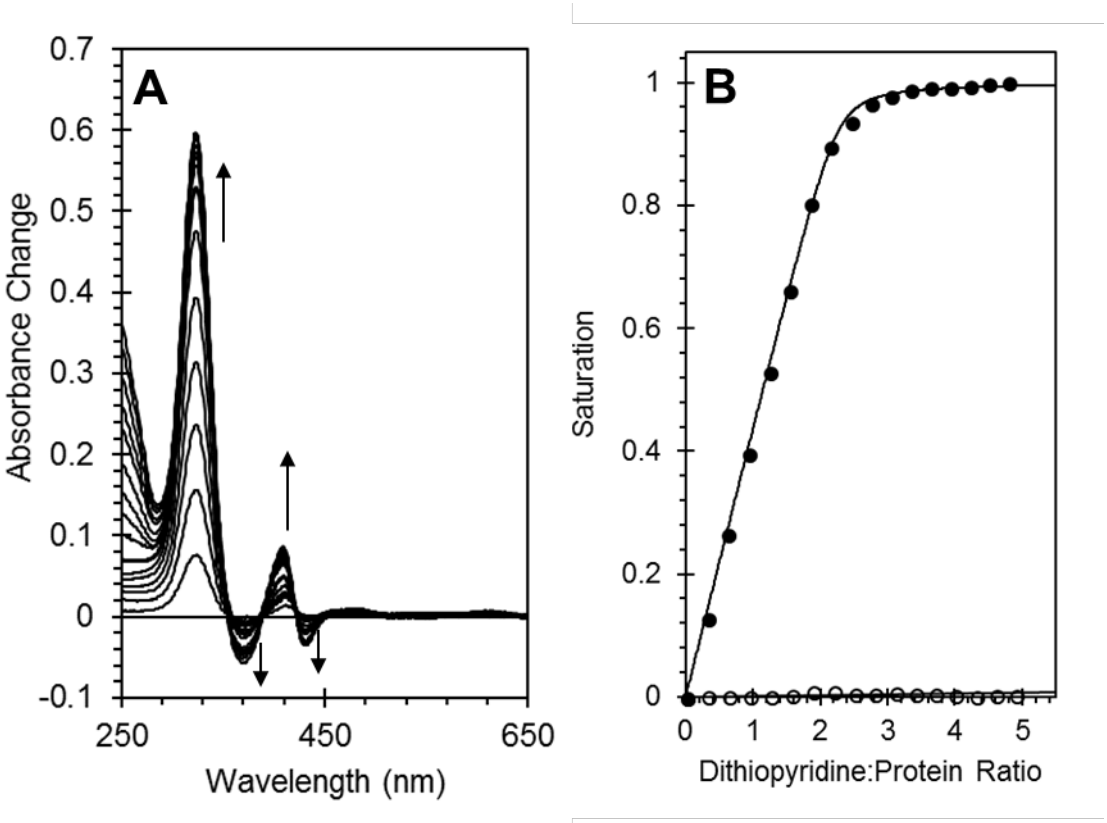

Figure 5.3.6.1. Surface exposed disulfide in the C/D region of the heme domain. (A) Protein (4 μM) was titrated with 4,4' dithiodipyridine and the optical changes followed for TCEP reduced Adgb. (B) Fractional saturation of dithiodipyridine binding to free sulfhydryl as a function of dithiodipyridine concentration for TCEP reduced (closed circles) and purified form (no/minimal disulfide reduction, open circles).

5.3.7 Identification of a pentacoordinate NO bound androglobin globin domain species by Electron Paramagnetic Resonance Spectroscopy and Ultrafast laser flash spectroscopy.

Adgb-GD binds to NO in the ferrous form to generate an unusual optical spectrum as observed earlier, suggesting a five-coordinate NO heme iron. This is supported by EPR at 10 K (Figure 5.3.7.1). The spectrum observed showed a characteristic three-line hyperfine signal, essentially identical to that reported for cytochrome c' from *Shewanella frigidimarina* and *Alcaligenes xylosoxidans* (Manole et al., 2015) This is again consistent with five-coordinate NO binding to the ferrous heme (Manole et al., 2015). Six-coordinate heme-NO EPR spectra are a typical nine line-shape pattern with a nitrogenous histidine ligand as the second axial ligand, creating a triplet of triplets (Zhao et al., 1998)

Transient absorption spectra observed following dissociation of the Adgb-GD NO complex with short light pulses are shown in Figure 5.3.7.2. The spectra are characterized by a broad bleaching around 390 nm due to the disappearance of the 5-coordinate NO-bound state and a relatively strong induced absorption centred at 427 nm assigned to the 4-coordinate NO-dissociated state (Negrerie et al., 2001) confirming the EPR (Fig 2d) data that the NO bound state of the ferrous Adgb is pentacoordinate.

Apart from small relaxation signals with a time constant of ~1.5 ps, corresponding to a blue shift of the induced absorption band (Figure 5.3.7.2A, inset) and assigned to vibrational cooling, the spectral evolution is characterized by a decay (associated spectra in the inset of Figure 5.3.7.2A) dominated by a 5.3 ps phase and a minor (~14%) 20 ps phase (Figure 5.3.7.2B). The remaining spectrum after these phases corresponds to only ~1% of the photo-dissociated NO, meaning that NO rebinding is almost completely geminate, implying that dissociated NO stays within the confines of the heme pocket and only minor quantities of NO escape the heme pocket. Rebinding of NO to the heme iron from bulk solution outside the heme pocket would be expected to occur on the μs to ms timescale, such as that observed with Mb and Cygb for NO or other gases such as CO. High-yield rebinding of NO to heme in a single 5-8 ps phase has been observed upon dissociation in all studied 5-coordinate heme-

NO complexes in proteins thus far studied (Kruglik et al., 2007, Liebl et al., 2013) In Adgb, however a slower, 20 ps phase of NO binding is also present. This finding suggests a relaxation process competing with initial NO rebinding, allowing NO to explore a larger conformational space, and indicating a less constrained heme pocket.

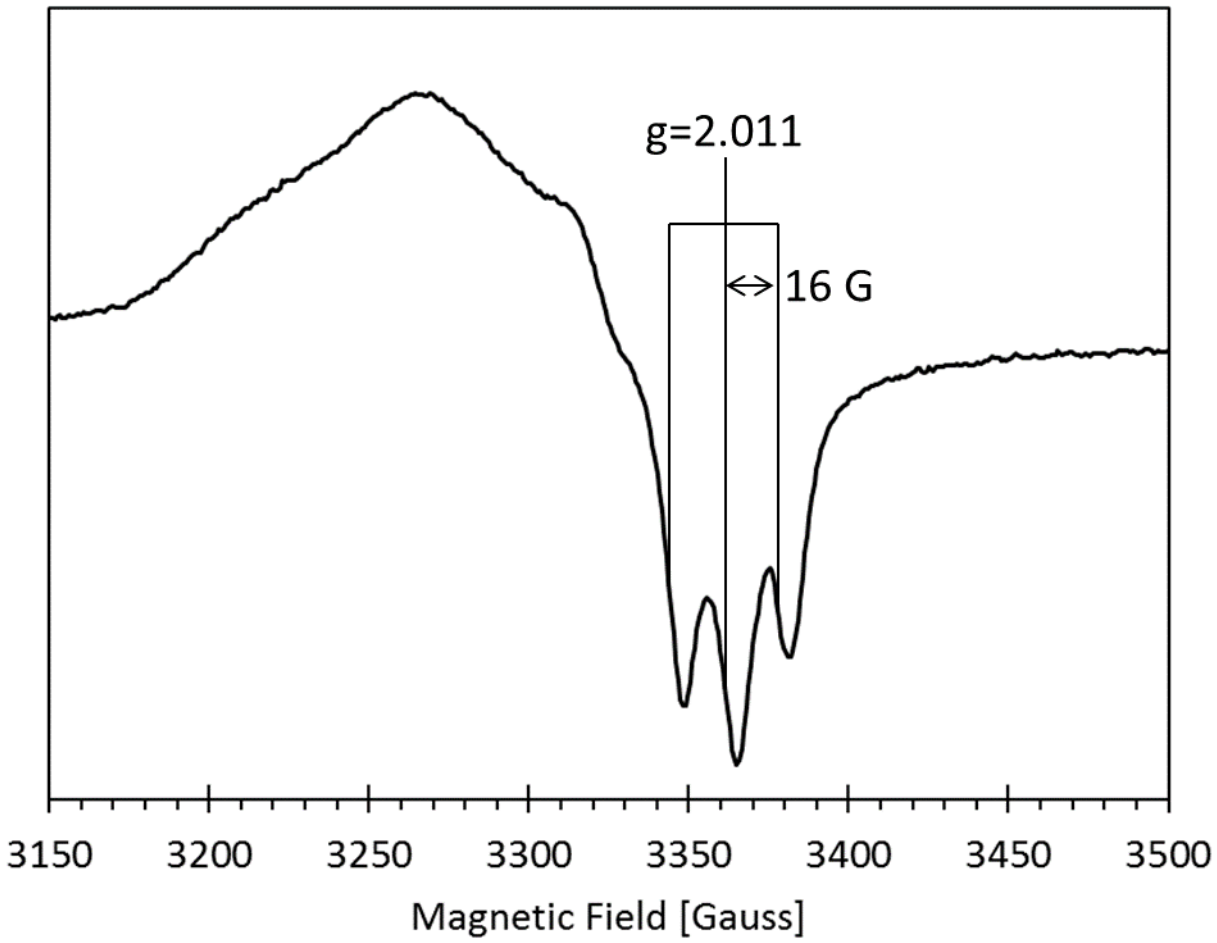

Figure 5.3.7.1. Androglobin globin domain Electron Paramagnetic Resonance spectra of ferrous-NO bound state.

An EPR spectrum of ferrous NO bound Adgb-GD, exhibiting three lines, separated by 16 G, around g= 2.011, typical of other EPR spectra of five coordinate NO binding such as cyt c'.

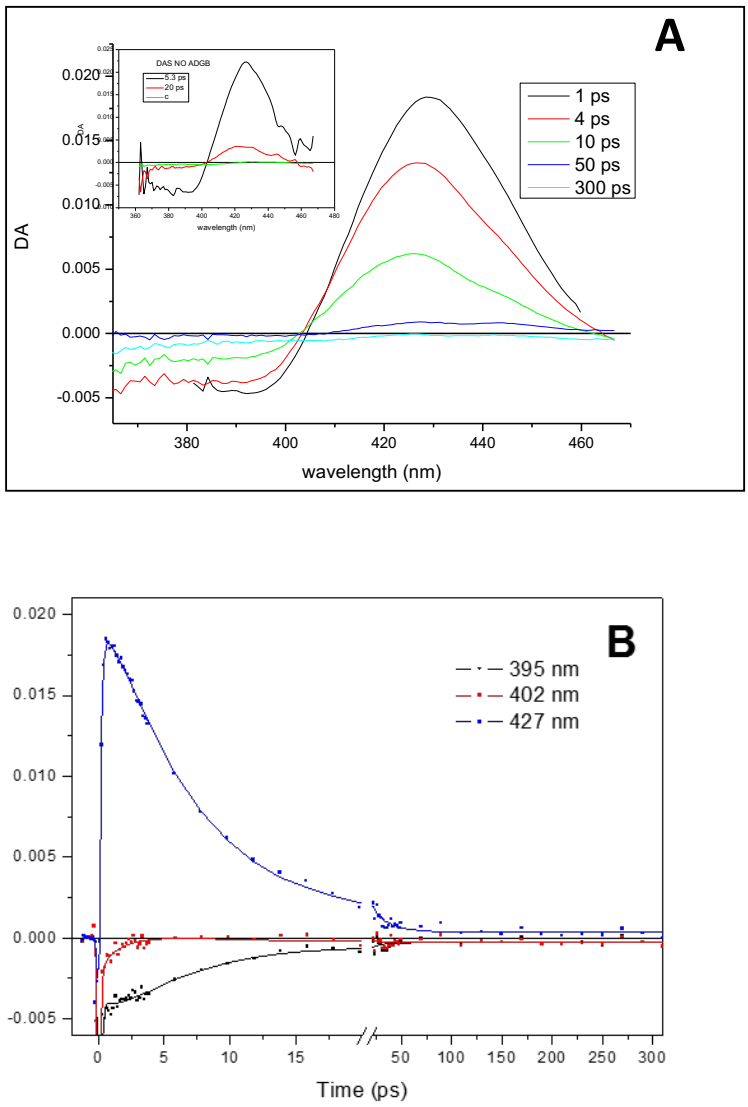

Figure 5.3.7.2. Ultrafast photo-dissociation and rebinding of NO from the ferrous androglobin globin domain five coordinate NO complex. (A) Transient absorption spectra after different delay times upon excitation at 570 nm. *Inset*: Decay Associated Spectra corresponding to the NO geminate rebinding phases obtained from a global analysis (B) Dual-timescale kinetics and fits at selected wavelengths.

5.4 Discussion

NIR of Adgb-GD has revealed this activity to be as fast as Cygb, also suggesting a potential physiological role for this activity, that is through NO homeostasis. However, further work is still needed to determine the role of the its sulphides on this activity, transition to pentacoordinate following generation of NO from nitrite.

Cygb is expressed in virtually all body tissues (Burmester et al., 2002), while Adgb-GD in localised primarily in the testes (Hoogewijs et al., 2012). In contrast with Cygb, the NO binding of androglobin is accompanied by structural transition to 5-coordinate species. This has been previously reported in other heme proteins such as cytochrome c' prime (Weber, 1982), but may be a unique activity of hexacoordinate androglobin in the hemoglobin family. However, more research is needed fully understand androglobin NO activity. It is interesting to note, however, that in the testis where Adgb is found, there are four Nitric Oxide Synthases (NOS), endothelial NOS (eNOS), inducible NOS (iNOS), and neuronal NOS (nNOS) and one testis-specific nNOS (TnNOS) (Lee and Cheng, 2008) NO has been proposed to play a unique role in modulating germ cell viability and development (Zini et al., 1996) with high NO concentrations exhibiting a deleterious role in the mobility of spermatozoa and thus acting on some aspects of male infertility (Lee and Cheng, 2008) This raises the possibility that Adgb could also play a role in NO homeostasis and hence germ cell viability.

The pH acid-alkaline transition of ferric androglobin observed was high spin to low spin. The reverse of what has been reported in heme proteins like myoglobin (Brunori et al., 1968). Similar high spin to low spin acid-alkaline transitions has been observed in cytoglobin(Balercia et al., 2004) (Reeder, Svistunenko and Wilson, 2011), but data from pH titration suggest acid alkaline transition independent of water ionisation but rather transition due to pH effect of amino acids close to heme pocket. Crystal structures of the androglobin in the two spin-states may solve this issue. Data from in house modelling and sequence analysis of androglobin revealed the presence of 4 cysteines, however, two of those are buried within the structure and two exposed and capable of forming and intramolecular disulfide bond. Data from present study suggests an intramolecular bond formation by the two surface exposed cysteines, the

would similar to the kind of bond formation (intramolecular disulphide bond), by cysteines present in Cygb and Ngb. The cysteines in Cygb modulates distal histidine coordination and ligand access to the distal coordination site (Reeder and Ukeri, 2018), more work is needed to explore the role of the cysteines of structural and ligand binding properties of Adgb-GD. Adgb is a novel chimeric globin to the human globin family, we have explored optical spectral properties of the globin domain depicting it as a hexacoordinate-like globin, however more pentacoordinate-like than Ngb and Cygb Figure 5.3.4.3. The NiR and NO binding activities all reveals a 5-C NO binding mechanism, the study of cytochrome c' by manole *et a*l 2015 suggests a proximal NO binding, spectral and sequence analysis suggests a 5-C NO binding however more work is needed to be to fully characterize the ligand binding properties of Adgb-GD.

Chapter 6

General Discussion

6.1. Nitrite reductase activity of cytoglobin is rapid, cysteines may be molecular switches hinting regulatory role of cytoglobin.

Unlike Hb and Mb, Cygb is hexacoordinated, with the distal histidine ligated to the central heme-iron in the absence of external ligand, the role of the distal histidine in hexacoordinate globins is not clearly understood (Burmester et al., 2002). However, studies proposed a gating mechanism similar to that of Mb and Hb were the distal histidine stabilises and modulates ligand ligation to the central heme iron (Birukou et al., 2010). Futhermore, the distal ligand in Mb and Hb doesn't coordinate to the central heme iron, suggesting additional or novel role(s) of hexacoordination in hexacoordinate human globin like Cygb. It been has been suggested that hexacoordination may be linked to regulatory or signalling roles in these globins in contrast to the sensing and enzymatic roles of Mb and Hb (Trent Iii et al., 2001). Cygb is a low abundance globin (Hankeln et al., 2005), hampering any potential transport and storage roles like Mb and Hb as higher concentration Mb and Hb outcompetes Cygb in any such scenario, making a regulatory role much more feasible. The NiR activity might be an avenue for such regulatory activity, with studies showing Cygb to be unregulated in hypoxic tissues, coupled with fact that this activity occurs in deoxygenated condition this strongly supports Cygb activity during cellular hypoxia (Emara et al., 2010, Reeder and Ukeri, 2018).

Cygb possess two surface exposed cysteines capable of forming a disulfide bond, this leads to cysteine dependent heterogeneity with the protein existing in three forms as a Dimer(s-s), Monomer(sh-sh) and Monomer(s-s) (figure 3.1.1 and 3.1.2). However, the state of the protein *in vivo* is suggested to be that of a monomer, due to the protein having a monomeric assembly at low concentration, and likely a monomer *in vivo* due to low expression levels (Lechauve et al., 2010). Studies in chapter two identified the roles of cysteines in the NiR activity of Cygb. In the Monomer(s-s) the modulating effect of the cysteines on the distal histidine (His81) makes the NiR activity rapid, see Figure 2.3.3.9, placed Cygb as the fastest mammalian NiR, and fastest NiR in the human globin family see Table 2.4.1. However the cysteines didn’t play a significant role the NOD activity see Figure 2.3.4.4, due to the rapid nature of this activity, data observed was that of relaxation of the distal histidine and not the NOD activity, but the

cysteine played a role in the relaxation of the distal ligand with relatively more rapid relaxation observed in the Monomer(sh-sh) and Dimer(s-s) populations in contrast with the Monomer(s-s) population. The rapid nature of the NiR activity in Cygb place it for a potential role in NO homeostasis.

The proximity of the surface exposed cysteines in monomeric Cygb, and ability of the cysteines to form bonds within a monomeric unit in oxidative environment in cells suggests free cysteines in Cygb might be sensitive to cellular environment (Cumming et al., 2004). Formation of intramolecular disulphide bonds can occur in oxidative environment activating the protein for hypoxic response (Backer et al., 2018), this bond maybe be disrupted in reductive environment deactivating the protein, the cysteine may essentially act as molecular switches or signal transducers. Ferric Monomer(s-s) population of Cygb interact with lipids like oleate resulting in hexacoordinate to pentacoordinate structural transition in the protein this is a behaviour unique to Cygb (Beckerson et al., 2015). Cygb is also a rapid lipid peroxidase, this activity may be couple to pentacoordinate structural transition associated with lipid bind, free-radical-catalysed lipid oxidation has been observed to generate biologically active molecules important to various cell signalling pathways (Reeder et al., 2011). This again points to potential regulatory role of this protein, in which cysteines act as molecular switches to signal transduction pathway.

6.2 Modulation of nitrite reductase and nitric oxide dioxygenase activities by mutagenesis which highlights similarities to ligand migration in myoglobin and hemoglobin

6.2.1 Evolutionary relationship Myoglobin, hemoglobin and Cytoglobin to ancestral cellular globin suggests related roles

Mb, Hb, Ngb and Ngb are believed to have evolved from a common ancestor, however Cygb and Mb are more closely related with gene duplication events placing them in the Clade, with Ngb evolved to separate lineage, Cygb share 30% sequence similarity with Mb (Burmester et

al., 2002). They also share structural similarity also with conservation and similar orientation of key residues (Phe(CD1), Val(E11), distal His(E7) and proximal His(F8)), the key structural difference is the E7 position and structural changes associated with Cys38(B2) and Cys83(E9) disulphide bond formation (Sugimoto et al., 2004). The last common ancestor of all vertebrates most likely possessed two kinds of globins Ngb kept its role as globin of the nervous system, which it possessed early in the evolution (Burmester et al. 2000). The other globins possibly differentiated into a cellular globin, which led to Mb and CYGBs on the one hand and Hb on the other. Despite low sequence similarity between Ngb and Cygb the E7 position in conserved.

6.2.2 Effectiveness of mutation highlights possible relatedness in ligand migration

Mutation of residues at the distal pocket in proximity to the central heme iron was effective in attenuating or enhancing the NOD or NiR activity, these residues selected where based on the work of (Scott et al., 2001, Varnado et al., 2013) and (Tejero et al., 2015) on Mb, Hb and Ngb, see also chapter 3.1. The finding was that Cygb mutations are effective in modulating the NiR and NOD activities, similar to those reported by (Scott et al., 2001, Varnado et al., 2013) and (Tejero et al., 2015a) for mutations in other globins. The results reported in chapter 3.3.2 and 3.3.3 demonstrated ligand migration to the central heme in Cygb iron involved interaction with residues of identical positions on Mb and Hb, this may mean potentially identical ligand migration pathway during exit and entry to the central heme iron in Mb, Hb and Cygb. Highlighting evolutionary relationship of these globins, and possible distinction in roles of Ngb and Cygb while, the latter is in the same clade with Mb and Hb suggesting some role similar or related to Mb and Hb. Ngb is more evolutionary ancient and its role may be distinct (Burmester et al., 2002).

6.2.3 Removal of the distal histidine enhances ligand accessibility to the central heme iron

The distal histidine mutation (His81A), was effective in enhancing NiR activity in Cygb see Table 3.3.2.1, and NO binding (Figure 3.3.1.2D) similar to result by (Scott et al., 2001, Varnado

et al., 2013) and (Tejero et al., 2015a) mutation of distal ligand to a smaller amino acid residue like alanine reduces steric hindrance and enhance access to the distal coordination site (Birukou et al., 2010). In Mb the distal histidine act a gate modulating ligand access to the central heme iron, and also actsto stabilise binding of ligands like oxygen binding to the central heme iron (Birukou et al., 2010). Differences in structural configuration of distal ligands in Mb (pentacoordinate) and Cygb (hexacoordinate) necessitate different role, the role of the distal histidine in Cygb might be a regulatory role, due to proximity of the Cys38(B2) and Cys83(E9) to His81(E7), formation of bonds between these cysteines in monomeric subunit of Cygb affects the penta-hexa equilibrium, this bond favours the pentacoordinate structural confirmation (Beckerson et al., 2015b). More work still needs to done to identify the precise role of the distal histidine in Cygb in contrast to Mb and Hb.

6.2.4 Introducing bulk to the distal pocket attenuates the NiR and NOD activity

The L46W mutation introduced bulk to the back of the distal pocket, in agreement with previous studies, this results in attenuation of activities (NOD activity in particular). Ligand like NO resides in temporary docking sites behind the distal histidine before formation of bond with central heme iron, or heme oxygen (in the case of NOD activity) or escape via the histidine gate, disrupting this docking sites may increase energy barrier for ligand escape or binding, another possible explanation maybe alternative routes for NO which is hindered by large side chains of amino acid residues like tryptophan (Scott et al., 2001). In the L46W mutant there appeared to be a concentration dependence during NO binding (Figure 3.3.1.2C), with the rate of NO binding faster that than that of wild-type protein (Monomer(s-s)), and the other mutants (L46F, and C38,83S), the L46W mutation resulted in structural changes that made this mutant pentacoordinate-like (see Figure 3.3.1.1D). This could explain the concentration dependence on NO, since this process involves one ligand, ligand can access directly via the histidine gate without need temporary docking sites. In multi-ligand activity like NOD or NiR it can be proposed that there is a need for temporary docking sites which was disrupted by the bulky tryptophan residue. This is consistent with results from chapter 4 where three temporary docking zones have been proposed to explain three kinetic species (three step recombination)

observed after ultrafast photolysis see Figure 4.3.4.1 and Figure 4.4.2. The L46W mutation had significant impact the NOD activity this resulted in observation of different kinetic properties in contrast with the wild-type, L46F and C38,83 mutation. The kinetics of the L46W showed concentration dependency on NO consumption, while the time courses of the wild-type, L46F and C38,83 mutation displayed a hyperbolic curve. As observed in chapter 2 (Figure 2.3.4.2), this kinetics is not that of the NOD activity but the relaxation of the distal histidine and the protein transition from a pentacoordinate to a hexacoordinate state, the NOD activity is over before the dead time of the stopped-flow ~1.2 ms and hence cannot be measured. The L46W mutation slowed down the NOD activity enough for the true measurement of this activity to be observed (Figure 3.3.3.1). The L46F mutation had an intermediate effect on the NiR and NOD activity due to phenylalanine side chain being 50% smaller than that of the Tryptophan residue, rate of these activities where halfway between the L46W mutant and the wild-type protein.

6.3 Probing effect of cysteines on ligand migration pathway with ultrafast and nanosecond flash photolysis

The distal heme pocket was probed with femto- and nano- second flash photolysis (chapter 4). The results revealed the cysteine have effect on ligand migration pathway and temporary docking sites, the present or absence of the intramolecular disulfide bond in Cygb plays a role in ligand entry and exit from the distal coordination site. With ultrafast photolysis ~95 % of photolysed species recombined geminately in Dimer(s-s) and Monomer(sh-sh)) and ~99 % geminate in Monomer(s-s). However three kinetic components were identified (Figure 4.3.4.1), while component I and II were virtually identical across protein populations (Monomer(s-s), Monomer(sh-sh), Dimer(s-s)) component III was identical in protein population without the intramolecular disulfide bonds (Monomer(sh-sh) and Dimer(s-s)), leading to the conclusion that this difference was introduced as a result of the intramolecular disulfide bond present in the Monomer(s-s). Cygb species with an intact intramolecular disulfides bond, will have a more compacted structure this, affecting ligand migration and ligand binding pockets.

Component I represent species in temporary docking sites closest to the distal central heme iron, Component II represents species in close by site, Component III can described as species in docking site more distant from the heme iron and potentially impacted by the present of absence of intramolecular disulphide bonds. Autodock ligand binding prediction software was further used to model the ligand binding modes of NO on monomeric Cygb, crystal structure with xenon pockets were used for the modelling. Three pockets were identified with Xenon structure, auto-dock predicted 7 ligand binding mode, of which 3 of these mode overlapped the xenon pockets (3 pockets), identified from experimental data. With other two in distal binding pocket, one in the proximal binding pocket, with one being more of an outlier. Binding modes where clustered into zones, zone 1 where docking sites closest to the heme iron, while zone 2 nearby docking site, with zone 3 being the more distant site (see Figure 4.4.2). Zone 2 and 3 overlapped the xenon pockets observed from experiment data. It should be noted that the structure used was that of the Monomer(sh-sh) form of the protein as the crystal structure of the Monomer(s-s) was not available at the time this work was done. The zones give a clue of the potential temporary docking zones for NO to occupy after photolysis but not the structural dynamics associated with present of absence of the intramolecular disulphide bond

The Ultrafast recombination kinetics was distinct from that of the nanosecond recombination Figure 4.3.3.1 and 4.3.4.1. The ultrafast kinetics was a three-step process with three components with the nanosecond flash photolysis displayed a monophasic kinetics showing a single component. Reasons for this may be the nanosecond laser having a much longer time scale and so many more photons compared to the femtosecond laser. The ultrafast photolysis data reveals the effect of cysteines on temporary docking sites in the heme pocket, while nanosecond flash photolysis looked at the effect of cysteines on exit and re-entry of NO to heme pocket after flash photolysis. We propose that from this data in scenarios where the distal histidine is out the way, cysteines play a role in the dynamics of temporary docking sites within the heme pocket, but not ligand entry and exit from the from the heme pocket.

6.4 Androglobin a chimeric globin with an elusive role

In chapter 5, our work on the novel androglobin globin domain (Adgb-GD), reveals a hexacoordinate-like protein, but is much more pentacoordinate-like than other hexacoordinate members of the human globin family (Ngb, Cygb). Cysteine assays identified two surface expose cysteines are capable of forming an intramolecular disulphide bond like Cygb Figure 5.3.6.1. Although more work needs to be done to clarify the role(s) of these cysteines, preliminary studies revealed they have an effect on the NiR activity Figure 5.3.2.1C-F. The spectral properties of the NiR activity reveals a 5-coordinate NO binding Figure 5.3.2.1A-B, which is distinct from other members of the human globin family. This may suggest a unique role for the globin different from other members of the human globin family. EPR spectra of the NO-bound species is consistent with that of 5-coordinate NO-bound species. While the position of the on the heme plane is not yet verified, we have suggested a proximal binding similar to that of cytochrome c' (see Figure 5.3.3.1) due similarities in the optical properties of the NO-bound species. Androglobin globin domain also displays a unique pH transition in contrast with other member of the human globin family, Adgb lacks the high spin component present at high pH, the high spin components in hemoglobins at high pH results from an OH group occupying the distal coordination site. Structural transition due to pH effects are therefore different from those other human globin members, with structural changes impedes access of the OH group to central heme iron.

Summary

Cygb Monomer(s-s) is a relatively rapid nitrite reductase, the fastest among the mammalian globins. A second order rate constant of ~30 M^{-1}-s^{-1} is biological significant enough to propose a role in NO homeostasis. The cysteines modulate the distal histidine and ligand binding the Monomer(s-s), these cysteines could act as switches or signal transducers by bond formation in oxidative environment activating the protein, or bond disruption in reductive environment deactivating the protein. Point mutations were effective in controlling NiR and NOD activities

this could be used as a foundation for developing mammalian cell models to probe the NiR and NOD in cells. The effectiveness of residues in similar orientation and position in Mb and Hb having this effect on Cygb highlights evolutionary relations of these globins supporting the idea of Cygb Hb and Mb evolving a singular cellular globin ancestor. Ultrafast and nanosecond flash photolysis showed in impacts on cysteines on temporary docking sites within the heme pocket and ligand migration in and out of the heme pocket, with the cysteines have an effect of temporary docking sites with the protein. Adgb-GD is hexacoordinate-like, it's also a rapid NiR activity in 5-coordinate NO binding similar to cytochrome c'. While much is still unknown about this globin, we have successful characterised spectra and biochemical properties that could serve as the basis for future work. These intriguing results lay the foundation of further studies into the mechanism and role of the Adgb and clearly suggests a novel role in NO regulation.

Chapter 7

References

Alayash, A., Patel, R. and Cashon, R., 2001. Redox Reactions of Hemoglobin and Myoglobin: Biological and Toxicological Implications. *Antioxidants & Redox Signaling*, 3(2), pp.313-327.

Amdahl, M., Sparacino-Watkins, C., Corti, P., Gladwin, M. and Tejero, J., 2017. Efficient Reduction of Vertebrate Cytoglobins by the Cytochrome b5/Cytochrome b5 Reductase/NADH System. *Biochemistry*, 56(30), pp.3993-4004.

Ascenzi, P., Marino, M., Polticelli, F., Coletta, M., Gioia, M., Marini, S., Pesce, A., Nardini, M., Bolognesi, M., Reeder, B. and Wilson, M., 2013. Non-covalent and covalent modifications modulate the reactivity of monomeric mammalian globins. *Biochimica et Biophysica Acta (BBA) - Proteins and Proteomics*, 1834(9), pp.1750-1756.

Astudillo, L., Bernad, S., Derrien, V., Sebban, P. and Miksovska, J., 2010. Probing the Role of the Internal Disulfide Bond in Regulating Conformational Dynamics in Neuroglobin. *Biophysical Journal*, 99(2), pp.L16-L18.

Astudillo, L., Bernad, S., Derrien, V., Sebban, P. and Miksovska, J., 2013. Reduction of the internal disulfide bond between Cys 38 and 83 switches the ligand migration pathway in cytoglobin. *Journal of Inorganic Biochemistry*, 129, pp.23-29.

Avivi, A., Gerlach, F., Joel, A., Reuss, S., Burmester, T., Nevo, E. and Hankeln, T., 2010. Neuroglobin, cytoglobin, and myoglobin contribute to hypoxia adaptation of the subterranean mole rat Spalax. *Proceedings of the National Academy of Sciences*, 107(50), pp.21570-21575.

Baldwin, J., 1976. Structure and function of haemoglobin. *Progress in Biophysics and Molecular Biology*, 29, pp.225-320.

Balercia, G., Moretti, S., Vignini, A., Magagnini, M., Mantero, F., Boscaro, M., Ricciardo-Lamonica, G. and Mazzanti, L., 2004. Role of Nitric Oxide Concentrations on Human Sperm Motility. *Journal of Andrology*, 25(2), pp.245-249.

Basu, S., Azarova, N., Font, M., King, S., Hogg, N., Gladwin, M., Shiva, S. and Kim-Shapiro, D., 2008. Nitrite Reductase Activity of Cytochromec. *Journal of Biological Chemistry*, 283(47), pp.32590-32597.

Beckerson, P., Reeder, B. and Wilson, M., 2015. Coupling of disulfide bond and distal histidine dissociation in human ferrous cytoglobin regulates ligand binding. *FEBS Letters*, 589(4), pp.507-512.

Beckerson, P., Svistunenko, D. and Reeder, B., 2015. Effect of the distal histidine on the peroxidatic activity of monomeric cytoglobin. *F1000Research*, 4, p.87.

Beckerson, P., Wilson, M., Svistunenko, D. and Reeder, B., 2014. Cytoglobin ligand binding regulated by changing haem-co-ordination in response to intramolecular disulfide bond formation and lipid interaction. *Biochemical Journal*, 465(1), pp.127-137.

Bellei, M., Bortolotti, C., Di Rocco, G., Borsari, M., Lancellotti, L., Ranieri, A., Sola, M. and Battistuzzi, G., 2018. The influence of the Cys46/Cys55 disulfide bond on the redox and spectroscopic properties of human neuroglobin. *Journal of Inorganic Biochemistry*, 178, pp.70-86.

Berman, H., 2000. The Protein Data Bank. *Nucleic Acids Research*, 28(1), pp.235-242.

Bholah, T., Neergheen-Bhujun, V., Hodges, N., Dyall, S. and Bahorun, T., 2015. Cytoglobin as a Biomarker in Cancer: Potential Perspective for Diagnosis and Management. *BioMed Research International*, 2015, pp.1-6.

Birben, E., Sahiner, U., Sackesen, C., Erzurum, S. and Kalayci, O., 2012. Oxidative Stress and Antioxidant Defense. *World Allergy Organization Journal*, 5(1), pp.9-19.

Birukou, I., Maillett, D., Birukova, A. and Olson, J., 2011. Modulating Distal Cavities in the α and β Subunits of Human HbA Reveals the Primary Ligand Migration Pathway. *Biochemistry*, 50(34), pp.7361-7374.

Birukou, I., Schweers, R. and Olson, J., 2010. Distal Histidine Stabilizes Bound O2and Acts as a Gate for Ligand Entry in Both Subunits of Adult Human Hemoglobin. *Journal of Biological Chemistry*, 285(12), pp.8840-8854.

Bonaventura, C., Henkens, R., Alayash, A., Banerjee, S. and Crumbliss, A., 2013. Molecular Controls of the Oxygenation and Redox Reactions of Hemoglobin. *Antioxidants & Redox Signaling*, 18(17), pp.2298-2313.

Boutaud, O., Moore, K., Reeder, B., Harry, D., Howie, A., Wang, S., Carney, C., Masterson, T., Amin, T., Wright, D., Wilson, M., Oates, J. and Roberts, L., 2010. Acetaminophen inhibits hemoprotein-catalyzed lipid peroxidation and attenuates rhabdomyolysis-induced renal failure. *Proceedings of the National Academy of Sciences*, 107(6), pp.2699-2704.

Bracke, A., Hoogewijs, D. and Dewilde, S., 2018. Exploring three different expression systems for recombinant expression of globins: Escherichia coli, Pichia pastoris and Spodoptera frugiperda. *Analytical Biochemistry*, 543, pp.62-70.

Brittain, T., Skommer, J., Raychaudhuri, S. and Birch, N., 2010. An Antiapoptotic Neuroprotective Role for Neuroglobin. *International Journal of Molecular Sciences*, 11(6), pp.2306-2321.

Brown, K., 1996. Erythrocyte Metabolism and Enzyme Defects. *Laboratory Medicine*, 27(5), pp.329-333.

Brunori, M., Giuffre, A., Nienhaus, K., Nienhaus, G., Scandurra, F. and Vallone, B., 2005. Neuroglobin, nitric oxide, and oxygen: Functional pathways and conformational changes. *Proceedings of the National Academy of Sciences*, 102(24), pp.8483-8488.

Burmester, T. and Hankeln, T., 2009. What is the function of neuroglobin?. *Journal of Experimental Biology*, 212(10), pp.1423-1428.

Burmester, T., Ebner, B., Weich, B. and Hankeln, T., 2002. Cytoglobin: A Novel Globin Type Ubiquitously Expressed inVertebrate Tissues. *Molecular Biology and Evolution*, 19(4), pp.416-421.

Burmester, T., Weich, B., Reinhardt, S. and Hankeln, T., 2000. A vertebrate globin expressed in the brain. *Nature*, 407(6803), pp.520-523.

Chakraborty, S., John, R. and Nag, A., 2014. Cytoglobin in tumor hypoxia: novel insights into cancer suppression. *Tumor Biology*, 35(7), pp.6207-6219.

Chun-Lap Lo, S. and Agar, N., 1986. NADH-methemoglobin reductase activity in the erythrocytes of newborn and adult mammals. *Experientia*, 42(11-12), pp.1264-1265.

Corti, P., Ieraci, M. and Tejero, J., 2016. Characterization of zebrafish neuroglobin and cytoglobins 1 and 2: Zebrafish cytoglobins provide insights into the transition from six-coordinate to five-coordinate globins. *Nitric Oxide*, 53, pp.22-34.

Corti, P., Xue, J., Tejero, J., Wajih, N., Sun, M., Stolz, D., Tsang, M., Kim-Shapiro, D. and Gladwin, M., 2016. Globin X is a six-coordinate globin that reduces nitrite to nitric oxide in fish red blood cells. *Proceedings of the National Academy of Sciences*, 113(30), pp.8538-8543.

Cumming, R., Andon, N., Haynes, P., Park, M., Fischer, W. and Schubert, D., 2004. Protein Disulfide Bond Formation in the Cytoplasm during Oxidative Stress. *Journal of Biological Chemistry*, 279(21), pp.21749-21758.

De Backer, J., Razzokov, J., Hammerschmid, D., Mensch, C., Hafideddine, Z., Kumar, N., van Raemdonck, G., Yusupov, M., Van Doorslaer, S., Johannessen, C., Sobott, F., Bogaerts, A. and Dewilde, S., 2018. The effect of reactive oxygen and nitrogen species on the structure of cytoglobin: A potential tumor suppressor. *Redox Biology*, 19, pp.1-10.

De Backer, J., Razzokov, J., Hammerschmid, D., Mensch, C., Hafideddine, Z., Kumar, N., van Raemdonck, G., Yusupov, M., Van Doorslaer, S., Johannessen, C., Sobott, F., Bogaerts, A. and Dewilde, S., 2018. The effect of reactive oxygen and nitrogen species on the structure of cytoglobin: A potential tumor suppressor. *Redox Biology*, 19, pp.1-10.

de Sanctis, D., Dewilde, S., Pesce, A., Moens, L., Ascenzi, P., Hankeln, T., Burmester, T. and Bolognesi, M., 2004. Mapping protein matrix cavities in human cytoglobin through Xe atom binding. *Biochemical and Biophysical Research Communications*, 316(4), pp.1217-1221.

de Sanctis, D., Pesce, A., Nardini, M., Bolognesi, M., Bocedi, A. and Ascenzi, P., 2004. Structure-Function Relationships in the Growing Hexa-Coordinate Hemoglobin Sub-Family. *IUBMB Life*, 56(11), pp.643-651.

Dewilde, S., Kiger, L., Burmester, T., Hankeln, T., Baudin-Creuza, V., Aerts, T., Marden, M., Caubergs, R. and Moens, L., 2001. Biochemical Characterization and Ligand Binding Properties of Neuroglobin, a Novel Member of the Globin Family. *Journal of Biological Chemistry*, 276(42), pp.38949-38955.

Dietz, G., 2011. Protection by neuroglobin and cell-penetrating peptide-mediated delivery in vivo: A decade of research. *Experimental Neurology*, 231(1), pp.1-10.

Dröge, J. and Makałowski, W., 2011. Phylogenetic analysis reveals wide distribution of globin X. *Biology Direct*, 6(1), p.54.

Edgar, R., 2004. MUSCLE: multiple sequence alignment with high accuracy and high throughput. *Nucleic Acids Research*, 32(5), pp.1792-1797.

Emara, M., Turner, A. and Allalunis-Turner, J., 2010. Hypoxic regulation of cytoglobin and neuroglobin expression in human normal and tumor tissues. *Cancer Cell International*, 10(1), p.33.

Eswar, N., 2003. Tools for comparative protein structure modeling and analysis. *Nucleic Acids Research*, 31(13), pp.3375-3380.

Fago, A., Hundahl, C., Dewilde, S., Gilany, K., Moens, L. and Weber, R., 2004. Allosteric Regulation and Temperature Dependence of Oxygen Binding in Human Neuroglobin and Cytoglobin. *Journal of Biological Chemistry*, 279(43), pp.44417-44426.

Fago, A., Mathews, A., Dewilde, S., Moens, L. and Brittain, T., 2006. The reactions of neuroglobin with CO: Evidence for two forms of the ferrous protein. *Journal of Inorganic Biochemistry*, 100(8), pp.1339-1343.

Fang, J., Ma, I. and Allalunis-Turner, J., 2011. Knockdown of Cytoglobin Expression Sensitizes Human Glioma Cells to Radiation and Oxidative Stress. *Radiation Research*, 176(2), pp.198-207.

Ferreira, J., Marcondes, M., Icimoto, M., Cardoso, T., Tofanello, A., Pessoto, F., Miranda, E., Prieto, T., Nascimento, O., Oliveira, V. and Nantes, I., 2015. Intermediate Tyrosyl Radical and Amyloid Structure in Peroxide-Activated Cytoglobin. *PLOS ONE*, 10(8), p.e0136554.

Fiocchetti, M., Cipolletti, M., Brandi, V., Polticelli, F. and Ascenzi, P., 2017. Neuroglobin and friends. *Journal of Molecular Recognition*, 30(12), p.e2654.

Flogel, U., Merx, M., Godecke, A., Decking, U. and Schrader, J., 2001. Myoglobin: A scavenger of bioactive NO. *Proceedings of the National Academy of Sciences*, 98(2), pp.735-740.

Fordel, E., Geuens, E., Dewilde, S., De Coen, W. and Moens, L., 2004. Hypoxia/Ischemia and the Regulation of Neuroglobin and Cytoglobin Expression. *IUBMB Life*, 56(11), pp.681-687.

Fordel, E., Thijs, L., Martinet, W., Lenjou, M., Laufs, T., Van Bockstaele, D., Moens, L. and Dewilde, S., 2006. Neuroglobin and cytoglobin overexpression protects human SH-SY5Y

neuroblastoma cells against oxidative stress-induced cell death. *Neuroscience Letters*, 410(2), pp.146-151.

Frehm, E., Bonaventura, J. and Gow, A., 2004. S-Nitrosohemoglobin: an allosteric mediator of NO group function in mammalian vasculature. *Free Radical Biology and Medicine*, 37(4), pp.442-453.

Frey, A. and Kallio, P., 2003. Bacterial hemoglobins and flavohemoglobins: versatile proteins and their impact on microbiology and biotechnology. *FEMS Microbiology Reviews*, 27(4), pp.525-545.

García-Horsman, J., Barquera, B., Rumbley, J., Ma, J. and Gennis, R., 1994. The superfamily of heme-copper respiratory oxidases. *Journal of Bacteriology*, 176(18), pp.5587-5600.

Gardner, A., Cook, M. and Gardner, P., 2010. Nitric-oxide Dioxygenase Function of Human Cytoglobin with Cellular Reductants and in Rat Hepatocytes. *Journal of Biological Chemistry*, 285(31), pp.23850-23857.

GARDNER, P., 2005. Nitric oxide dioxygenase function and mechanism of flavohemoglobin, hemoglobin, myoglobin and their associated reductases. *Journal of Inorganic Biochemistry*, 99(1), pp.247-266.

Garrocho-Villegas, V., Gopalasubramaniam, S. and Arredondo-Peter, R., 2007. Plant hemoglobins: What we know six decades after their discovery. *Gene*, 398(1-2), pp.78-85.

Haines, B., Demaria, M., Mao, X., Xie, L., Campisi, J., Jin, K. and Greenberg, D., 2012. Hypoxia-inducible factor-1 and neuroglobin expression. *Neuroscience Letters*, 514(2), pp.137-140.

Halligan, K., Jourd'heuil, F. and Jourd'heuil, D., 2009. Cytoglobin Is Expressed in the Vasculature and Regulates Cell Respiration and Proliferation via Nitric Oxide Dioxygenation. *Journal of Biological Chemistry*, 284(13), pp.8539-8547.

Hamdane, D., Kiger, L., Dewilde, S., Green, B., Pesce, A., Uzan, J., Burmester, T., Hankeln, T., Bolognesi, M., Moens, L. and Marden, M., 2003. The Redox State of the Cell Regulates the Ligand Binding Affinity of Human Neuroglobin and Cytoglobin. *Journal of Biological Chemistry*, 278(51), pp.51713-51721.

Hamdane, D., Kiger, L., Dewilde, S., Green, B., Pesce, A., Uzan, J., Burmester, T., Hankeln, T., Bolognesi, M., Moens, L. and Marden, M., 2004. Coupling of the heme and an internal disulfide bond in human neuroglobin. *Micron*, 35(1-2), pp.59-62.

HANKELN, T., EBNER, B., FUCHS, C., GERLACH, F., HABERKAMP, M., LAUFS, T., ROESNER, A., SCHMIDT, M., WEICH, B. and WYSTUB, S., 2005. Neuroglobin and cytoglobin in search of their role in the vertebrate globin family. *Journal of Inorganic Biochemistry*, 99(1), pp.110-119.

Hargrove, M., 2000. A Flash Photolysis Method to Characterize Hexacoordinate Hemoglobin Kinetics. *Biophysical Journal*, 79(5), pp.2733-2738.

Hederstedt, L., 2012. Heme A biosynthesis. *Biochimica et Biophysica Acta (BBA) - Bioenergetics*, 1817(6), pp.920-927.

Helms, C., Gladwin, M. and Kim-Shapiro, D., 2018. Erythrocytes and Vascular Function: Oxygen and Nitric Oxide. *Frontiers in Physiology*, 9.

Hoffman, B. and Gibson, Q., 1978. On the photosensitivity of liganded hemoproteins and their metal-substituted analogues. *Proceedings of the National Academy of Sciences*, 75(1), pp.21-25.

Holt, S., Reeder, B., Wilson, M., Harvey, S., Morrow, J., Roberts, L. and Moore, K., 1999. Increased lipid peroxidation in patients with rhabdomyolysis. *The Lancet*, 353(9160), p.1241.

Hoogewijs, D., Ebner, B., Germani, F., Hoffmann, F., Fabrizius, A., Moens, L., Burmester, T., Dewilde, S., Storz, J., Vinogradov, S. and Hankeln, T., 2011. Androglobin: A Chimeric

Globin in Metazoans That Is Preferentially Expressed in Mammalian Testes. *Molecular Biology and Evolution*, 29(4), pp.1105-1114.

Huang, Z., 2005. Enzymatic function of hemoglobin as a nitrite reductase that produces NO under allosteric control. *Journal of Clinical Investigation*, 115(8), pp.2099-2107.

International Journal of Molecular Sciences, 2017. Comparative Response of Brain to Chronic Hypoxia and Hyperoxia. 18(9), p.1914.

Jayaraman, T., Tejero, J., Chen, B., Blood, A., Frizzell, S., Shapiro, C., Tiso, M., Hood, B., Wang, X., Zhao, X., Conrads, T., Mallampalli, R. and Gladwin, M., 2011. 14-3-3 Binding and Phosphorylation of Neuroglobin during Hypoxia Modulate Six-to-Five Heme Pocket Coordination and Rate of Nitrite Reduction to Nitric Oxide. *Journal of Biological Chemistry*, 286(49), pp.42679-42689.

Jia, L., Bonaventura, C., Bonaventura, J. and Stamler, J., 1996. S-nitrosohaemoglobin: a dynamic activity of blood involved in vascular control. *Nature*, 380(6571), pp.221-226.

Jin, K., Mao, X., Xie, L., Khan, A. and Greenberg, D., 2008. Neuroglobin protects against nitric oxide toxicity. *Neuroscience Letters*, 430(2), pp.135-137.

Kakar, S., Hoffman, F., Storz, J., Fabian, M. and Hargrove, M., 2010. Structure and reactivity of hexacoordinate hemoglobins. *Biophysical Chemistry*, 152(1-3), pp.1-14.

Kawada, N., Kristensen, D., Asahina, K., Nakatani, K., Minamiyama, Y., Seki, S. and Yoshizato, K., 2001. Characterization of a Stellate Cell Activation-associated Protein (STAP) with Peroxidase Activity Found in Rat Hepatic Stellate Cells. *Journal of Biological Chemistry*, 276(27), pp.25318-25323.

Kobayashi, K., Tamura, M. and Hayashi, K., 1982. Kinetic analysis of the recombination of nitric oxide with ferrihemoproteins by the flash photolysis method. *Biochemistry*, 21(4), pp.729-732.

Kriegl, J., Bhattacharyya, A., Nienhaus, K., Deng, P., Minkow, O. and Nienhaus, G., 2002. Ligand binding and protein dynamics in neuroglobin. *Proceedings of the National Academy of Sciences*, 99(12), pp.7992-7997.

Kruglik, S., Lambry, J., Cianetti, S., Martin, J., Eady, R., Andrew, C. and Negrerie, M., 2006. Molecular Basis for Nitric Oxide Dynamics and Affinity withAlcaligenes xylosoxidansCytochromeć. *Journal of Biological Chemistry*, 282(7), pp.5053-5062.

Latina, A., Viticchiè, G., Lena, A., Piro, M., Annicchiarico-Petruzzelli, M., Melino, G. and Candi, E., 2015. ΔNp63 targets cytoglobin to inhibit oxidative stress-induced apoptosis in keratinocytes and lung cancer. *Oncogene*, 35(12), pp.1493-1503.

Lechauve, C., Chauvierre, C., Dewilde, S., Moens, L., Green, B., Marden, M., Célier, C. and Kiger, L., 2010. Cytoglobin conformations and disulfide bond formation. *FEBS Journal*, 277(12), pp.2696-2704.

Lee, J., Kim, H., Kim, D. and Gye, M., 2006. EFFECTS OF CALCIUM CHANNEL BLOCKERS ON THE SPERMATOGENESIS AND GENE EXPRESSION IN PERIPUBERTAL MOUSE TESTIS. *Archives of Andrology*, 52(4), pp.311-318.

Lee, N. and Cheng, C., 2008. Nitric Oxide and Cyclic Nucleotides: Their Roles in Junction Dynamics and Spermatogenesis. *Oxidative Medicine and Cellular Longevity*, 1(1), pp.25-32.

Li, H., Hemann, C., Abdelghany, T., El-Mahdy, M. and Zweier, J., 2012. Characterization of the Mechanism and Magnitude of Cytoglobin-mediated Nitrite Reduction and Nitric Oxide Generation under Anaerobic Conditions. *Journal of Biological Chemistry*, 287(43), pp.36623-36633.

Liebl, U., Lambry, J. and Vos, M., 2013. Primary processes in heme-based sensor proteins. *Biochimica et Biophysica Acta (BBA) - Proteins and Proteomics*, 1834(9), pp.1684-1692.

Lilly, B., Dammeyer, K., Marosis, S., McCallinhart, P., Trask, A., Lowe, M. and Sawant, D., 2018. Endothelial cell-induced cytoglobin expression in vascular smooth muscle cells contributes to modulation of nitric oxide. *Vascular Pharmacology*, 110, pp.7-15.

Liu, X., El-Mahdy, M., Boslett, J., Varadharaj, S., Hemann, C., Abdelghany, T., Ismail, R., Little, S., Zhou, D., Thuy, L., Kawada, N. and Zweier, J., 2017. Cytoglobin regulates blood pressure and vascular tone through nitric oxide metabolism in the vascular wall. *Nature Communications*, 8(1).

Liu, X., Follmer, D., Zweier, J., Huang, X., Hemann, C., Liu, K., Druhan, L. and Zweier, J., 2012. Characterization of the Function of Cytoglobin as an Oxygen-Dependent Regulator of Nitric Oxide Concentration. *Biochemistry*, 51(25), pp.5072-5082.

Liu, X., Tong, J., Zweier, J., Follmer, D., Hemann, C., Ismail, R. and Zweier, J., 2013. Differences in oxygen-dependent nitric oxide metabolism by cytoglobin and myoglobin account for their differing functional roles. *FEBS Journal*, 280(15), pp.3621-3631.

Luchsinger, B., Rich, E., Gow, A., Williams, E., Stamler, J. and Singel, D., 2003. Routes to S-nitroso-hemoglobin formation with heme redox and preferential reactivity in the subunits. *Proceedings of the National Academy of Sciences*, 100(2), pp.461-466.

Luyckx, E., Everaert, B., Van der Veken, B., Van Leuven, W., Timmermans, J., Vrints, C., De Meyer, G., Martinet, W. and Dewilde, S., 2017. Cytoprotective effects of transgenic neuroglobin overexpression in an acute and chronic mouse model of ischemic heart disease. *Heart and Vessels*, 33(1), pp.80-88.

Lv, Y., Wang, Q., Diao, Y. and Xu, R., 2008. Cytoglobin:A Novel Potential Gene Medicine for Fibrosis and Cancer Therapy. *Current Gene Therapy*, 8(4), pp.287-294.

Makino, M., Sugimoto, H., Sawai, H., Kawada, N., Yoshizato, K. and Shiro, Y., 2006. High-resolution structure of human cytoglobin: identification of extra N- and C-termini and a

new dimerization mode. *Acta Crystallographica Section D Biological Crystallography*, 62(6), pp.671-677.

Manole, A., Kekilli, D., Svistunenko, D., Wilson, M., Dobbin, P. and Hough, M., 2015. Conformational control of the binding of diatomic gases to cytochrome c′. *JBIC Journal of Biological Inorganic Chemistry*, 20(4), pp.675-686.

Martínková, M., Kitanishi, K. and Shimizu, T., 2013. Heme-based Globin-coupled Oxygen Sensors: Linking Oxygen Binding to Functional Regulation of Diguanylate Cyclase, Histidine Kinase, and Methyl-accepting Chemotaxis. *Journal of Biological Chemistry*, 288(39), pp.27702-27711.

Mathai, C., Jourd'heuil, F., Lopez-Soler, R. and Jourd'heuil, D., 2020. Emerging perspectives on cytoglobin, beyond NO dioxygenase and peroxidase. *Redox Biology*, 32, p.101468.

McRonald, F., Risk, J. and Hodges, N., 2012. Protection from Intracellular Oxidative Stress by Cytoglobin in Normal and Cancerous Oesophageal Cells. *PLoS ONE*, 7(2), p.e30587.

Motoyama, H., Komiya, T., Thuy, L., Tamori, A., Enomoto, M., Morikawa, H., Iwai, S., Uchida-Kobayashi, S., Fujii, H., Hagihara, A., Kawamura, E., Murakami, Y., Yoshizato, K. and Kawada, N., 2013. Cytoglobin is expressed in hepatic stellate cells, but not in myofibroblasts, in normal and fibrotic human liver. *Laboratory Investigation*, 94(2), pp.192-207.

Mukai, M., Savard, P., Ouellet, H., Guertin, M. and Yeh, S., 2002. Unique Ligand−Protein Interactions in a New Truncated Hemoglobin fromMycobacterium tuberculosis†. *Biochemistry*, 41(12), pp.3897-3905.

Nardini, M., Pesce, A., Milani, M. and Bolognesi, M., 2007. Protein fold and structure in the truncated (2/2) globin family. *Gene*, 398(1-2), pp.2-11.

Nayak, G., Prentice, H. and Milton, S., 2009. Role of neuroglobin in regulating reactive oxygen species in the brain of the anoxia-tolerant turtleTrachemys scripta. *Journal of Neurochemistry*, 110(2), pp.603-612.

Négrerie, M., Bouzhir, L., Martin, J. and Liebl, U., 2001. Control of Nitric Oxide Dynamics by Guanylate Cyclase in Its Activated State. *Journal of Biological Chemistry*, 276(50), pp.46815-46821.

Nicolis, S., Monzani, E., Ciaccio, C., Ascenzi, P., Moens, L. and Casella, L., 2007. Reactivity and endogenous modification by nitrite and hydrogen peroxide: does human neuroglobin act only as a scavenger?. *Biochemical Journal*, 407(1), pp.89-99.

Oleksiewicz, U., Liloglou, T., Tasopoulou, K., Daskoulidou, N., Bryan, J., Gosney, J., Field, J. and Xinarianos, G., 2013. Cytoglobin has bimodal: tumour suppressor and oncogene functions in lung cancer cell lines. *Human Molecular Genetics*, 22(16), pp.3207-3217.

Ostojic, J., 2006. Neuroglobin and Cytoglobin: Oxygen-Binding Proteins in Retinal Neurons. *Investigative Ophthalmology & Visual Science*, 47(3), pp.1016-1023.

Ostojić, J., 2008. Patterns of Distribution of Oxygen-Binding Globins, Neuroglobin and Cytoglobin in Human Retina. *Archives of Ophthalmology*, 126(11), p.1530.

Pesce, A., Bolognesi, M., Bocedi, A., Ascenzi, P., Dewilde, S., Moens, L., Hankeln, T. and Burmester, T., 2002. Neuroglobin and cytoglobin. *EMBO reports*, 3(12), pp.1146-1151.

Pesce, A., De Sanctis, D., Nardini, M., Dewilde, S., Moens, L., Hankeln, T., Burmester, T., Ascenzi, P. and Bolognesi, M., 2004. Reversible hexa- to penta-coordination of the heme Fe atom modulates ligand binding properties of neuroglobin and cytoglobin. *IUBMB Life*, 56(11), pp.657-664.

Pesce, A., Nardini, M., Dewilde, S., Ascenzi, P., Burmester, T., Hankeln, T., Moens, L. and Bolognesi, M., 2002. Human neuroglobin: crystals and preliminary X-ray diffraction

analysis. *Acta Crystallographica Section D Biological Crystallography*, 58(10), pp.1848-1850.

Petersen, M., Dewilde, S. and Fago, A., 2008. Reactions of ferrous neuroglobin and cytoglobin with nitrite under anaerobic conditions. *Journal of Inorganic Biochemistry*, 102(9), pp.1777-1782.

Proceedings of the Royal Society of London. Series B. Biological Sciences, 1962. Absorption spectra and some other properties of cytochrome c and of its compounds with ligands. 156(965), pp.429-458.

Rajendram, R. and Rao, N., 2006. Neuroglobin in normal retina and retina from eyes with advanced glaucoma. *British Journal of Ophthalmology*, 91(5), pp.663-666.

Reeder, B. and Ukeri, J., 2018. Strong modulation of nitrite reductase activity of cytoglobin by disulfide bond oxidation: Implications for nitric oxide homeostasis. *Nitric Oxide*, 72, pp.16-23.

Reeder, B., 2017. Redox and Peroxidase Activities of the Hemoglobin Superfamily: Relevance to Health and Disease. *Antioxidants & Redox Signaling*, 26(14), pp.763-776.

Reeder, B., Cutruzzolà, F., Bigotti, M., Watmough, N. and Wilson, M., 2007. Histidine and not tyrosine is required for the Peroxide-induced formation of haem to protein cross-linked myoglobin. *IUBMB Life*, 59(8), pp.477-489.

Reeder, B., Svistunenko, D. and Wilson, M., 2011. Lipid binding to cytoglobin leads to a change in haem co-ordination: a role for cytoglobin in lipid signalling of oxidative stress. *Biochemical Journal*, 434(3), pp.483-492.

Reuss, S., Saaler-Reinhardt, S., Weich, B., Wystub, S., Reuss, M., Burmester, T. and Hankeln, T., 2002. Expression analysis of neuroglobin mRNA in rodent tissues. *Neuroscience*, 115(3), pp.645-656.

Reuss, S., Wystub, S., Disque-Kaiser, U., Hankeln, T. and Burmester, T., 2016. Distribution of Cytoglobin in the Mouse Brain. *Frontiers in Neuroanatomy*, 10.

Riener, C., Kada, G. and Gruber, H., 2002. Quick measurement of protein sulfhydryls with Ellman's reagent and with 4,4′-dithiodipyridine. *Analytical and Bioanalytical Chemistry*, 373(4-5), pp.266-276.

Roesner, A., Fuchs, C., Hankeln, T. and Burmester, T., 2004. A Globin Gene of Ancient Evolutionary Origin in Lower Vertebrates: Evidence for Two Distinct Globin Families in Animals. *Molecular Biology and Evolution*, 22(1), pp.12-20.

Rowland, L., Campbell, P., Mavingire, N., Wooten, J., McLean, L., Zylstra, D., Thorne, G., Daly, D., Boyle, K., Whang, S., Unternaehrer, J. and Brantley, E., 2018. Putative tumor suppressor cytoglobin promotes aryl hydrocarbon receptor ligand–mediated triple negative breast cancer cell death. *Journal of Cellular Biochemistry*, 120(4), pp.6004-6014.

Sanctis, D., Dewilde, S., Pesce, A., Moens, L., Ascenzi, P., Hankeln, T., Burmester, T. and Bolognesi, M., 2004. Crystal Structure of Cytoglobin: The Fourth Globin Type Discovered in Man Displays Heme Hexa-coordination. *Journal of Molecular Biology*, 336(4), pp.917-927.

Sawai, H., Kawada, N., Yoshizato, K., Nakajima, H., Aono, S. and Shiro, Y., 2003. Characterization of the Heme Environmental Structure of Cytoglobin, a Fourth Globin in Humans†. *Biochemistry*, 42(17), pp.5133-5142.

Sawai, H., Makino, M., Mizutani, Y., Ohta, T., Sugimoto, H., Uno, T., Kawada, N., Yoshizato, K., Kitagawa, T. and Shiro, Y., 2005. Structural Characterization of the Proximal and Distal Histidine Environment of Cytoglobin and Neuroglobin. *Biochemistry*, 44(40), pp.13257-13265.

Schmidt, M., Gerlach, F., Avivi, A., Laufs, T., Wystub, S., Simpson, J., Nevo, E., Saaler-Reinhardt, S., Reuss, S., Hankeln, T. and Burmester, T., 2003. Cytoglobin Is a Respiratory Protein in Connective Tissue and Neurons, Which Is Up-regulated by Hypoxia. *Journal of Biological Chemistry*, 279(9), pp.8063-8069.

Scott, E., Gibson, Q. and Olson, J., 2000. Mapping the Pathways for O2Entry Into and Exit from Myoglobin. *Journal of Biological Chemistry*, 276(7), pp.5177-5188.

Shaw, R., Omar, M., Rokadiya, S., Kogera, F., Lowe, D., Hall, G., Woolgar, J., Homer, J., Liloglou, T., Field, J. and Risk, J., 2009. Cytoglobin is upregulated by tumour hypoxia and silenced by promoter hypermethylation in head and neck cancer. *British Journal of Cancer*, 101(1), pp.139-144.

Shigematsu, A., Adachi, Y., Matsubara, J., Mukaide, H., Koike-Kiriyama, N., Minamino, K., Shi, M., Yanai, S., Imamura, M., Taketani, S. and Ikehara, S., 2008. Analyses of Expression of Cytoglobin by Immunohistochemical Studies in Human Tissues. *Hemoglobin*, 32(3), pp.287-296.

Shivapurkar, N., Stastny, V., Okumura, N., Girard, L., Xie, Y., Prinsen, C., Thunnissen, F., Wistuba, I., Czerniak, B., Frenkel, E., Roth, J., Liloglou, T., Xinarianos, G., Field, J., Minna, J. and Gazdar, A., 2008. Cytoglobin, the Newest Member of the Globin Family, Functions as a Tumor Suppressor Gene. *Cancer Research*, 68(18), pp.7448-7456.

Singh, S., Canseco, D., Manda, S., Shelton, J., Chirumamilla, R., Goetsch, S., Ye, Q., Gerard, R., Schneider, J., Richardson, J., Rothermel, B. and Mammen, P., 2013. Cytoglobin modulates myogenic progenitor cell viability and muscle regeneration. *Proceedings of the National Academy of Sciences*, 111(1), pp.E129-E138.

Singh, S., Zhuo, M., Gorgun, F. and Englander, E., 2013. Overexpressed neuroglobin raises threshold for nitric oxide-induced impairment of mitochondrial respiratory activities and stress signaling in primary cortical neurons. *Nitric Oxide*, 32, pp.21-28.

Smagghe, B., Sarath, G., Ross, E., Hilbert, J. and Hargrove, M., 2006. Slow Ligand Binding Kinetics Dominate Ferrous Hexacoordinate Hemoglobin Reactivities and Reveal Differences between Plants and Other Species†. *Biochemistry*, 45(2), pp.561-570.

Smagghe, B., Trent, J. and Hargrove, M., 2008. NO Dioxygenase Activity in Hemoglobins Is Ubiquitous In Vitro, but Limited by Reduction In Vivo. *PLoS ONE*, 3(4), p.e2039.

Sugimoto, H., Makino, M., Sawai, H., Kawada, N., Yoshizato, K. and Shiro, Y., 2004. Structural Basis of Human Cytoglobin for Ligand Binding. *Journal of Molecular Biology*, 339(4), pp.873-885.

Sun, F., Mao, X., Xie, L., Greenberg, D. and Jin, K., 2013. Neuroglobin Protein is Upregulated in Alzheimer's Disease. *Journal of Alzheimer's Disease*, 36(4), pp.659-663.

Tejero, J., Kapralov, A., Baumgartner, M., Sparacino-Watkins, C., Anthonymutu, T., Vlasova, I., Camacho, C., Gladwin, M., Bayir, H. and Kagan, V., 2016. Peroxidase activation of cytoglobin by anionic phospholipids: Mechanisms and consequences. *Biochimica et Biophysica Acta (BBA) - Molecular and Cell Biology of Lipids*, 1861(5), pp.391-401.

Tejero, J., Kapralov, A., Baumgartner, M., Sparacino-Watkins, C., Anthonymutu, T., Vlasova, I., Camacho, C., Gladwin, M., Bayir, H. and Kagan, V., 2016. Peroxidase activation of cytoglobin by anionic phospholipids: Mechanisms and consequences. *Biochimica et Biophysica Acta (BBA) - Molecular and Cell Biology of Lipids*, 1861(5), pp.391-401.

Tejero, J., Sparacino-Watkins, C., Ragireddy, V., Frizzell, S. and Gladwin, M., 2015. Exploring the Mechanisms of the Reductase Activity of Neuroglobin by Site-Directed Mutagenesis of the Heme Distal Pocket. *Biochemistry*, 54(3), pp.722-733.

Tiso, M., Tejero, J., Basu, S., Azarov, I., Wang, X., Simplaceanu, V., Frizzell, S., Jayaraman, T., Geary, L., Shapiro, C., Ho, C., Shiva, S., Kim-Shapiro, D. and Gladwin, M., 2011. Human Neuroglobin Functions as a Redox-regulated Nitrite Reductase. *Journal of Biological Chemistry*, 286(20), pp.18277-18289.

Tong, J., Zweier, J., Huskey, R., Ismail, R., Hemann, C., Zweier, J. and Liu, X., 2014. Effect of temperature, pH and heme ligands on the reduction of Cygb(Fe3+) by ascorbate. *Archives of Biochemistry and Biophysics*, 554, pp.1-5.

Totzeck, M., Hendgen-Cotta, U., Kelm, M. and Rassaf, T., 2014. Crosstalk between Nitrite, Myoglobin and Reactive Oxygen Species to Regulate Vasodilation under Hypoxia. *PLoS ONE*, 9(8), p.e105951.

Totzeck, M., Hendgen-Cotta, U., Luedike, P., Berenbrink, M., Klare, J., Steinhoff, H., Semmler, D., Shiva, S., Williams, D., Kipar, A., Gladwin, M., Schrader, J., Kelm, M., Cossins, A. and Rassaf, T., 2012. Nitrite Regulates Hypoxic Vasodilation via Myoglobin-Dependent Nitric Oxide Generation. *Circulation*, 126(3), pp.325-334.

Trent, J. and Hargrove, M., 2002. A Ubiquitously Expressed Human Hexacoordinate Hemoglobin. *Journal of Biological Chemistry*, 277(22), pp.19538-19545.

Trent, J., Hvitved, A. and Hargrove, M., 2001. A Model for Ligand Binding to Hexacoordinate Hemoglobins†. *Biochemistry*, 40(20), pp.6155-6163.

Trent, J., Watts, R. and Hargrove, M., 2001. Human Neuroglobin, a Hexacoordinate Hemoglobin That Reversibly Binds Oxygen. *Journal of Biological Chemistry*, 276(32), pp.30106-30110.

Trott, O. and Olson, A., 2009. AutoDock Vina: Improving the speed and accuracy of docking with a new scoring function, efficient optimization, and multithreading. *Journal of Computational Chemistry*, p.NA-NA.

Tsujino, H., Yamashita, T., Nose, A., Kukino, K., Sawai, H., Shiro, Y. and Uno, T., 2014. Disulfide bonds regulate binding of exogenous ligand to human cytoglobin. *Journal of Inorganic Biochemistry*, 135, pp.20-27.

Uppal, S., Kumar, A., Shandilya, M., Mukhi, N., Singh, A., Kateriya, S., Kaur, J. and Kundu, S., 2016. Penta- and hexa-coordinate ferric hemoglobins display distinct pH titration profiles measured by Soret peak shifts. *Analytical Biochemistry*, 510, pp.120-128.

Vallone, B., Nienhaus, K., Brunori, M. and Nienhaus, G., 2004. The structure of murine neuroglobin: Novel pathways for ligand migration and binding. *Proteins: Structure, Function, and Bioinformatics*, 56(1), pp.85-92.

Van Doorslaer, S., Dewilde, S., Kiger, L., Nistor, S., Goovaerts, E., Marden, M. and Moens, L., 2002. Nitric Oxide Binding Properties of Neuroglobin. *Journal of Biological Chemistry*, 278(7), pp.4919-4925.

Van Thuy, T., Thuy, L., Yoshizato, K. and Kawada, N., 2017. Possible Involvement of Nitric Oxide in Enhanced Liver Injury and Fibrogenesis during Cholestasis in Cytoglobin-deficient Mice. *Scientific Reports*, 7(1).

Varnado, C., Mollan, T., Birukou, I., Smith, B., Henderson, D. and Olson, J., 2013. Development of Recombinant Hemoglobin-Based Oxygen Carriers. *Antioxidants & Redox Signaling*, 18(17), pp.2314-2328.

Vinogradov, S. and Moens, L., 2008. Diversity of Globin Function: Enzymatic, Transport, Storage, and Sensing. *Journal of Biological Chemistry*, 283(14), pp.8773-8777.

Vinogradov, S., Hoogewijs, D., Bailly, X., Mizuguchi, K., Dewilde, S., Moens, L. and Vanfleteren, J., 2007. A model of globin evolution. *Gene*, 398(1-2), pp.132-142.

Wen, J., Wu, Y., Wei, W., Li, Z., Wang, P., Zhu, S. and Dong, W., 2017. Protective effects of recombinant human cytoglobin against chronic alcohol-induced liver disease in vivo and in vitro. *Scientific Reports*, 7(1).

YOSHIZATO, K., THUY, L., SHIOTA, G. and KAWADA, N., 2016. Discovery of cytoglobin and its roles in physiology and pathology of hepatic stellate cells. *Proceedings of the Japan Academy, Series B*, 92(3), pp.77-97.

Zhang, J., Pei, Y., Yang, W., Yang, W., Chen, B., Zhao, X. and Long, S., 2018. Cytoglobin ameliorates the stemness of hepatocellular carcinoma via coupling oxidative-nitrosative stress signals. *Molecular Carcinogenesis*, 58(3), pp.334-343.

Zhang, S., Li, X., Jourd'heuil, F., Qu, S., Devejian, N., Bennett, E., Jourd'heuil, D. and Cai, C., 2017. Cytoglobin Promotes Cardiac Progenitor Cell Survival against Oxidative Stress via the Upregulation of the NFκB/iNOS Signal Pathway and Nitric Oxide Production. *Scientific Reports*, 7(1).

Zhao, Y., Hoganson, C., Babcock, G. and Marletta, M., 1998. Structural Changes in the Heme Proximal Pocket Induced by Nitric Oxide Binding to Soluble Guanylate Cyclase†. *Biochemistry*, 37(36), pp.12458-12464.

Zhao, Y., Hoganson, C., Babcock, G. and Marletta, M., 1998. Structural Changes in the Heme Proximal Pocket Induced by Nitric Oxide Binding to Soluble Guanylate Cyclase†. *Biochemistry*, 37(36), pp.12458-12464.

Zini, A., O'Bryan, M., Magid, M. and Schlegel, P., 1996. Immunohistochemical Localization of Endothelial Nitric Oxide Synthase in Human Testis, Epididymis, and Vas Deferens Suggests a Possible Role for Nitric Oxide in Spermatogenesis, Sperm Maturation, and Programmed Cell Death1. *Biology of Reproduction*, 55(5), pp.935-941.

Zuckerman, B., Abergel, Z., Zelmanovich, V., Romero, L., Abergel, R., Livshits, L., Smith, Y. and Gross, E., 2017. Characterization of gene expression associated with the adaptation of the nematode C. elegans to hypoxia and reoxygenation stress reveals an unexpected function of the neuroglobin GLB-5 in innate immunity. *Free Radical Biology and Medicine*, 108, pp.858-873.

Zweier, J. and Ilangovan, G., 2020. Regulation of Nitric Oxide Metabolism and Vascular Tone by Cytoglobin. *Antioxidants & Redox Signaling*, 32(16), pp.1172-1187.